Evaluating the Influence of the Forestry Reclamation Approach on Water Quality and Hydrology on Appalachian Coal Mines

Final Report

Christopher Barton[1], Tanja Williamson[2], Carmen Agouridis[3], Kevin Yeager[4], Morgan Gerlitz[3], William Bond[4], Kenton Sena[5] and Scott Aldridge[6]

[1]University of Kentucky, Department of Forestry and Natural Resources; [2]USGS OH-KY-IN Water Science Center; [3]University of Kentucky, Department of Biosystems and Agricultural Engineering; [4]University of Kentucky, Department of Earth and Environmental Sciences; [5]University of Kentucky, Honors College; [6]USDA-NRCS

*This draft manuscript is distributed solely for purposes of scientific peer review. Its content is deliberative and predecisional, so it must not be disclosed or released by reviewers. Because the manuscript has not yet been approved for publication by the U.S. Geological Survey (USGS), it does not represent any official USGS finding or policy.

**Any use of trade, firm, or product names is for descriptive purposes only and does not imply endorsement by the U.S. Government.

TABLE OF CONTENTS

LIST OF TABLES

LIST OF FIGURES

I. EXECUTIVE SUMMARY

Since the passage of the Surface Mine Control and Reclamation Act (SMCRA) of 1977, surface coal mines in Appalachia have largely been reclaimed as hayland pasture and wildlife habitat instead of the forest land type that existed prior to mining. Many components of the natural forest's hydrologic cycle are altered in reclaimed grasslands and shrublands due to the lack of canopy cover and changes to physical properties of the soil. Canopy interception (and interception loss) are expected to be lower in conventionally reclaimed grassland sites due to less structural complexity of the canopy (fewer layers of vegetation and less surface area). Soils at conventionally reclaimed grassland sites tend to be compacted by design, thus limiting infiltration and rooting volume. The combined influences result in reduced subsurface flow and ET, in exchange for increased overland flow, storm response, and potentially increased erosion and sedimentation. Reclamation using forestry reclamation approach (FRA) should (with time and forest development) provide a canopy that functions similar to a natural forest and provide soil that better promotes infiltration and water storage, which can be utilized by tree roots. As such, use of FRA should result in higher ET over reclaimed grasslands, providing a higher ability of the basin to buffer storm events. In theory, restoration of the forest will restore lost hydrologic function with regards to water use and cycling. Similarly, the return of the forests should also aid in the recovery of lost ecosystem functions (including those that provide ecosystem services regarding air, water and soil quality). Few studies have tried to confirm or negate these hydrologic interactions until now. A multi-faceted project was undertaken to examine the influence of FRA on water resources with the following objectives:

1. Compare hydrological function (including streamflow, canopy interception, stemflow, soil-water storage, and soil saturated hydraulic conductivity) across a variety of surface mine reclamation strategies and ages, including those listed above to evaluate the influence of FRA on the water cycle.
2. Use a sediment record to evaluate the effectiveness of differing reclamation techniques for minimizing runoff and erosion. The timing and magnitude of the erosional pulse from lands cleared and then reclaimed using FRA and conventional reclamation are comparable; whereas fundamental differences exist between the nature of sediments shed from control (unmined/unreclaimed) sites versus sites reclaimed by either FRA or conventional reclamation, reflecting the much longer timescales required to effect recovery in terms of sediment types and post reclamation.
3. Compare water quality attributes across a variety of surface-mine reclamation strategies, including conventional grassland reclamation, Forestry Reclamation approach (FRA), and unmined forests to assess FRA effectiveness for water pollution control.

4. Model annual evapotranspiration (AET) at the watershed scale under differing reclamation strategies, including those listed above using input variables collected from objective 1.

Major findings from the study include:

1. Canopy interception and throughfall in FRA plots followed expected trends for non-mined maturing forests. Interception rates varied with tree type and age with 10- and 20-year old FRA coniferous stands exhibiting about 44% and 40% of rainfall, respectively. The lowest interception rate (6%) occurred with 10-year old FRA deciduous plots that had not achieved canopy closure. Interception rates for the 20-year old FRA deciduous trees that had achieved canopy closure, however, were equivalent to those for the non-mined 100-year forest stand. Due to self-thinning, the 100-year forest stand had lower interception and higher throughfall than the 20-year FRA stands and the 10-year coniferous stand. Because mean annual streamflow is inversely related to interception, it is hypothesized that mined watersheds reforested using the FRA will exhibit decreased water yields for at least 20-40 years before experiencing a steady flow rate as the forest matures.
2. Grain size analysis and radionuclide data provided data for understanding the complex erosion, sediment transport and depositional processes following coal mine reclamation in eastern Kentucky. The Guy Cove watershed, which was logged in the 1920s, mined in the mid-1990s and reclaimed using the FRA in 2008, showed an increase of sediment loading due to the logging followed by a gradual reduction in sediment load as the forest regenerated. Sediment loads increase due to the mining, but significant reductions have occurred through the reclamation period. The most recent few years, during a period where canopy closure was achieved, exhibit the lowest sediment deposition rates of the record. It is likely that a reduction in throughfall (increased interception as explained above), an increase (presence of) in the thickness of the litter layer, and a lower erosive energy of precipitation hitting the forest floor have slowed erosion in the watershed.
3. Stream and watershed functions were restored on a valley fill (Guy Cove) using natural channel design and FRA. After 10 years, tree growth and survival are quite good for most species, particularly in the uplands. By 2019, canopy closure was evident across the entire watershed. The state of the young forest should greatly influence the hydrology of the watershed through increased canopy interception and increased evapotranspiration. On the portion of the main channel located on the crown, water quality has improved greatly (99, 89 and 53% reduction in Mn, sulfate and EC, respectively). Overall water quality in the watershed has also exhibited considerable

improvement (92, 85 and 49% reduction in Mn, sulfate and EC, respectively). EC levels in the 760-m section on the crown have remained below 500 µS since 2017.

4. Saturated hydraulic conductivity (Ksat) measurements and soil physical analysis indicated that the conventionally reclaimed grassland site had the lowest total porosity and a relatively high field capacity, which resulted in a soil profile that cannot efficiently move water in the sub-surface during precipitation events. Modeled potential evapotranspiration and streamflow from this site resulted in a flashy hydrology with little to no baseflow between storms. Ksat on FRA soils were higher at the 0 to 20-cm depth than the 20-40-cm depth, which suggest that water can infiltrate but slows as it moves into the deeper soil profile. Because of the lower porosity and Ksat with depth, models for each of the mine reclamation strategies resulted in a more water limited environment for plant growth and flashier streamflow. Projected climate conditions were examined in order to understand if hydrologic changes from mine-reclamation might be exacerbated during the coming century. Projected water limitations due to increased temperatures from climate change suggest that FRA sites could experience increased soil-water deficits in summer months that would lead to decreased streamflow and plant-available water.

I.I. OVERVIEW

In the steep sloping hills of central Appalachia, water resource issues abound. Whether the culprit is coal mining, timber harvesting, straight piping of sewage or any number of construction or agricultural activities, discussing the impact of land use on water quality and quantity in the region is often emotionally, and sometimes politically, fueled. Natural resource extraction (coal, gas, timber) has been the primary economic driver in the region for over a century. Although these activities provide jobs and revenue, degradation of water quality and compromised water supplies from resource extraction are regularly documented. Linked with the consequences of global climate change, the status of the region's water resources for the foreseeable future are unknown. Management solutions developed to protect water resources from these issues are needed. The University of Kentucky's Robinson Forest provides an ideal setting to examine impacts of land-use on water resources. The forest contains a hydrologic network that has been continuously monitored since the early 1970s. Additionally, resource extraction in the form of timber harvesting and surface coal mining have occurred on the site resulting in a myriad of land disturbance types and time-since impacted. Thus, we have the capability to examine how recent mining and reclamation practices (with sites ranging from 1 to 20 years since planted) may be affecting forest regeneration and its influence on watershed function (annual streamflow, storm flow response, evapotranspiration, water chemistry, erosion). We also have the ability to examine what measures could be employed to minimize

these effects, for example, implementing the Forestry Reclamation Approach. Lastly, we can utilize climate and forest range modeling techniques to examine the recovery (restoration or natural regeneration) of forest stands and watershed function at the watershed scale. A better understanding of how land-use and restoration influence water resources in the region will allow us to predict and prepare for associated economic, environmental, social, and/or infrastructure costs that may arise in response to change.

Background

Mixed hardwood forests of the Appalachian region provide valuable ecosystem services, not the least of which is maintenance of freshwater resources. Unfortunately, Appalachian forests are threatened by a variety of short- and long-term pressures, including climate change, invasive species expansion, and resource extraction. Surface mining for coal is one of the most important drivers of land use change in the Appalachian region, reducing native forest cover, causing forest fragmentation, and eliminating native soil (Wickham et al. 2013). In addition to these significant impacts to terrestrial ecosystems, surface mining impairs the region's valuable water resources. A widening body of literature implicates surface mining, even after reclamation, in long-term water quality impacts including impaired chemistry (Bernhardt et al. 2012; Lindberg et al. 2011) and altered macroinvertebrate assemblages (Pond et al. 2008; Pond 2010). Surface mining has also been linked to alterations in hydrological function, typically related to a combination of drastically reduced infiltration rates (due to heavy soil compaction) and reduced evapotranspiration (ET) rates (Negley and Eshelman, 2006). The solution to some of these problems may lie in improved mine reclamation techniques.

Recently, an interdisciplinary team of researchers, practitioners, and regulators formed the Appalachian Regional Reforestation Initiative (ARRI) and developed the Forestry Reclamation Approach (FRA) (Burger et al., 2005; Adams, 2017). The FRA has been found to be successful in establishing native hardwoods on surface mined land throughout the region (e.g. Zipper et al., 2011). In addition, research suggests that heavy compaction on conventionally reclaimed surface mines can be mitigated using a bulldozer with a ripping shank (e.g., Burger et al., 2013). Compaction-mitigated sites can also be successfully reforested to native mixed-mesophytic forests. Although the FRA has been thoroughly tested for utility in reforestation, few studies have investigated the potential for FRA techniques to reduce long-term water quality, hydrology and erosion issues associated with surface mining and conventional reclamation.

Native forest systems are characterized by a complex water budget and understanding natural forest hydrology is critical for restoring natural hydrologic cycling to a disturbed system. In a natural unmined watershed, water enters the forest as precipitation (Figure 1). Some

precipitation is intercepted by trees, litter, and other vegetation before reaching the mineral soil (termed “interception”). Interception rates in hardwood forests vary with season (lower interception during the dormant season) and forest composition (e.g., coniferous vs. various hardwood forest types). A portion of interception is evaporated from the canopy and does not reach the forest floor (termed “canopy interception loss”). An additional portion of interception flows along the tree stems and trunk directly to the soil (termed “stemflow”). The portion of interception that falls through the canopy and reaches the forest floor is termed “throughfall.” Throughfall can be further intercepted by the litter layer, a portion of which will be evaporated (termed “litter interception loss”). These processes have been well-studied in eastern forests and equations are available to estimate throughfall and stemflow from precipitation of natural stands (e.g., Helvey and Patric, 1965).

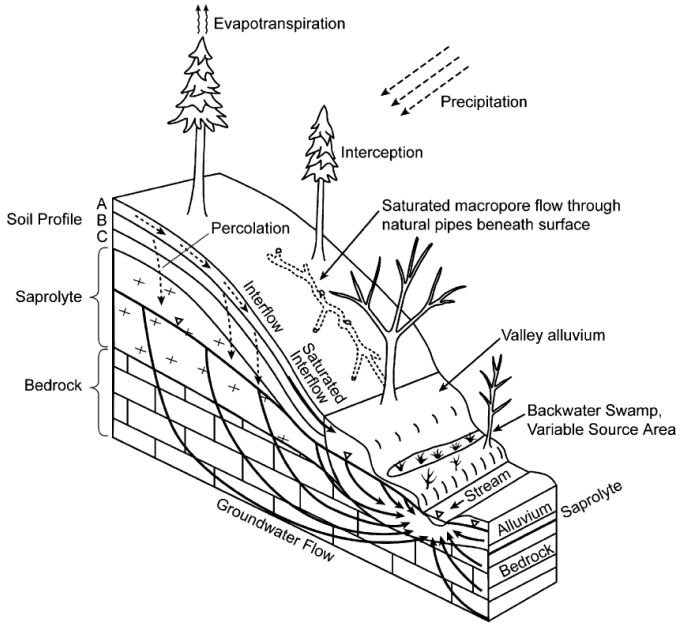

Figure 1: Hydrologic cycling in a native forest system, figure from Neary et al., 2009.

Water that reaches the mineral soil, termed net precipitation, seeps into the soil (infiltration), with some percolating further into the soil to recharge groundwater storage or move laterally (interflow) downslope towards streams. Soil water is taken up by trees and other vegetation and is transpired into the atmosphere in combination with water evaporating directly from soil and water-body surfaces (evapotranspiration; ET). Water also follows subsurface flowpaths, formed by a combination of soil structure and rooting patterns. In natural forest systems, rainwater primarily flows via these subsurface flowpaths and interflow into stream channels (Figure 1). Overland flow on the land surface does not contribute significantly to unaltered stream systems except in extreme cases in which storm events are particularly intense or soil infiltration rates are particularly low (Neary et al. 2009).

In a traditionally reclaimed site (grassland) many components of the natural forest's hydrologic cycle are altered due to the lack of canopy cover and changes to physical properties of the soil. Canopy interception (and interception loss) are expected to be lower in conventionally reclaimed sites due to less structural complexity of the canopy (fewer layers of vegetation and less surface area). Soils at conventionally reclaimed sites tend to be compacted by design, thus limiting infiltration, pore space to store water for plants and enable water movement, and rooting volume. The combined influences result in reduced subsurface flow and ET, in exchange for increased overland flow, flashier storm response, and potentially increased erosion and sedimentation (Miller and Zegre, 2014). Reclamation using FRA should (with time and forest development) provide a canopy that functions similar to a natural forest and provide soil that promotes infiltration and water storage, which can be utilized by tree roots (Sena et al., 2014; Taylor et al., 2009). As such, use of FRA should result in higher ET over reclaimed grasslands, including accessing deeper soil layers and building a network of larger pores, providing a higher ability of the basin to buffer storm events. In theory, restoration of the forest will restore lost hydrologic function with regards to water use and cycling.

Similarly, the return of the forests should also aid in the recovery of lost ecosystem functions (including those that provide ecosystem services regarding air, water and soil quality). Unfortunately, few studies have tried to confirm or negate these hydrologic interactions. Moreover, the FRA is a relatively new concept (in terms of forest growth) so sites that are old enough to conduct these types of experiments have only recently become available.

TESTING THE FORESTRY RECLAMATION APPROACH

Surface mine reclamation in the U.S. is regulated under the Surface Mine Control and Reclamation Act (SMCRA) of 1977, part of which was aimed at reducing the threat of erosion and landslides from surface-mined sites throughout the steeply sloped Appalachian region, like that in Robinson Forest. Reclamation under SMCRA, through years of interpretation and enforcement, eventually matured into what is now considered traditional or conventional surface mine reclamation in the region, characterized by heavy "mine-soil" compaction and final land-uses of pasture/grassland or wildlife habitat (grassland/shrublands). Altered, and sometimes damaging, stream response, characterized by high peak flows after rain events and higher mean annual discharge, has been linked both to reduced ET due to replacement of forest with herbaceous vegetation (Hornbeck et al. 1970) and reduced infiltration due to soil compaction (Ritter and Gardner 1993). In the U.S., Ferrari et al. (2009) modeled flood response in surface mined land in Virginia and observed that flood magnitude increased with increased surface mined area. In other studies, forestry operations that remove forest cover were found to increase overall water yield, but not increase flood volume (Witt et al., 2015). Thus, the

heavy compaction associated with typical surface-mine reclamation produced a flashier hydrograph, with a higher peak and smaller recession that resulted in the same total volume of water in response to the same precipitation event. Another study in Maryland (Negley and Eshleman 2006) found that storm-event runoff from a watershed influenced by surface mining was significantly higher than runoff from an undisturbed forested watershed. The authors attributed this difference in storm response to heavy compaction on the surface-mined watershed, which reduced infiltration rates from 30 cm/hr in the reference basin to < 1 cm/hr in the surface-mined basin.

A clear biological indicator of water toxicity associated with surface mining is macroinvertebrate community impairment. Pond et al. (2008) found that sensitive macroinvertebrate taxa were largely extirpated from streams draining surface mines. Subsequent research continues to identify strong correlations between mining and water quality impairment (e.g., elevated specific conductance (EC), SO_4, Se) (Lindberg et al. 2011). Also, researchers continue to implicate mine drainage in declines of sensitive macroinvertebrate taxa and salamanders in eastern Kentucky headwater streams (Pond 2010, 2011; Muncy et al., 2014) and altered biofilm function/development in southeast Ohio (Smucker and Vis 2011). Finally, Hopkins et al. (2013) confirmed that these effects (elevated EC, SO_4, Al) can be observed even in streams draining legacy mine sites long after conventional reclamation (>10 years).

FRA has been demonstrated to be successful at reforestation on Appalachian rcoal mines. However, very little is known about how FRA techniques influence long-term water quality, hydrology, or sediment erosion on reclaimed sites. In a column-leaching study of mine spoils, Orndorr et al. (2015) found that EC and concentrations of specific ions declined rapidly over the first few leach cycles. Similarly, Sena et al. (2014), working on 1-acre experimental FRA test plots in eastern Kentucky, found that EC of interflow decreased to the 300-500μS/cm threshold identified by Pond et al. (2008) as a critical threshold for macroinvertebrate community integrity within nine years of plot construction. On these same plots in Kentucky, Taylor et al. (2009) found that surface runoff was not a significant component of the water budget, and that runoff curve numbers were similar to undisturbed forest sites. Nine years after plot establishment, Sena et al. (2014) found an ET effect on water budgeting, with lower interflow from treed plots during the growing season than the dormant season. However, we have not found any studies evaluating influence of FRA techniques on water resources at the watershed scale.

FRA leaves a ~1.5-m deep surface layer of loose spoils and top soil, which is leveled under dry conditions with as few passes as possible. SMCRA mandates back-to-contour spoil placement to

approximate natural slopes, which in this region exceed 20% in many locations. Assessing how FRA as applied to steeply sloping terrain relates to soil and sediment erosion and sediment yields is a critical research need. While a body of literature exists on the relation between traditional mine reclamation methods and soil erosion (e.g., Toy 1989; Loch 2000; Sheoran et al. 2010), there has been little research to date on the FRA approach and soil erosion.

Headwater stream systems are also significantly impacted by surface mining. For example, surface mining results in the production of excess spoil or overburden, which is often placed in adjacent valleys resulting in the creation of valley fills. These valley fills bury headwater streams which in turn can negatively impact downstream ecosystems. Restoring headwater stream systems and their ecosystem services requires an understanding of the interconnectedness of hydrologic, geomorphic and ecological processes (Kauffman et al., 1997). As seen in the Stream Function Pyramid, restoration of aquatic communities occurs when the more basic functions of hydrology, hydraulics, geomorphology and physiochemistry have been restored (Harman et al., 2012). According to Harman et al. (2012), the foundation of restoring streams involves reestablishing hydrologic functions such as precipitation-runoff relations and flow duration. Recent research on stream restoration on mined lands at the University of Kentucky's Guy Cove suggests that FRA can play a vital role in reestablishing storm event hydrology (Blackburn-Lynch, 2015).

Previous work involving this hydrologic modeling approach evaluated streamflow, soil-water storage, and streamflow permanence. The Cumberland Plateau was included in regional calibration of the Kentucky Water Availability Tool for Environmental Resources (WATER) decision support system (DSS). Robinson Forest was one of two Kentucky field sites used to simulate soil-water movement and storage (Williamson et al., 2015a,b). Recently funded work integrates samples from the Natural Resources Conservation Service's (NRCS) National Rapid Carbon Assessment (RaCA) in order to extend this hydrologic modeling to a larger geographic area and frame the results in the context of agricultural resiliency for a 30-yr, normalized record centered on 2050 (Baker et al., 2015). Work supported by the USGS Water Census (Williamson et al., 2015b) validated ET estimates for a mixed forest community using a mix of Ameriflux and Soil-Surface Energy Balance simulations (Senay et al., 2013) for the Delaware River Basin (DRB) with the intention of understanding water availability given projected changes in climate (Frumhoff et al., 2007). In each case, the hydrologic model is being used to understand the effects of climate and land-use change by integrating Coupled Model Intercomparison Project (CMIP) general circulation model (GCM) data using a change-factor approach for precipitation, temperature, and potential evapotranspiration (PET). This research will further improve our ability to simulate the water budget that controls streamflow in forested regions that provide drinking water to large portions of the U.S., including populations that are geographically

isolated from alternative sources. The encapsulation of this hydrologic modelling approach (WATER) in a DSS that is already used by regulators and resource managers in several states ensures transferability of this knowledge to objectively consider how land-use, and reforestation (FRA) might affect streamflow and water availability.

Working to consistently improve reclamation approaches on surface coal mining sites in mountainous regions is critically important for many reasons, including the mitigation of environmental impacts derived from excessive landscape erosion (Carroll et al. 2000; Espigares et al. 2011), and down-slope geomorphic adjustments (e.g., Jaeger 2015). To better promote native forest regeneration, FRA has become widely utilized in the Appalachian region, and works in part by delivering minimally-compacted spoils to the landscape to improve reforestation success (Zipper et al. 2011.). Numerous studies have utilized standard plot methods to quantify the soil erodibility of surface mining reclamation sites by employing the Revised Universal Soil Loss Equation (RUSLE) (e.g., McIntosh and Barnhisel 1993; Toy et al. 1999). RUSLE enjoys widespread use in predicting annual soil loss per unit area, and does consider varying soil properties, land surface conditions, and management practices. However, there are often differences between what RUSLE will predict in terms of soil erodibility, and what actual sediment yields are, and these differences are undoubtedly related to two major sources of uncertainty, (1) actual landscape heterogeneity not captured by the model, and (2) assumptions required for RUSLE that minimize or over-simplify actual geomorphic processes that contribute to erosion (e.g., Kinnell 2005, 2008; Parsons et al. 2006; Rejman et al. 1999).

The focus here is to utilize sediment cores collected from depositional environments located downstream from three sub-catchments with different mining and reclamation histories (unmined [control], conventionally reclaimed, and FRA) to quantify how sediment yields from these areas have changed over time. Approaches including the use of sediment cores (which will provide data on sediment composition, texture [grain size], organic carbon content, and radionuclide activities [^{7}Be, ^{137}Cs, ^{210}Pb]), have been successfully employed in a range of watersheds to assess basin sediment budgets and yields and their changes over time (e.g., Walling 1999; Wilkinson et al. 2009; Porto et al. 2009, 2011).

1. EVALUATING THE INFLUENCE OF THE FORESTRY RECLAMATION APPROACH ON CANOPY INTERCEPTION AND THROUGHFALL

1.1 INTRODUCTION

1.1.1 Appalachian Region

The Appalachian region covers about 531,000 km^2, including all of West Virginia and parts of Alabama, Kentucky, Ohio, Pennsylvania, and Virginia (ARC,2019). The rugged terrain is dominated by mixed mesophytic forest of oak (*Quercus* sp.), yellow poplar (*Liriodendron tulipfera*), hickory (*Carya* sp.), and American Beech (*Fagus grandifolia*) (Braun, 1950; Carpenter and Rumsey, 1976). The landscape is "mature" with a dense stream network that dissects the region coupled with high topographic relief (Davis, 1899). Underlain by Pennsylvanian sandstone, shale, siltstone, and coal parent material, soils are thin with limited fertility (Smalley, 1984; Kalisz et al., 1987). Coal mining is common in the region as is agriculture in the valleys.

1.1.2 Coal Mining – Historical Context

Numerous environmental problems, such as landslides, erosion, flooding, instream sedimentation, and poor water quality, prompted Congress to enact the Surface Mining Control and Reclamation Act (SMCRA) of 1977. These problems were largely associated with essentially unregulated mining and reclamation methods. For instance, operators commonly used the "shoot and shove" method whereby operators blasted rock to reach the coal seam and then pushed spoil over the edge of the bench. This practice created unstable outslopes and exposed high walls, some exceeding 100 ft in height (Zipper, 1990; Haering et al., 2004).

After the enactment of SMCRA, regulators focused on regrading to achieve land stability and approximate original contour (AOC) while reducing erosion and subsequent sedimentation of streams (Angel et al., 2005). This "mining-grading- topsoiling" mindset resulted in highly compacted lands planted with fast-growing herbaceous vegetation (Smith, 1980; Graves et al., 2000; AGI, 2006; Zipper et al., 2011). Trees, which were once planted at similar rates as grasses, in states such as Kentucky, gave way to grasses and legumes (Brothers, 1990). Tree survival on compacted lands, and in the face of fierce competition from herbaceous vegetation, was poor (Skousen et al., 2009; Zipper et al., 2011). Economically, hand planting trees was laborious and more costly than sowing grasses by mechanical means such as hydroseeders or airplanes. The reduced costs of planting grasses were balanced the increased grading costs (Brothers, 1990). Socially, the less steep and more easily traveled landscape of the graded grassed lands was appealing to many landowners (Smith, 1980). Grasses, which grow more quickly than trees,

allowed operators to meet reclamation bonding requirements within the required short term (e.g., five-year period, 90% ground cover) (Roberts et al., 1998; Holl et al., 2009; USEPA, 2011).

Even with the decline in coal production, surface coal mining is a major industry in northern and central Appalachia accounting for up to 20% of employed persons in some Kentucky and West Virginia counties (Ruppert, 2001; Bowen, 2018). As of 2008, coal extraction under the U.S. Surface Mining Control and Reclamation Act (SMCRA) had occurred on more than 600,000 ha (6,000 km^2) of the region with two-thirds in the Central Appalachian states of Kentucky, Tennessee, Virginia, and West Virginia (Zipper et al., 2011; Pericak, 2018). Since the early 1970's, the Central Appalachian region has experienced more than a 9% change in land use, predominately associated with an increase in coal mining, decrease in forested area, and an increase in grasslands/shrubs (Townsend et al., 2008; Sayler, 2016). The increase in grasslands/shrubs reflects the conversion of previously active mines to reclaimed or abandoned ones.

1.1.3 Hydrologic Impacts

Converting a forested watershed to a grassed one, even without the complicating factors of soil compaction, alters ecosystem functions such as nutrient cycling, water storage, carbon sequestration, habitat provision, and temperature moderation (Saunders et al., 1991; Osborne and Kovacic, 1993; Mao and Cherkauer, 2009; Zipper et al., 2011). Hydrologic processes such as interception, infiltration, evapotranspiration, and runoff are altered due to changes in vegetation type (Negley, 2006; Sena et al., 2014) and increased soil compaction from heavy equipment operations used to regrade the mine spoil (Wells et al., 1983; Jorgensen and Gardner, 1987; Hoomehr et al., 2005; Simmons 2008; Ferrari, 2009). Conversion of forested lands to mined and then grasslands, has been shown to increase both runoff volumes and peak flows (Negley, 2006; Taylor et al., 2009), negatively impact receiving streams (Wiley and Brogan, 2003; Miller and Zégre, 2014). Increase runoff volumes and peak can also result in eroded streambanks, incised channels, and homogenous streambeds (Booth, 1990; Rhoads, 1995).

Forests play a critical role in managing how water moves across the landscape. Forested canopy has the potential to intercept nearly 25% of the precipitation associated with a storm depending on tree age and type; storm depth, duration, and intensity; and wind speed (Jackson, 1975; Miralles et al., 2010). Llorens et al. (1997) found that a 33-year old pine forest (Pinus sylvestris) in the Mediterranean mountains of Spain intercepted, on average, 24% of rainfall over a 30-month period with a maximum rate of 49%. Bryant et al. (2005) measured

interception rates ranging from 17-22% in five forest types (pine, mixed forest, lowland hardwood, pine planation, and upland hardwood) in Georgia. Diego et al. (2010), using the Climate Prediction Center morphing technique (CMORPH) precipitation product and the Gash analytical model, determined that needleleaf forests intercepted 22% of rainfall followed by broadleaf deciduous forests at 19% and then broadleaf evergreen forests at 13%. In a review of the literature, Levia et al. (2006) noted that between 77-83% of rainfall becomes throughfall in deciduous forests while coniferous forests display a wider range of 47-91%.

Prior work suggests interception and throughfall rates are linearly correlated with rainfall depth with greater interception rates occurring for small storms meaning greater throughfall rates occurred for larger ones (Helvey and Patric, 1965; Pressland, 1973, Carlyle-Moses, 2004). Pressland (1973) noted that rainfall duration is also correlated with interception rates. Tanaka et al. (2015) noted that rainfall depth and duration account for nearly the entire throughfall rate during the leafing and leafed phases of teak trees.

1.1.4 Reforestation

Forests in the Central Appalachians rank as one of the world's most diverse non-tropical ecosystems (Ricketts et al., 1999; Zipper et al., 2011). These forests provide habitat to numerous plants and fauna, sequester carbon, reduce runoff peaks and volumes, and protect water quality (Wickham et al., 2007; Ricketts et al., 2009). Post-SMCRA reclamation techniques, which promoted the conversion of forests to grasslands, resulted in the loss of these forested ecosystem services. The use of heavy earthwork equipment to grade and compact spoils resulted in low tree growth and survival, low infiltration rates, increased peak flows, and increased runoff volumes (Bonta et al., 1997; Bradshaw, 1997; Graves et al., 2000; Guebert and Gardner, 2001; Shukla et al., 2004; Skousen et al., 2009).

The Forestry Reclamation Approach (FRA) is a prescription for reclaiming mined lands in such a way as to promote tree growth while addressing pre-SMCRA concerns of land stability, erosion, and sedimentation concerns (Angel et al., 2005; Zipper et al., 2011). The FRA consists of five steps:

1. Create a suitable rooting medium, at least 1.5 m (4 ft) deep, using topsoil, weathered sandstone, and/or best available material.
2. Minimize compaction by only loosely grading rooting medium.
3. Minimize competition by using tree-compatible ground covers.
4. Plant early successional trees for wildlife and soil stability and commercially valuable crop trees.
5. Use proper tree planting techniques.

Angel et al. (2005) and Zipper et al. (2011) provide details and research supporting each step. The Office of Surface Mining, Reclamation and Enforcement, through the Appalachian Regional Reforestation Initiative, provides Forest Reclamation Advisories to address questions related to reclaim coal mined lands for forested post-mining land uses.

Research indicates that FRA is effective at promoting tree growth and survival (Graves et al., 2000; Skousen et al., 2009; Sena et al., 2015), accelerating soil development (Miller et al., 2012; Sena et al., 2018), improving water quality (Agouridis et al., 2012; Daniels et al., 2016), and restoring hydrologic response in the form of reduced peak flows and runoff volumes (Taylor et al., 2009a, 2009b; Sena et al., 2014).

Due to the short time that FRA has been in practice (e.g., less than 25 years), the literature lacks direct comparisons between mature FRA forests and mature non-FRA forests. However, in mature non-FRA forests, studies have investigated the changes of throughfall and runoff (Haydon 1995), evapotranspiration (ET), water yield (Cornish 2001), and macropore development (Colloff 2010). Colloff (2010) found that macropore development and infiltration increased over time after reforestation of agricultural lands. Haydon (1995) found that interception and runoff had an inverse relationship that changed with the age of a mountain ash forest recovering from forest fire; canopy interception peaked around 30 years of forest maturity before declining. Cornish (2001) studied the water yield of a eucalypt forest following logging and found that water yield first increased and then declined past pre- logging levels over the 16-year study.

While these hydrologic changes were attributed to a number of factors as trees aged including increases in water use by growing trees, it may also be related to self-thinning of the forest causing a reduction in canopy cover. Self-thinning is a natural process by which larger trees outcompete smaller trees resulting in fewer trees per area as the tree biomass increases with stand age. A mature forest in Appalachia, such as that at Robinson Forest, has a tree density of around 150 trees per acre. With FRA, the recommended planted tree density is 700 trees per acre. This assumes an initial 70% survival rate on mine sites resulting in 490 trees per acre. Because of the young age of FRA, it has yet to be determined if these plots will experience self-thinning similar to that of natural forest regrowth.

1.1.5 Objectives

Until now, no studies existed evaluating interception (and hence throughfall) rates associated with trees grown using the FRA – prompting many questions. At what point do trees planted in

accordance with FRA guidelines begin to intercept rainfall at rates similar to mature forests? How does tree type, coniferous versus deciduous, influence interception? This latter question has important implications for watershed managers in light of climate impacts such as the northern migration of trees species (Woodwall et al., 2009; Lafleur et al., 2010) and changing rainfall patterns (Dore, 2005) as well as potential land management changes such as the establishment and harvesting of woody biomass plantations (Xu et al., 2002).

The objective of this study was to evaluate the effect of the FRA on precipitation throughfall by comparing 10-, 20-, and 100-year old tree plots consisting of coniferous or deciduous trees. Understanding how throughfall amounts vary with tree age and type is critical to characterizing the environment created by individual reclamation strategies and managing post-mined landscapes to address critical watershed functions associated with water quantity and quality.

1.2 METHODS

1.2.1 Study Site

The research project was conducted at the University of Kentucky's Robinson Forest and the Starfire Mine (currently Little Elk Mine) which are in southeastern Kentucky in the Cumberland Plateau section of the Appalachian Plateaus province of the Appalachian Highlands (Figure 1.1). These adjacently located study sites are situated in the Appalachian mixed mesophytic forest region, which is characterized by hills and valley with elevation differences ranging from 385 to 610 m (Smalley, 1986). The average annual rainfall is 118 cm and the climate is humid and temperate with daily mean summer temperatures ranging from 30 to 18°C and winter temperatures ranging from -5 to 6°C (Cherry, 2006; USDC, 2002). Weather is highly variable throughout the year with long periods of low intensity rainfall during the winter months and high intensity storm events that typically occur during the summer and early fall months (Husic et al., 2019).

Robinson Forest (latitude 37.450° N, longitude 83.183° W) is an approximately 6,000 ha research and teaching forest that consists of a main block approximately 4,200 ha in size and seven other discontinuous areas. The forest is characterized by steep-side slopes, averaging 45%, coupled with a hydrologically restrictive geologic layer consisting of interbedded sandstone, siltstone, shale, and coal (McDowell et al., 1981). Robinson Forest was clear cut between 1890 and 1920 with subsequent mixed-mesophytic forest regeneration dominated by oaks (*Quercus* spp.), hickories (*Carya* spp.), and yellow poplar (*Liriodendron tulipifera* L.) (Overstreet, 1984; Witt, 2012; Villines et al., 2015).

Starfire Mine (latitude 37.400° N, longitude 83.117° W) is in Perry and Knott Counties. Since the early 1980s, the mine has operated as a mountain-top removal operation whereby multiple coal seams were extracted using dragline and truck/shovel techniques (Barton et al., 2017). Most of this area was reclaimed as hay and pastureland on compacted spoils, using traditional techniques. In 1996 and 1997, 1-ha reclamation cells were created overtop reclaimed mined land by utilizing spoil (non-acidic shale and sandstone overburden) from the active mining operation (Angel et al., 2006). Spoil was placed in accordance with the FRA (Burger et al., 2005; Zipper et al., 2011), and the site was planted with eastern white pine (*Pinus strobus*), white ash (*Fraxinus Americana*), black walnut (*Juglans nigra*), yellow poplar, white oak (*Quercus alba*), and northern red oak (*Quercus ruba*) 1-year old nursery stock bare root seedlings (Angel et al., 2006).

1.2.2 Treatments

Treatments were comprised on 10-, 20-, and 100-year old coniferous and deciduous tree plots located at either Robinson Forest or Starfire Mine. Tree plots were established as monocultures. A "traditional" or grass-only plot was established at Starfire Mine adjacent to the 20-year old plots; this area had been in grassland also for 20-years. For this study, each plot was 10 m x 10 m in size.

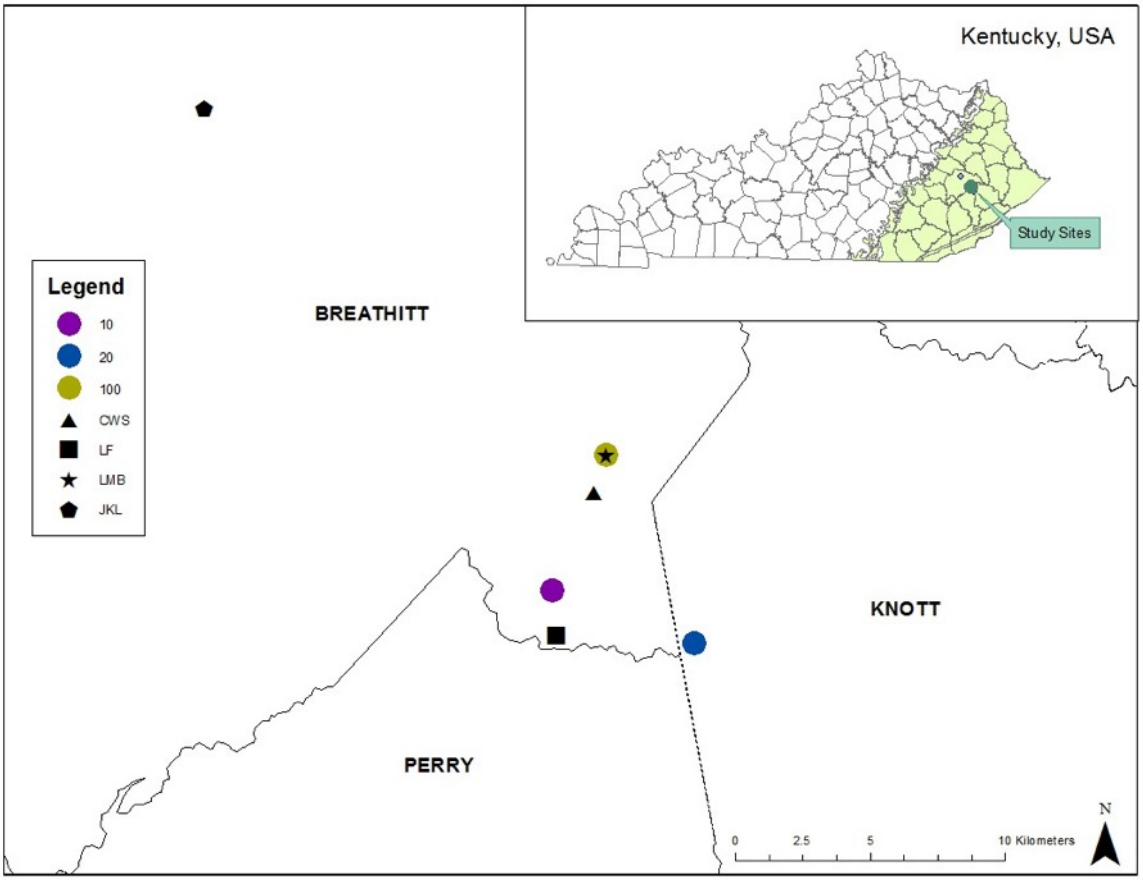

Figure 1.1. Tree plots are in eastern Kentucky (shaded area indicates Appalachian Plateaus physiographic province) near the intersection of Breathitt, Perry, and Knott counties. 10=10-year-old plots, 20=20-year-old plots, 100=100-year-old plots, CWS=Camp weather station, LF=Laurel Fork weather station, LMB=Little Millseat Branch weather station, and JKL=Jackson National Weather Service weather station.

1.2.2.1 10-year Old Plots

The 10-year old tree plots (37.428° N 83.177° W) were established on an 810-ha section of Robinson Forest that was mined during the mid-1990s. The site was ripped, in accordance with FRA No. 4 (Sweigard et al., 2007), and subsequently planted in 2007. The coniferous plot, used in this study, contained 25 loblolly pines while the deciduous plot contained ten red oaks (Table 1.1, Figures 1.2-1.3). Autumn olive (*Elaeagnus umbellate*) has invaded the understory of the deciduous plot but not the coniferous one. The estimated overstory density, as measured by a Model-A spherical densiometer in June 2017, was 97% for the coniferous plot and 61% for the deciduous plot.

Table 1.1. Number of trees and equivalent density per plot.

Plot[1]	No. of Trees	Density (trees/km2)
10C	25	2,500
10D	10	1,000
20C	21	2,100
20D	32	3,200
100C	17	1,700
100D	21	2,100
Traditional grassland	0	0

[1]10C=10 year coniferous, 10D=10 year deciduous, 20C=20 year coniferous, 20D=20 year deciduous, 100C=100 year coniferous, 100D=100 year deciduous, and traditional = grass only.

Figure 1.2. The 10-year old coniferous tree plot contained 25 loblolly pines. Photo courtesy of Matt Barton, University of Kentucky, Agricultural Communications Services.

Figure 1.3. The 10-year old deciduous tree plot contained ten red oaks and had a thick understory dominated by autumn olive (*Elaeagnus umbellate*).

1.2.2.2 20-year Old Plots

The 20-year old tree plots (37.410° N 83.118° W) were established and planted at Starfire Mine in 1997. The coniferous plot contained 21 white pines while the deciduous plot contained 32 white oaks (Table 1.1, Figures 1.4-1.5). The estimated overstory density, as measured by a Model-A spherical densiometer in June 2017, was 94% for the coniferous plot and 96% for the deciduous plot.

Figure 1.4. The 20-year old coniferous plot contained 21 white pines.

Figure 1.5. The 20-year old deciduous tree plot contained 32 white oaks.

1.2.2.3 100-year Old Plots

The 100-year old non-mined tree plots (37.473° N 83.153° W) were established in the Little Millseat watershed which is a 77.9 ha watershed located in the main block of Robinson Forest. Elevations in the watershed range from 304 m to 451 m. The watershed is characterized by steep slope (25-60%), dense drainage network (drainage density of 0.0038 m m^{-2}), and a narrow valley with well-drained soils (Hayes, 1991; Cherry, 2006). The coniferous plot contained 17 eastern hemlocks (*Tsuga Canadensis*) while the deciduous plots each contained 21 white oaks (Table 1.1, Figure 1.6-1.7). The estimated overstory density, as measured by a Model-A spherical densiometer in June 2017, was 93% for the coniferous plot and 95% for the deciduous plot.

Figure 1.6. The 100-year old coniferous tree plot contained 17 eastern hemlocks.

Figure 1.7. The 100-year old deciduous tree plots contained 21 white oaks.

1.2.2.4 Traditional Grassland

A non-forested plot was established on a 20-year old traditionally reclaimed section of Starfire Mine adjacent to the 20-year old tree plots. Reclamation was conducted in accordance with the Surface Mining Control and Reclamation Act of 1997 resulting in a highly compacted surface dominated by tall fescue (*Festuca arundinacea*) and sericea lespedeza (*Lespedeza cuneate*) (Figure 1.8). During the summer months, the grasses grew to a height of approximately 1.1 m which was greater than the height of the rain gauges. The control plot was not used in the statistical analyses (Section 1.2.4) but was used to validate precipitation measurements.

Figure 1.8. The control plot was dominated by grasses such as tall fescue and sericea lespedeza.

1.2.3 Hydrologic Data

Precipitation data were obtained from three University of Kentucky weather stations (Camp, Little Millseat, and Laurel Fork) and the National Weather Service's Jackson, Kentucky weather station (JKL, latitude 37.592° N, longitude 83.316° W). The Camp (CWS, latitude 37.461° N, longitude 83.159° W), Little Millseat (LMB, latitude 37.473° N, longitude 83.153° W), and Laurel Fork (LF, latitude 37.413° N, longitude 83.176° W) weather stations are all within 7.5-km radius of all the tree plots (Figure 1.1). The JKL weather station is about 20 km from the closest tree plot and 25 km from the furthest. At the CWS and LMB weather stations, precipitation data were recorded at 15-min intervals while precipitation data were recorded at 60-minute intervals at LF and 5-min at JKL. All University of Kentucky weather stations used a tipping bucket rain gauge linked to a Campbell Scientific CR10X data logger to collect precipitation data (Cherry, 2006). To reduce the effect of local random errors associated with tipping bucket rain gages, storm event data from all four weather stations were averaged (Ciach, 2002). Repeated measures ANOVA on Ranks were used to compare storm event depths and durations between the weather stations as well as the average of all four weather stations.

Twelve stands, with a 46 cm x 46 cm platform, were randomly distributed in each tree plot (Helvey and Patric, 1965; Bryant et al., 2005; Levia and Frost, 2006). Each platform stand was

located 61 cm above the ground surface. A Rain Collector II tipping bucket rain gage (Davis Instruments, Haywood, CA, USA) equipped with a Hobo Event Data Logger (Onset Computer Corporation, Cape Cod, MA, USA) was located atop each platform. The rain gages were used to record throughfall timing and depth. Rain gages were mounted on the corner of each stand. Biweekly, rain gages were rotated clockwise around the stands to account for variations in canopy coverage to provide a more accurate representation of throughfall throughout the tree plots (Helvey and Patric, 1965; Lloyd, 1988; Bryant et al., 2005; Levia and Frost, 2006). Prior work indicated stemflow accounted for less than 2% of net rainfall, and as such, this parameter was not measured (Lorens, 1997). Though evaporation rates were not measured in this study, other researchers have found that this type of funneled rain gage looses between 0 and 4% of captured throughfall to evaporation (Thimonier, 1998).

Throughfall data were collected for a one-year period (May 18, 2017 to May 19, 2018). For each storm event, throughfall depths from all twelve rain gages (throughfall stands) within each plot were aggregated to determine plot median throughfall depths. If a throughfall data collector's performance was compromised due to clogging (e.g., leaf litter accumulation or biofilm blockage of funnel tip) or wildlife damage to the tipping bucket, at the time of biweekly data download, data from that data collector was not used in computing the plot's storm event throughfall median value. On average, across the plots, approximately 10 rain gages were operational for a storm event.

Repeated measures ANOVA on ranks (a nonparametric ANOVA using rank-transformed data) were used to compare throughfall depths within treatments (plots) over multiple periods in time (Johnson et al., 2002; Singe et al., 2013). Median values and rank-based statistics were used due to the heterogenous (non-normal) distribution of throughfall within the plots (Table 1.2), a phenomenon noted by other researchers (Shachnovich et al., 2008; Tanaka et al., 2015). All plots showed a significant difference among tipping buckets within the plot. The greatest variability within a single plot type was seen in the 10-year deciduous plots. These plots include a high variability of canopy cover due to poor oak survival that created micro-areas with little canopy cover with patches of non-oak plants that grew to very dense cover. Tree growth also differed between species, which could also contribute to differences. In 2014, tree volume for pine (192,551 cm^3) was drastically greater than that observed for oak (1,250 cm^3) at this site (Hansen et al., 2015).

Table 1.2. Results of comparing tipping buckets, within plots, using repeated measures ANOVAs. Values reported are median throughfall depths in mm.

Tipping Bucket	Plot[1]						
	10C	10D	20C	20D	100C	100D	Traditional
1	3.81	7.37	4.95	5.97	5.33	6.60	7.11
2	4.19	8.89	3.30	5.84	5.33	7.11	6.60
3	3.18	7.87	2.67	4.45	6.10	7.37	7.37
4	3.81	7.87	4.57	5.84	5.08	6.86	6.22
5	4.32	7.11	3.43	5.59	4.32	6.86	6.60
6	3.30	6.10	4.06	6.86	5.84	5.08	7.62
7	5.08	7.11	3.30	5.84	4.83	5.33	6.35
8	5.68	4.32	4.32	4.83	6.60	6.35	7.75
9	3.68	5.59	3.05	5.33	3.30	6.60	8.64
10	3.56	7.24	3.81	1.52	5.84	5.59	7.49
11	3.43	7.37	3.81	6.10	5.72	5.59	6.10
12	3.56	6.60	3.81	4.06	5.33	7.24	7.49
p-value[2]	<0.001	0.014	<0.001	<0.001	<0.001	<0.001	<0.001

[1]10C=10 year coniferous, 10D=10 year deciduous, 20C=20 year coniferous, 20D=20 year deciduous, 100C=100 year coniferous, 100D=100 year deciduous, and control = grass only.
[2]p=value noted for within column (plot) comparisons.

1.2.4 Statistical Analysis

A generalized linear mixed model (GLMMIX) in Statistical Analysis Software 9.4 (SAS, 2016) was used to test for differences in natural log transformed throughfall depths due to tree age (10, 20, and 100 years) and tree type (coniferous, deciduous) (α=0.05). Storm intensity, storm duration, and leaf-on (May through September) and leaf-off (November through February) periods served as covariates. Storm depth was not included in the model because it was highly correlated with storm duration (Section 1.3.1). Storm intensity and duration were modeled as random effects. The Tukey test was used for multiple comparisons between tree plot type and age when significant differences were present (α=0.05).

1.3 RESULTS AND DISCUSSION

1.3.1 Precipitation Characteristics

A total of 113 storm events occurred during the study period of May 2017 through May 2018. Total rainfall depths ranged from 1,261 mm at LMB to 1,434 mm at LF while rainfall durations ranged from 15 minutes at CWS to 37 hours at LF. Most rainfall events were small and short (Figures 1.9-1.10). Levia (2006) found storm magnitude and duration were important factors affecting throughfall. Across all weather stations, about 85% of the recorded storms had rainfall depths of 20 mm or less and durations of 12 hours or less. The two storms with the highest recurrence interval (comparing to 20-yr Design Storms of Lexington-Fayette Country Stormwater Manual) were close to the 5-year storm depth at 41.4 mm and 39.3 mm for 1.11 hr and 0.96 hr, respectively. The third highest reoccurrence interval was for a 6.25 hr storm with 57.0 mm of rainfall. Most of the storms were below the 1-year recurrence interval. Rainfall depth and duration displayed significant positive relationships for all four weather stations as well as the average of these stations (Figure 1.11). Table 1.3 shows the comparison of median storm event depth and duration between the weather stations. The LF weather station had a significantly higher median storm event depth as compared to LMB and a significantly longer median duration as compared to all other weather stations individually and averaged. The LF weather station recorded data at the largest interval, 1 hour, which may account for its difference with regards to median storm duration. The significant linear relationship between depth and duration, at these weather stations, was similar but stronger than that found by Austen and Claborn (1974) who noted a correlation of 0.409 between these two parameters for storm events in Lubbock, Texas.

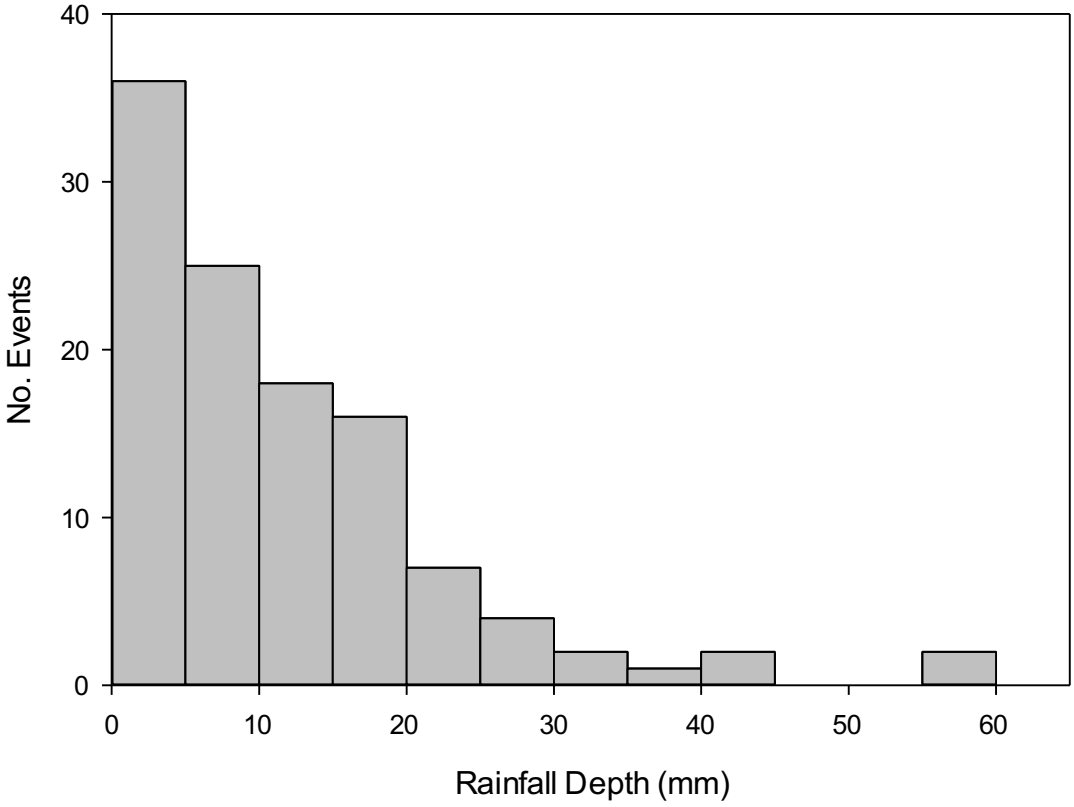

Figure 1.9. Distribution of rainfall depths as averaged over all four weather stations.

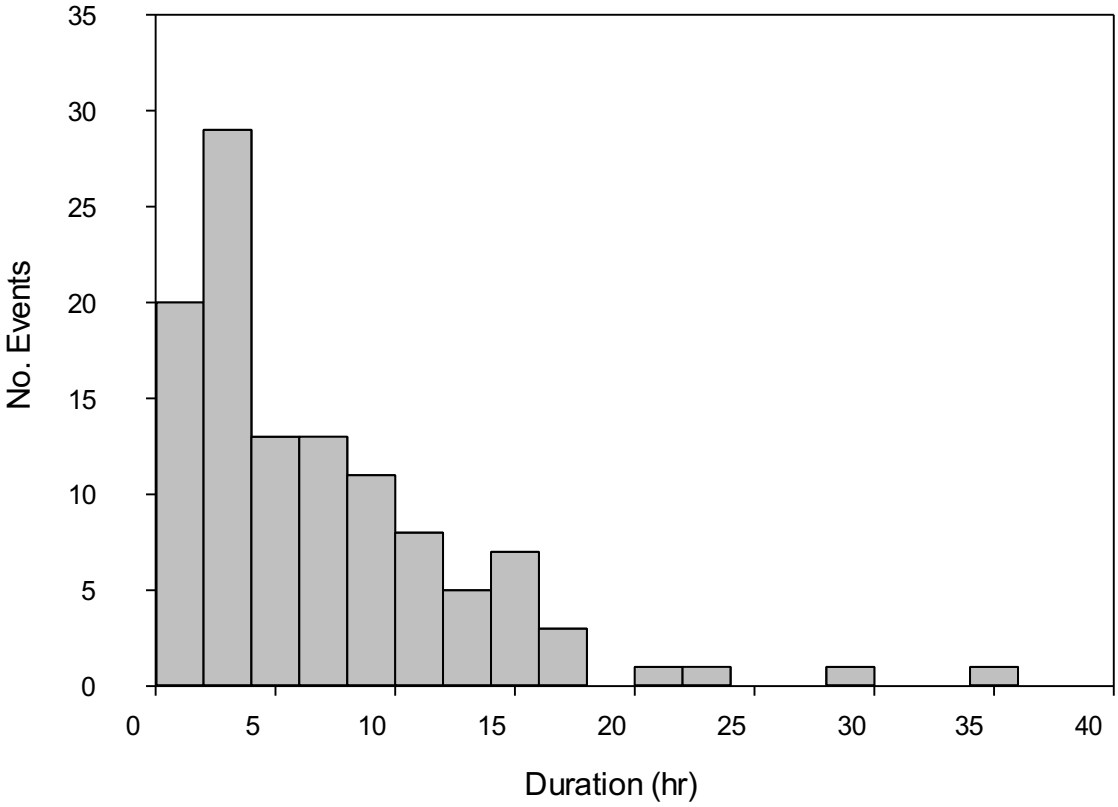

Figure 1.10. Distribution of rainfall durations as averaged over all four weather stations.

Table 1.3. Results of comparing storm event depth and duration from weather stations using repeated measures ANOVAs.

Weather station[1]	Median depth (mm)	Median duration (hr)
CWS	8.64 ab	5.00 b
LMB	7.62 b	4.85 b
LF	9.14 a	6.00 a
JKL	8.20 ab	5.45 b
Average (n=4)	8.45 ab	5.14 b

[1]CWS=Camp, LMB=Little Millseat Branch, LF=Laurel Fork, and JKL=Jackson. Statistical differences within column noted by differing letters (α=0.05).

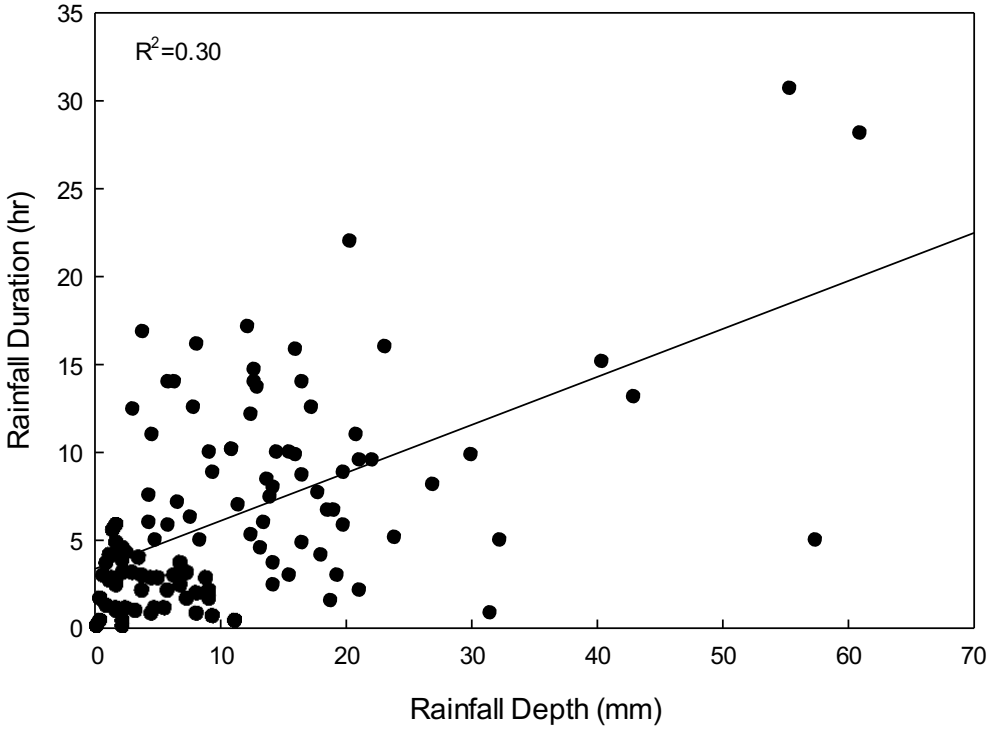

Figure 1.11. The relationship between rainfall depth and duration for the Camp weather station was significant (R2=0.30, p<0.001).

Storm events displayed seasonal differences across winter (December- February), spring (March-May), summer (June-August), and autumn (September- November) time periods for duration and average intensity but not depth (Tables 1.4-1.5). No statistical differences were found between winter and summer storm event depths. Storm event durations were significantly longer during the winter months as compared to the summer ones. Summer storms were significantly more intense as compared to winter events. Long periods of low intensity rainfall during the winter months and high intensity storm events in the summer and early fall are typical for this region (Husic et al., 2019).

Table 1.4. Results of comparing seasonal variations in storm event durations using a one-way ANOVA. Values displayed are medians and units are in hr.

Weather station[1]	Winter[2]	Spring	Summer	Autumn
CWS	8.30 a	5.00 ab	3.35 b	5.00 ab
LMB	8.85 a	4.63 ab	4.15 b	6.00 ab
LF	9.50 a	5.50 a	3.00 b	8.89 a
JKL	8.78 a	5.15 ab	4.00 b	6.43 ab
Median (n=4)	9.02 a	5.03 ab	3.31 b	6.25 ab

[1]CWS=Camp, LMB=Little Millseat Branch, LF=Laurel Fork, and JKL=Jackson.
[2]Winter=December through February, spring=March through May, summer=June through August, and autumn=September through November.
Statistical differences within rows noted by differing letter (α=0.05).

Table 1.5. Results of comparing seasonal variations in storm event average intensities using a one-way ANOVA. Values displayed are medians and units are in mm.

Weather station[1]	Winter[2]	Spring	Summer	Autumn
CWS	1.23 b	1.64 ab	2.76 a	1.28 b
LMB	1.24 ab	1.45 ab	2.20 a	1.13 b
LF	1.10 b	1.28 ab	1.94 a	1.09 b
JKL	1.15 b	1.39 b	2.56 a	1.34 b
Median (n=4)	1.12 b	1.55 ab	2.37 a	1.23 b

[1]CWS=Camp, LMB=Little Millseat Branch, LF=Laurel Fork, and JKL=Jackson.
[2]Winter=December through February, spring=March through May, summer=June through August, and autumn=September through November.
Statistical differences within rows noted by differing letter (α=0.05).

1.3.2 Throughfall Characteristics

Throughfall was significantly affected by storm event duration and depth but not intensity considering both tree types (coniferous and deciduous) and all ages (10, 20, and 100 years) (Appendix E). Increases in depth and duration resulted in significantly larger throughfall depths while the effect of increased intensity increased throughfall depths for the 10- and

100-year old plots but not the 20-year old ones. Prior research has shown that throughfall rates are related to storm duration and intensity (Llorens et al., 2003; Levia and Frost, 2006). Crockford and Richardson (2000) noted that interception was strongly related to rainfall duration and intensity as higher interception rates were generally associated with low intensity long duration events and low interception rates were often linked to high intensity short duration events. Bryant et al. (2005) noted that short duration, low level intensity storms were associated with lower throughfall depths (i.e., higher interception rates) for five forest communities in western Georgia, USA. Miralles et al. (2010) noted that regions such as Scandinavia and northern Canada that are characterized by long duration storm events had higher interception losses than areas dominated by short duration convective storms yielding large annual rainfall amounts.

1.3.3 Traditional Grassland

For the traditional site (grass only), throughfall data were collected for 99 storm events during the period of June 2017 through May 2018. During this period, 1165 mm of rainfall occurred of which 1088 mm or about 93% was recorded in the throughfall collectors. It is possible that some rainfall was intercepted by the grasses in the summer, though it is also likely that the difference between precipitation and throughfall depths may be attributable to localized (micro) variations in rainfall patterns and losses from evaporation, splash, and wetting of the collector surface (Thimonier, 1998; Levia and Frost, 2006). In some instances, negative throughfall values were recorded (e.g., throughfall depths exceeding rainfall depths). Similar occurrences were noted in prior throughfall studies with some authors attributing this cause to wind (Robson et al., 1994; Crockford et al., 2000; Levia and Frost, 2006).

1.3.4 Treatment Effects

Throughfall was significantly influenced by tree type (coniferous, deciduous) and age (10, 20, 100 years). Considering all ages, coniferous trees had significantly lower throughfall depths and captured more in the canopy relative to deciduous trees (Table 1.6). The median throughfall depth for coniferous trees (all ages combined) was 3.8 mm and was 5.8 mm for deciduous trees (all ages combined). The effect of age depended on tree type (Figure 1.12). For coniferous trees, significant differences were present between the 10- and 100-year plots as well as the 20- and 100-year plots but not the 10- and 20-year plots. For deciduous trees, the 20-year plot differed significantly from the 10- and 100-year plots; however, the 10- and 100- year plots did not differ. Unlike the other plots, the 10-year deciduous plot contained large numbers of invasive shrubs such as Autumn Olive can impact tree growth, and hence

canopy cover, in the plot (Orr et al., 2005; Dukes et al. 2009). Canopy cover for the 10-year deciduous plot in June 2017 was much lower, at 61%, than the other plots which had values of 93% or greater. For both coniferous and deciduous stands, the 100-yr old canopy had relatively lower interception and higher throughfall and was most similar to the grassland.

Table 1.6. Results of the comparison of tree type and age. Values displayed are median throughfall depths in mm.

Age (years)	Coniferous	Deciduous
10	3.50 b,y	6.17 a,x
20	3.34 b,y	5.00 a,y
100	4.84 b,x	6.21 a,x

Statistical differences within row (a,b) and columns (x,y) noted by differing letter (α=0.05).

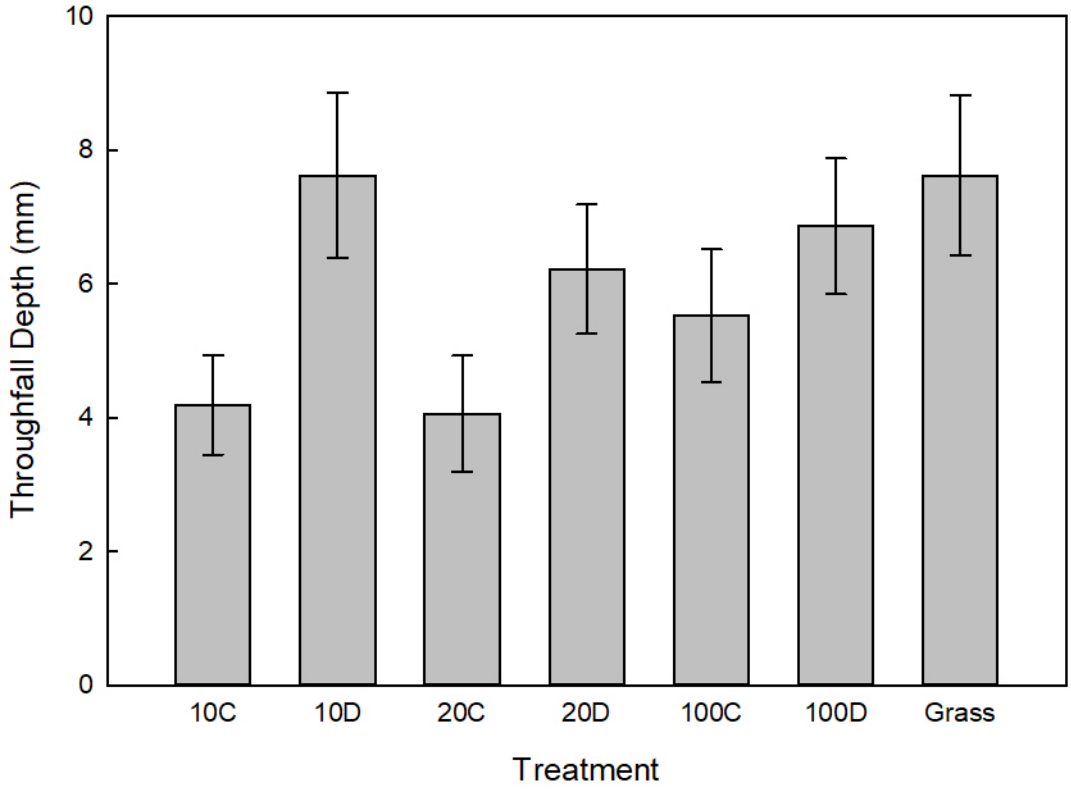

Figure 1.12. Throughfall depth depended on tree type and age. C indicates coniferous, D is deciduous, and the numbers indicate tree age in years. Error bars indicate standard error for each plot.

As the plots aged, the difference between coniferous and deciduous throughfall depths decreased from 2.67 mm at 10-years to 1.66 mm at 20-years and 1.37 mm at 100-years. The increase in throughfall depth over time and the reduction in differences between vegetation types with age may be attributable in part to self-thinning (Westoby, 1984; McCarthy et al., 1991). Recognizing that throughfall depths decrease with age could have watershed implications, particularly in instances where tree stands are not allowed to fully mature such as with woody biomass production where stands may be harvested between 10- and 20-years of age (Caldwell, 2018). Such strategies may benefit disturbed landscapes such as mined lands which undergo drastic ecosystem changes that often result in the transformation of forested environments to grassed ones (Zipper et al., 2011) and hence increased runoff peaks and volumes (Jorgensen and Gardner, 1987; Guebert and Gardner, 2001; Shukla et al., 2004). As demonstrated by Kuczera (1987) and Haydon et al. (1996), interception and water

yield is not a linear relationship with forest age. Interception increases rapidly peaking between 20 and 40 years before steadily declining. Similarly, water yields are nonlinear, and instead have a reversed curve as yields rapidly decrease to their lowest between 20 and 40 year before steadily increasing.

Interception rates, defined here as the amount of rainfall that did not become throughfall, varied with tree type and age (Figure 1.13). The highest interception rates occurred with the 10- and 20-year old coniferous plots where about 44% and 40% of rainfall, respectively. The lowest interception rate occurred with the 10-year old deciduous plots that is mixed with a dense understory of Autumn Olive. At about 6%, this plot was equivalent to the grassland plot. The lower level of overstory density in this plot meant that some throughfall collectors were essentially in the "open" with no canopy cover above them. The interception rates found in this study have a wider range than those reported by Bryant et al. (2005) for five forest communities in the southeast US, which recorded interception rates between 17 and 22% for stands 13-65 years old and opposite trends of interception as a function of age for coniferous and deciduous plots. Interception rates for the 20-year old deciduous plot at Starfire were equivalent to those for the 100-year deciduous plot at Little Millseat (Figure 1.13).

For deciduous trees, the throughfall depths were significantly influenced by the seasonal presence or absence of leaves (i.e., leaf on and leaf off) (Table 1.7). The median throughfall depth, for all years combined, was 7.52 mm with leaves on and 5.55 mm with leaves off. When examining the interaction between year and presence/absence of leaves, only the 100-year old plot was significant at $\alpha=0.05$; the 10-year old plot was significant at $\alpha=0.10$ ($p=0.055$).

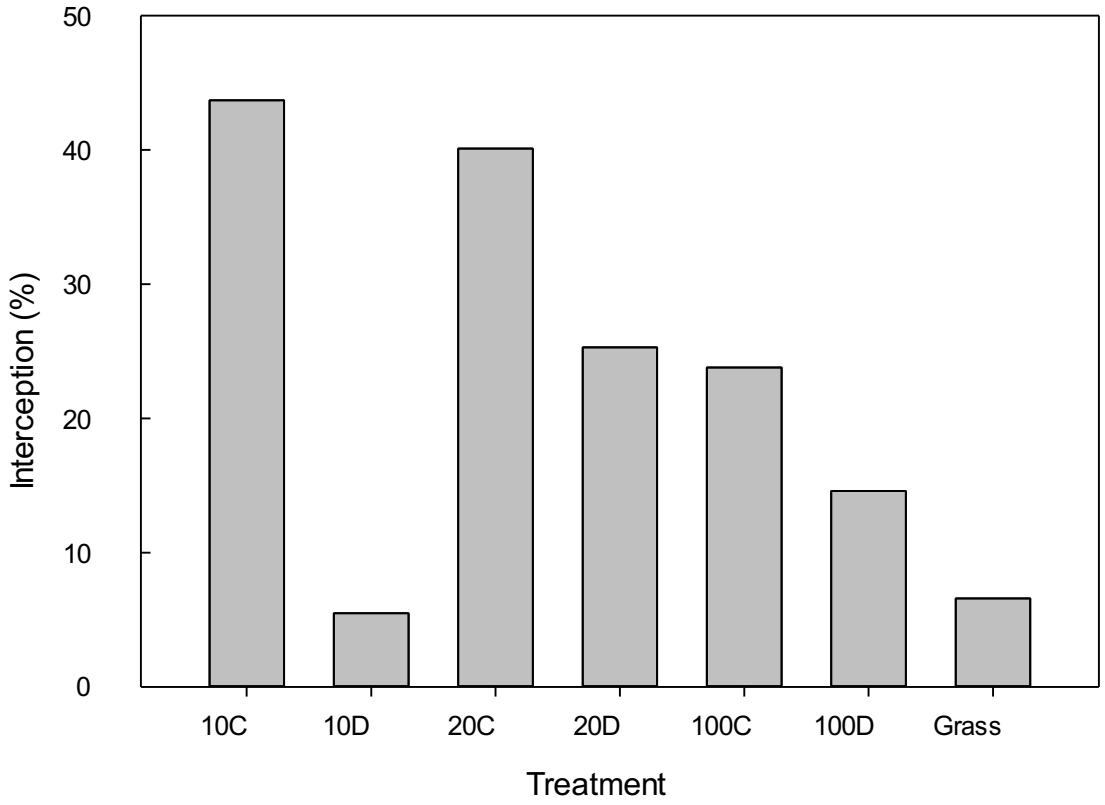

Figure 1.13. Interception rates for each plot. C indicates coniferous, D is deciduous, and the numbers indicate tree age in years.

1.4 CONCLUSIONS

Precipitation patterns in this study followed a seasonal trend with the highest intensity, shortest duration storms occurring during the summer months and the least intense, longest duration storms occurring during the winter months. Higher average precipitation levels occurred in 2018 as it was the wettest year on record. Rainfall characteristics significantly influenced throughfall patterns across the treatments. Tree type and age significantly influenced throughfall rates with coniferous trees intercepting more rainfall as compared to deciduous ones. For coniferous trees, throughfall depths were significantly greater for the 100-year plot as compared to the 10- and 20-year old plots. Self-thinning is a potential cause for this difference, indicating that both deciduous and coniferous FRA stands are regrowing in similar way to that of a natural forest stand. For the deciduous plots, the presence of invasive species in the 10-year plot resulted in large areas of open canopy and hence higher throughfall depths. Interestingly, interception rates for the 20-year plot increased as the forest matured and canopy closure was achieved. While it is not clear whether invasive species caused poor survival

of the 10-year oak trees or if poor survival allowed incursion of the invasive species, the results from this study show the importance of species survival rates on interception and that low survival rates could negatively impact or at least delay the hydrologic recovery of the area. Hall (2017) concluded that coniferous trees (shortleaf and loblolly pine) experience more rapid growth than deciduous trees (northern red oak, white oak, and chestnut oak) on reclaimed mined lands, a benefit for outcompeting invasive grasses which are common to such areas. Hansen et al. (2015) observed a similar trend at the site where the 10-yr plots were established.

It is likely that these results were influenced by the amount of precipitation received in 2018. Since the rainfall was not the result of a few high intensity storms, but rather many events, it is possible that short periods between events and residual water in the canopy and branch network increased the amount of throughfall seen across all plots.

The Forest Reclamation Approach is a proven method for re-establishing forested ecosystems on mined lands (Graves et al., 2000; Skousen et al., 2009; Agouridis et al., 2012; Sena et al., 2015). Results from this study indicate that the trees grown using FRA are following an expected pattern with regards to throughfall (Kuczera, 1987; Haydon et al., 1996) and complement prior FRA-focused runoff and infiltration studies (Taylor et al., 2009a; Taylor et al., 2009b; Sena et al., 2015). Because mean annual streamflow is inversely related to interception, it is hypothesized that mined watersheds reforested using the FRA will exhibit decreased water yields for at least 20-40 years before experiencing a steady flow rate as the forest matures. These patterns indicate that using FRA will allow natural hydrologic function to be restored and could reduce the flooding that is associated with sites restored as grassland.

2. The Forestry Reclamation Approach: Measuring Sediment Mass Accumulation Rates in Reclaimed Mine Lands and Naturally Regenerated Logged Forests of Eastern Kentucky

2.1 INTRODUCTION

Coal mining in its various forms has led to many detrimental impacts on the environment, some of which persist for years, decades, or much longer after mining activities have decreased or ceased entirely. Coal mining affects plant and animal life, soils, sediments, water quality, and the atmosphere. The effects on plant life are seen in areas where mountain top removal mining practices and accompanying valley fills have led to decreased botanical biodiversity in the region (e.g., Meier et al. 1995; Schuler and Gillespie 2000; Wyatt and Silman 2010; Sheoran et al. 2010; Ussiri and Lal 2005). This decrease in plant diversity not only reduces viable habitats for wildlife, but also decreases future timber production prospects due to the loss of commercially important native hardwood trees. Mining has also been shown to increase sediment loading in adjacent streams during storm flow events (e.g., Bonta 2007; Mangena and Brent 2006). A study from the late 1960s showed that wildlife was heavily impacted by the disturbance of over 800,000 acres of land, resulting in 5,000 miles of streams and some 13,800 acres of impoundments being contaminated by both sediment and acid drainage due to mining in Appalachia (Boccardy and Spaulding 1968).

From 1992 to 2006, areas throughout Appalachia with the highest mining activity were shown to have lost up to 7.6% of the total forest area (Wickham et al. 2007). The loss of interior forests is as significant as the loss of total forests because it leads to habitat fragmentation for native wildlife. The loss of interior forests was up to 5% greater than the loss of total forested land where strip mining occurred (Wickham et al. 2013). Mining activities affect both soils and sediments, primarily by erosion, including the loss of topsoil from mining activity (Holl and Cairns 1994; Kozlowski 1999). Topsoil loss from mining inhibits the regrowth of native hardwood tree species, in part due to losses of organic material and seeds (Bradshaw and Chadwick 1980).

Runoff from mined areas often shows decreases in water quality, which can be further degraded by valley fills, in part by the burial and/or capture of headwater streams (e.g., Ryan and Meiman 1996; Palmer et al. 2010). Adverse, but generally localized, effects from mining on water quality include: increases in electrical conductivity (EC), increased dissolved concentrations of sulfate and various heavy metals, organic matter (OM) enrichment, and increased turbidity, resulting in lower invertebrate density and decreased plant diversity in these riparian systems (e.g., Bernhardt et al. 2012; Fritz et al. 2010; Price and Wright 2016; Swer and Singh 2004).

Extensive logging occurred in eastern hardwood forests in the late 1800 and early 1900s. Logging can significantly change soil erosion rates, stream flow, and surface water quality (Arthur et al. 2007; Hatten et al. 2018). Deforestation has been shown to cause large changes in microbial communities in sandy soils (Crowther et al. 2014). Regions that have been previously logged have shown a decline in soil-nutrient availability due to the removal of OM (Brais et al. 1995; Hamlett et al. 1990; Huang et al. 1996). Due to the demand for greater timber production, mechanized logging operations are still prevalent within Appalachian hardwood forests (Wang et al. 2005).

Like mining, logging operations can adversely affect soils by increasing compaction and decreasing the pore space that retains water in the soil (Reisinger et al. 1988). Increased soil compaction and disturbances on steep slopes can lead to higher rates of overland flow and resulting erosion, which subsequently drive higher sediment fluxes to nearby streams and increased sedimentation (Martin 1988; Martin and Hornbeck 1994). Areas around streams can potentially be affected the most by increased compaction due to a reduction in soil-water retention from increased bulk density and reduced macropore spacing (Moehring and Rawls 1970; Greacen and Sands 1980).

2.1.1 Objectives

This study examined erosion and sediment movement patterns in watersheds due to longstanding and spatially extensive mining and logging activities. These disturbances have drastically altered regions of eastern Kentucky from their natural state and have led to damaged topsoil, or topsoil that has been removed entirely (Mensah 2015). This study compared the effect of different reclamation techniques on sediment accumulation rates in reclaimed mine lands. We also examined sediment dynamics in logging sites that have naturally regenerated for comparison.

2.2 METHODS

2.2.1 Study Location

This study is mainly focused on four separate reclaimed coal mines, and three previously logged sites, for a total of seven research sites. The sites include (1) Robinson Forest Little Millseat (RFMS_17T), the naturally regenerated riparian control site, (2) Robinson Forest Guy Cove (RFGC_17T, RFGC_17PC_A, RFGC_17PC_B), (3) Valley Fill Williams Branch (VFWB_17PC_A), (4) Robinson Forest Field Branch (RFFB_18T), (5) Starfire mine (SFMC_15), (6) Bent Mountain mine

(BM_07), and (7) Robinson Forest naturally regenerated drainage divide control site (FCA_15). The Bent Mountain mines are located within the Johns Creek drainage basin that covers an area of 581 km^2. All other research sites are found within the Troublesome Creek drainage basin, which encompasses an area of 637 km^2 (Figure 2.1). Sites RFGC, VFWB, SFMC, and BM_07 were previously mined. Sites RFMS, RFFB, and FCA were previously logged (Table 2.1). Little Millseat, Guy Cove, Field Branch, and Williams Branch were sampled within riparian areas. Robinson Forest drainage divide was sampled from a ridgetop on the drainage divide, while Starfire and Bent Mountain were sampled from upland areas because the recontouring process resulted in relatively uniform, flat areas with no distinct channel. Topography of individual sites was characterized from high resolution DEMs using ArcGIS.

The RFMS site was logged around 1923 (94 years prior to sampling) and naturally regenerated from seed and stump sprouts (Gough 2013). The FCA site was logged around 1925 (90 years prior to sampling), and then naturally regenerated. The RFFB site was logged in 1982 (36 years before sampling), and then naturally regenerated. The RFGC site was logged in the 1920s, mined in the mid-1900s, reclaimed as pasture 20 years ago (1997), and subsequently restored using FRA in 2008 (see Chapter 3). The VFWB site was mined and reclaimed as pasture five years before sampling (2012). The SFMC and BM sites were both mined, and both then reclaimed using FRA 18 years (1997), and 12 years (2004) prior to sampling, respectively. SFMC was constructed using mine spoil to a depth up to 6 feet.

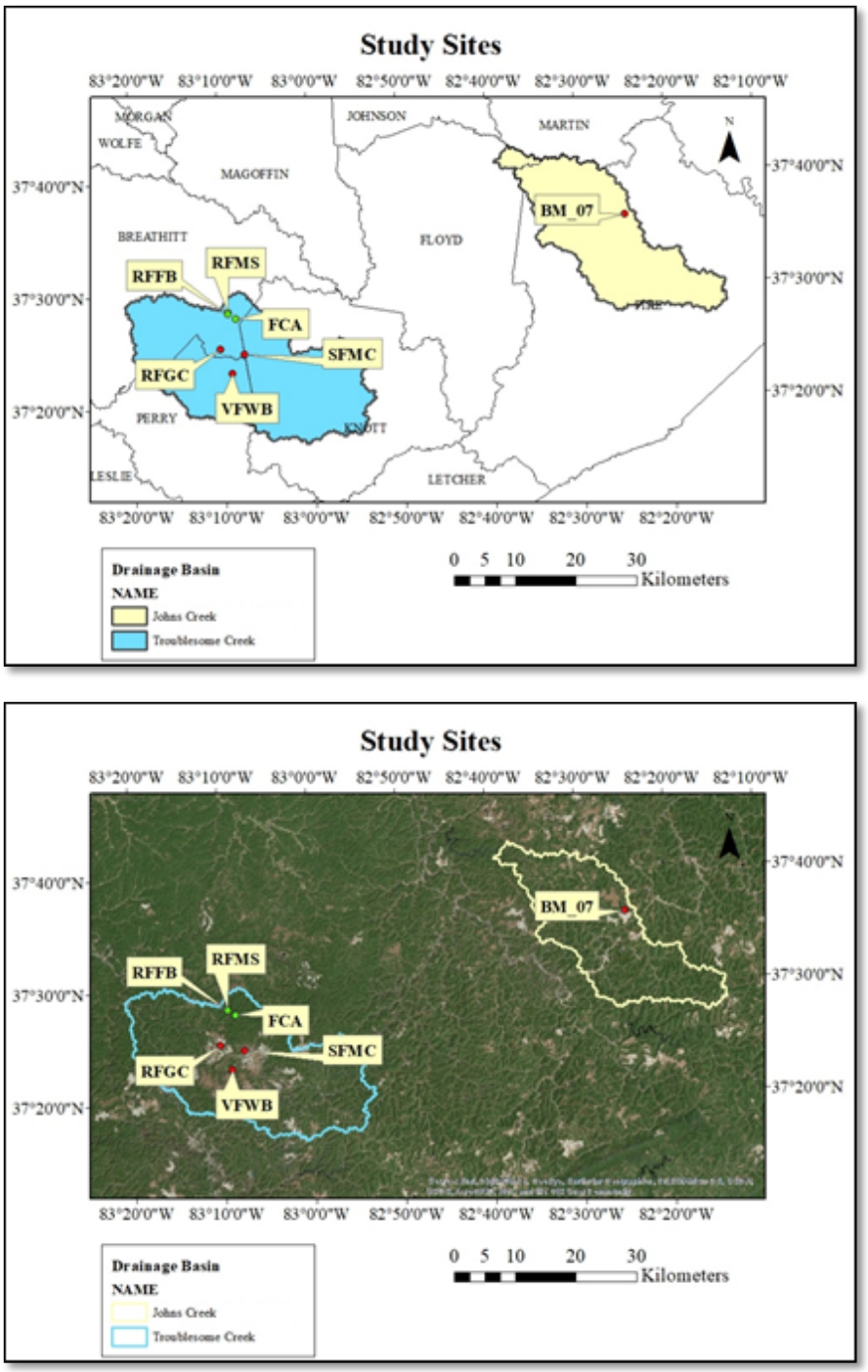

Figure 2.1. Locations of all mined (red) and logged (green) study sites. The top map shows site locations within the Johns Creek and Troublesome Creek drainage basins, and the Kentucky counties within which each are located. The bottom map shows 2016 satellite imagery (ArcGIS 10.5) for all sites.

Table 2.1. Study sites summary, including types of disturbances, when reclamation occurred, reclamation methods, upland contributing area, and when sites were sampled.

Site	Disturbance	Year regenerated or reclaimed	Method	Upslope Area (ha)	Year Sampled
RFMS	Logged	1923	Natural Regeneration	79	2017
FCA	Logged	1925	Natural Regeneration	0.6	2015
RFFB	Logged	1982	Natural Regeneration	9	2018
RFGC	Mined	1997 and 2008	Pasture and FRA	40	2017
VFWB	Mined	2012	Pasture	41	2017
BM_07	Mined	2004	FRA	na*	2016
SFMC	Mined	1997	FRA	na	2015

na = End dump spoil on mine bench, so no upland contributing area.

2.2.2 Core and Trench Sample Collection

At each site, sediment cores and trench samples were collected where possible. A total of six trenches were sampled for all of the study sites. Trenches were excavated with a shovel to a depth of 50-cm and width of approximately 2-m, or until the water table was reached, and sampled at 2-cm intervals using two-meter sticks braced against the side of the trench wall. All samples were bagged and held in cold storage until processing began. Sediment cores (Figure 2.2) were collected from each of the sites, if possible, for a total of three cores, utilizing aluminum core sleeves (10-cm diameter).

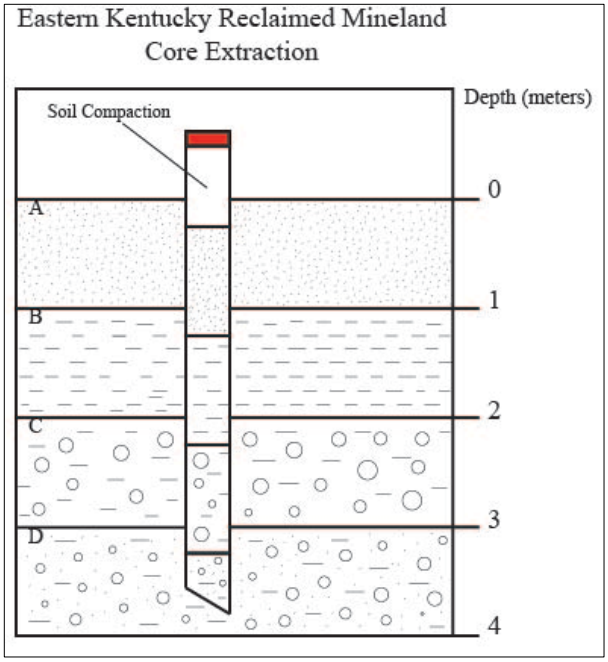

Figure 2.2. Hypothetical sediment profile of reclaimed mine land with core extraction (top of core in red). Example sediment layers include fine-grained sands (A), silt/clays (B), silt/clays with larger erratic cobbles (C), and sand/silt with large cobbles (D).

Aluminum core sleeves were used due to the common presence of large clastic materials; reclaimed mine land soils can contain up to 80% rock fragments derived from bedrock exposed by mining (e.g., Haering et al. 2004; Jaeger 2015). Core sampling depths ranged up to ~1 m with the intention of recovering sediment representing pre- and post-disturbance (mining or logging) periods for analysis and comparison. Each casing was physically driven into the sediment, and headspace was measured for each core prior to extraction to account for soil compaction during sampling (core shortening). Sediment accumulation rates are expressed in terms of mass accumulation rates to account for core shortening. All cores were sealed after extraction to minimize the risk of sediment mixing. Finally, cores and trench materials were transported to and stored at the Sedimentary and Environmental Radiochemistry Research Laboratory (SER_2L), Department of Earth and Environmental Sciences, at the University of Kentucky in preparation for physical, geochemical, and radiochemical analyses.

2.2.3 Core and Trench Sample Processing

Core casings were cut longitudinally using a rotary saw, with care taken to minimize disturbance of the sediment inside. After the casings were cut, medium gauge piano wire was used to cut through the sediments inside, allowing the core to be split open longitudinally. All cores were

then photographed at a fixed distance of 1 m directly above, and described noting changes in grain size, textures, facies and color based on comparison to the Munsell soil color chart (Munsell, 1998).

All cores were sectioned at uniform intervals to provide sediment aliquots for various analyses. The first step was the collection of bulk density plugs for RFMS, RFGC, VFWB, and RFFB. Bulk density was not measured for SFMC, BM_07, and FCA. Bulk density was calculated using:

$$Bd = \frac{M_s}{V_t}$$

where M_s is the mass of dried soil, and V_t is the total volume. Each plug was collected at 2-cm intervals spanning the full length of each core. The bulk density data allow sediment accumulation rates to be presented as linear accumulation rates. Each plug was placed into a pre-weighed 40-ml aluminum tin, weighed, and dried at 70° C for 24 hours (or longer as needed). All sample were then re-weighed and archived.

The first 50 cm of each core was divided into 1-cm sections, and the remainder was sectioned at 2-cm intervals. All samples were placed into pre-weighed 250-ml aluminum tins, weighed and dried at 70° C. After 48 hours, dried samples were re-weighed. All samples were then wet sieved (as needed) to remove macro OM and coarse clastic materials (larger than 0.05 cm) that were independently dried and weighed.

Trenches were excavated using shovels until bedrock or the water table was reached. Meter sticks were used to sample trench walls at 2-cm intervals, with samples removed using a hand spade and then bagged on site for transport. All core and trench samples were separated into aliquots for physical, radiochemical, and stable carbon isotope analyses. All radiochemical aliquots were homogenized using a Retsch RM200 mortar grinder.

2.2.4 Grain Size

Grain size analysis was utilized to assess changes in sedimentary environments over the period of record for each set of samples (cores, trenches), and among sites. Changes in particle size can reflect changes in transport energy and deposition (Robinson and Slingerland 1998; Koestner et al. 2011). Grain size distribution data were compiled for all cores and trenches sampled. Analysis of push cores was completed at 1-cm intervals from 0-50 cm, and at 2-cm intervals from 50 cm to the end of the core. Trenches were quantified at 2 cm intervals.

Sample aliquots for grain size were weighed at 5-10 g and placed into 250 ml clear Pyrex beakers. Samples were then treated with 10 ml each of sodium hexametaphosphate, acetone, de-ionized water, and concentrated hydrogen peroxide (H_2O_2). Micro organic material was oxidized using H_2O_2, preventing it from acting as a binding agent that can potentially skew mineral grain size data (Hillier 2001; Yeager et al. 2005). Sodium hexametaphosphate is a common dispersion agent that increases the surface area of the sample to facilitate OM oxidation by H_2O_2 (Plouffe et al. 2001). Samples were treated with H_2O_2 at room temperature for ~24 hours, and then heated at 100° C on hotplates while receiving 5-10 ml additions of H_2O_2 until obvious reactions ceased.

After removal of micro organic material, samples were rinsed into 50 ml centrifuge tubes and treated with magnesium chloride (MgCl; if needed) to flocculate any fine suspended sediment. Each sample was then centrifuged using an Allegra 14-X centrifuge at 2,000 rpm, and treated with additional MgCl until the water in the sample was clear, and decanted. This process was repeated three times to remove excess H_2O_2. Samples were placed into pre-weighed tins, dried in an oven at 70° C for 24 hours, and sieved to remove particles larger than 2 mm in diameter. Material larger than 2 mm (gravel) was weighed and bagged separately to be included in the grain-size determinations. Gravels were removed from samples due to particle size constraints of the Malvern Mastersizer. Once dried and re-weighed, samples were analyzed using a Malvern Mastersizer S2000 to obtain grain-size measurements for particles ranging from 0.02 µm to 2,000 µm (2 mm). Grain size data for each sample is presented as fractions of clay (< 4 µm), silt (63-4 µm), and sand (2 mm-63 µm) according to the Wentworth scale (Wentworth, 1922).

2.2.5 Radiochemistry

Radionuclide data have been used to estimate short-term sediment mixing depths, to establish a time frame for sediment deposition, and to determine sediment accumulation rates at these sites, whenever possible (e.g., Al Hamarneh et al. 2003; Rice 1986). This was accomplished by analyzing samples to determine activity concentrations of the fallout radionuclides Cesium-137 (^{137}Cs), Lead-210 (^{210}Pb), and Beryllium-7 (^{7}Be). ^{7}Be, given its short half-life ($t_{1/2}$ = 53 d), was used to provide information on short-term (≈1 year) sediment mixing depths (Krishnaswami et al. 1980; Sharma et al. 1987).

The radionuclides ^{137}Cs and ^{210}Pb were used to determine sediment accumulation rates (Baskaran 2011; Matisoff et al. 2002). ^{137}Cs has a half-life of 30.2 years (Ritchie and McHenry 1990). Large activity concentrations of ^{137}Cs appear in soils and sediments beginning in 1952, due to increases in the number and magnitudes of above-ground thermo-nuclear weapon tests,

which reached their maxima in 1963 (e.g., Yeager et al. 2007; Ritchie and McHenry 1990). The largest activity concentration peaks typically represent 1963, due to the onset of the Partial Nuclear Test Ban Treaty in 1964. Sediment accumulation rates are calculated using ^{137}Cs here by:

$$S = \frac{R_{peak}}{T}$$

where S = sediment accumulation rate, R_{peak} = the depth (or cumulative mass depth) at which the ^{137}Cs peak activity concentration appears, and T = time since 1963.

The radionuclide ^{210}Pb has a half-life of 22.3 years and is part of the Uranium-238 decay series (Figure 2.3).

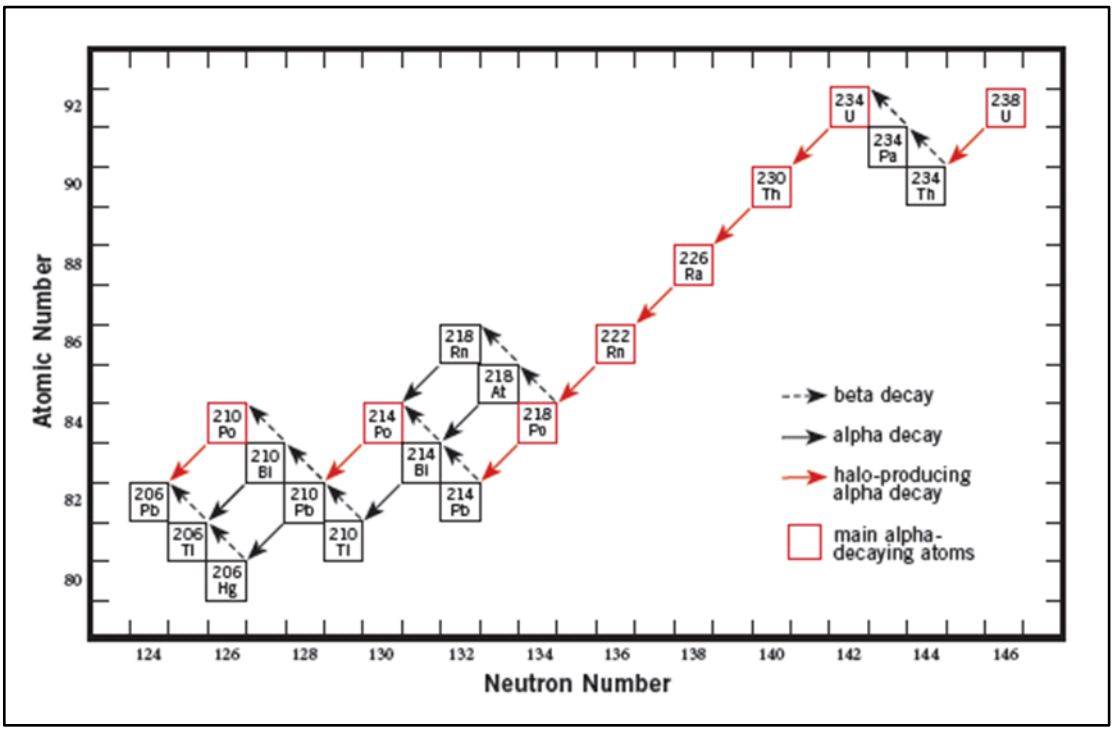

Figure 2.3. ^{238}U decay series (University of Wisconsin, wisc.edu).

Excess ^{210}Pb ($^{210}Pb_{ex}$) is that fraction of total ^{210}Pb delivered to soils through atmospheric fallout (principally bound to accumulating sediments), where it is combined with the supported fraction ($^{210}Pb_{sup}$) of total ^{210}Pb ($^{210}Pb_{tot}$), which is produced by the *in-situ* decay of ^{238}U series isotopes in rocks, sediments, and soils (Walling et al. 2011; Benmansour et al. 2011). Supported

^{210}Pb is determined using the mean value of the lowermost 3-5 samples at depth in the $^{210}Pb_{tot}$ profile. $^{210}Pb_{ex}$ is calculated using:

$$^{210}Pb_{ex} = {}^{210}Pb_{tot} - {}^{210}Pb_{sup}$$

Sediment chronologies are calculated using the constant rate of supply model (Lubis 2013):

$$t = \frac{1}{\lambda} \times ln(A_o/A)$$

where λ = the decay constant of ^{210}Pb (0.031 yr^{-1}), A_o = $^{210}Pb_{ex}$ inventory of the entire sediment section, and A = $^{210}Pb_{ex}$ inventory below the sample being dated. Sediment mass accumulation rates are determined using the equation:

$$S_a = \frac{\Delta m}{\Delta t}$$

where Δm is the change in mass depth, and Δt is the change in time (Yeager et al. 2005, 2007). The three assumptions used for this model are: (1) $^{210}Pb_{ex}$ is delivered to sediments at a constant rate through time, (2) the initial concentration of ^{210}Pb in the sediment is variable, and (3) rates of sediment accumulation are variable. Sediment linear accumulation rates are calculated by dividing S_a by the mean bulk density of the sediment section.

The expected $^{210}Pb_{ex}$ inventory from atmospheric deposition alone (537.42 mBq cm^{-2}; Santschi et al. 1999; Baskaran et al. 1993) is used to compare against measured values at all sites to estimate net deposition or erosion over the last ~100 years. The expected $^{210}Pb_{ex}$ inventory was calculated by dividing the expected flux of $^{210}Pb_{ex}$ (16.66 mBq cm^{-2} yr^{-1}; Turekian et al. 1977) by the ^{210}Pb decay constant (0.031 yr^{-1}). The expected ^{137}Cs inventory from atmospheric deposition alone has also been calculated (135.20 mBq cm^{-2}; Walling 1998; Larsen 1984). This was calculated using ^{90}Sr as a proxy for ^{137}Cs with the value decay corrected for 2016 using the equation:

$$A_t = A_0 \times e^{\lambda t}$$

Where A_t is the activity at 2016, A_0 is the original activity, λ is the decay constant for ^{137}Cs (0.023 yr^{-1}) and t is the time elapsed (from 1983 to 2016, see Larsen 1984). Calculated radionuclide inventories can be compared to those expected from atmospheric deposition alone to assess if study sites are net depositional or erosional. All of the radionuclides considered here (^{7}Be, ^{137}Cs, ^{210}Pb) readily adsorb onto fine-grained sediments at Earth's surface (^{210}Pb also adsorbs onto POC; e.g., Ab Razak et al. 1996; Wan et al. 2005; Vaaramaa et al. 2010) due to their low solubility and geochemistry (e.g., Baskaran 2011; Matisoff et al. 2002).

2.2.5.1 Alpha Spectrometry

Alpha spectrometry was used to determine activity concentrations of total ^{210}Pb in samples. This was accomplished using acid digestion with concentrated hydrochloric (HCl), nitric (HNO_3), and hydrofluoric acids (HF). Sample material (~1 g) was placed into pre-weighed Teflon beakers and spiked with 500 µL of ^{209}Polonium tracer (National Institute of Standards and Technology (NIST), SRM-4326A) that allows for the quantification of ^{210}Po. The tracer ^{209}Po was used because it does not occur in nature and has a half-life of 102 years. Polonium-210 is a naturally occurring, alpha emitting radionuclide (Rani et al. 2014). A major assumption of this method is that ^{210}Po and ^{210}Pb are in equilibrium with one another (Persson and Holm 2011). Samples received multiple treatments with the three concentrated acids (HF, HNO_3, HCl) under heat (~110-135° C) until the sediment was completely dissolved. Samples were then brought up in 50 ml of 1.5 normal HCl, heated to 100° C, and stirred for 15 minutes. Ascorbic acid was then added to bind free Fe in the solution (e.g., Narita et al., 1989; Miura et al., 1999; Vesterbacka and Ikaheimonen, 2005). Silver plates (1 cm^2) were added to each sample and allowed to set at 100° C for 2.5 hours as the sample was stirred. Polonium in solution was bound to the silver plates (e.g., Santschi et al., 1999; Poet et al., 1972), which were then analyzed using a Canberra 7200 Integrated Alpha spectrometer.

2.2.5.2 Gamma Spectrometry

Gamma spectrometry was used to determine activity concentrations of ^{137}Cs and ^{7}Be. Homogenized samples were placed into 10 ml test tubes and packed at a ratio of 1 g : 1 ml to match all standards used. The sediment standards used included Ocean Sediment Powder (NIST, SRM-4357) and Rocky Flats Soil Number 2 (NIST, SRM-4353A). To ensure that equal geometries were obtained, samples received small additions of silica gel (if needed) as filler. Samples were then sealed with epoxy and allowed to grow into equilibrium for 21 days to prevent radon (^{222}Rn) from escaping the sample. Samples were then analyzed using Canberra High Purity Germanium well detectors and multi-channel analyzers (DSA-1000).

2.2.6 Particulate Organic Carbon and Stable Carbon Isotopes

Particulate organic carbon (POC) concentrations were determined, and used to derive POC inventories within, and fluxes to these sediments. Stable carbon isotope analysis of organic carbon was used to characterize the source of plant material at each site (Hobbie and Werner 2004). All aliquots for POC and stable isotopes were analyzed at the Kentucky Stable Isotope

Geochemistry Laboratory (KSIGL), Department of Earth and Environmental Sciences, at the University of Kentucky.

The supplies of organic carbon and nitrogen to soils in eastern Kentucky are primarily controlled by atmospheric inputs, OM decay, microbial processes, and the types and densities of *in situ* vegetation (e.g., Compton et al., 2007; Updegraff et al., 1995; Fornara and Tilman, 2008). POC inventories have been calculated for the upper 10 cm of all study sites, and POC fluxes were calculated for all sites where sediment accumulation rates could be determined. For trenched sites, the surface is represented by the first measurement taken from 0-2 cm. In push cores, the surface is represented by the mean of the POC measurements taken at the 0-1 and 1-2 cm intervals.

Carbon isotope data, quantifying the presence of ^{13}C relative to the more common ^{12}C, were compared with radionuclide data to identify and constrain, if possible, the timeframe when the dominant vegetation at study sites shifted from C4- to C3-dominated plant communities. C4 pathway plants are predominately grasses, while all trees utilize the C3 pathway. While C4 pathway plants are usually grasses, there are some grasses that are C3 plants. Before resource extraction, each of the sites were forested drainage basins forests (C3). After sites were cleared of vegetation, reclamation included a combination of different grasses (C4), tree planting as part of FRA, or natural regeneration of forest. This change in isotopic values was used to determine if OC stored in these sediments recorded the transitions.

Stable isotopic values of carbon derived from OM present in soils and sediments are commonly coupled with geochronology to infer past climatic shifts as reflected by major changes in vegetation, including changes from cooler climate C3 pathway plants, to warmer climate C4 pathways plants (e.g., Phillips and Gregg, 2001; Stevenson et al., 2005; Kohn, 2010). Plant matter acts as a reservoir for atmospheric carbon (Bernoux et al., 1998; Peterson and Fry 1987), which is isotopically fractionated depending on plant type. Values of $\delta^{13}C$ from organic sources (i.e., plant matter in soil) were compared with known value ranges of differing photosynthetic pathways; $\delta^{13}C$ (describing the depletion of ^{13}C relative to a standard) values for C3 pathway plants (forests) range from -20‰ to -35‰, and C4 pathways (grassland) have a range of -11‰ to -15‰ (Dawson et al., 2002; Kohn, 2010). Isotopic ratios of carbon are expressed in the form:

$$X = \left(\frac{R_{Sample} - R_{Standard}}{R_{Standard}}\right) \times 1000$$

where X represents $\delta^{13}C$, and R represents $^{13}C/^{12}C$.

Sample aliquots for stable carbon isotope and POC analyses were bathed in dilute HCl (10%) and heated in an oven for 1 hour at 100° C to remove inorganic carbon. Then samples were filtered, dried, weighed, and rolled into tin capsules (≈5 mg). Each sample was then run through an elemental analyzer (Costech ECS 4010 EA), and from there into an isotope ratio mass spectrometer (Thermo Finnigan Delta Plus XP, Thermo Fisher Scientific, Inc.) by continuous flow through (Conflo IV, Thermo Fisher Scientific, Inc.). All POC and stable isotope samples have been compared against certified standards, including Acetanilide (SRM-141D), USGS 40 (SRM-8573), USGS 41 (SRM-8574), and NIST (SRM-1515). All data collected were corrected for drift and linearity. Calculated carbon isotope values were compared to the international Vienna PeeDee Belemnite (V-PDB) standard (O'Leary 1988).

2.3 RESULTS

2.3.1 Reclaimed Mine Land Digital Elevation Models (DEM)

High resolution DEMs were acquired for all sites using ArcGIS to demonstrate topographic relief in mined sites RFGC, VFWB, BM_07, and SFMC (Figure 2.4) and logging sites RFMS, RFFB, and FCA (Figure 2.5). Logging sites exhibited rugged terrain and high relief. The Starfire (SFMC) and Bent Mountain (BM_07) are located on relatively flat mountain-top mining benches. Whereas, RFGC and VFWB were at the toe of valley fills. Five separate valley fills are located within the sub-basin including the study site at Guy Cove (RFGC). These valley fills can be identified by terraced topographic areas. The study site VFWB has four additional valley fills near the site for a total of five, all within the sub-basin that includes this site. However, the valley fills located at RFGC and VFWB are downstream of the site where cores and trenches were collected. As such, we anticipate that column characteristics are indicative of land-use activities in their respective watersheds only and not influenced by other upstream disturbances.

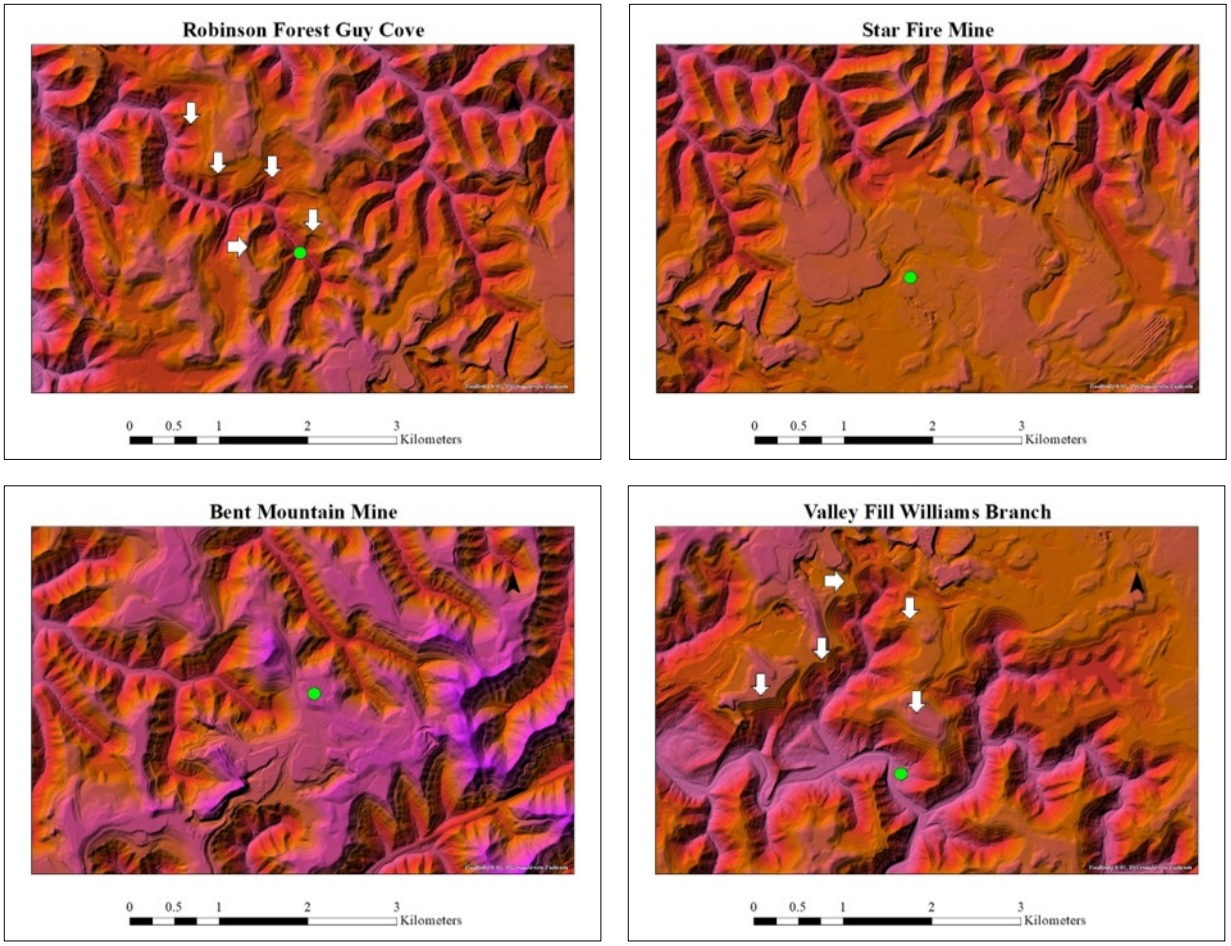

Figure 2.4. High resolution DEMs of reclaimed mine lands around study sites at Robinson Forest Guy Cove (top left – RFGC), Star Fire Mine (top right – SFMC), Bent Mountain Mine (lower left BM), and Valley Fill Williams Branch (bottom right - VFWB). Valley fills near VFWB and RFGC are shown by white arrows.

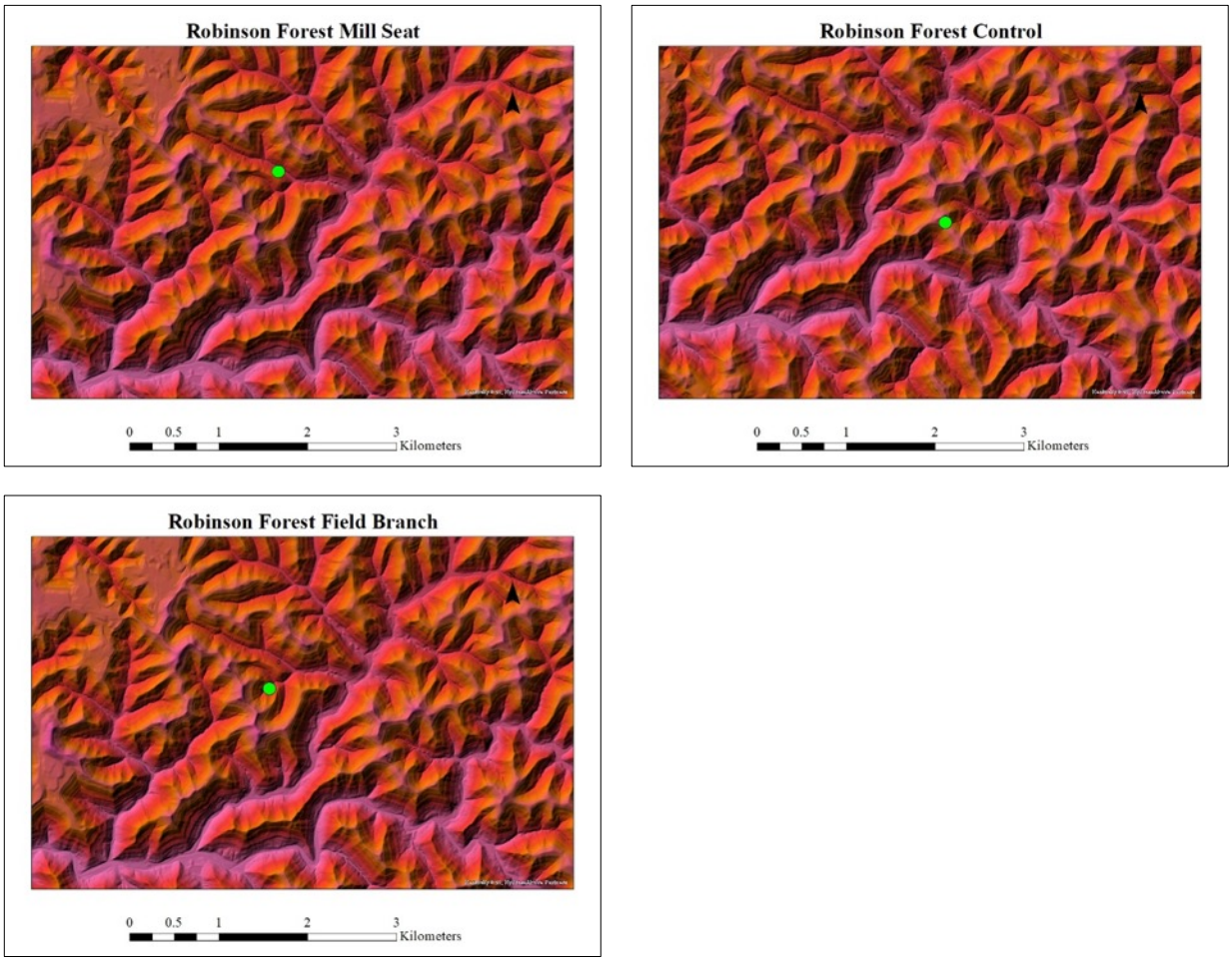

Figure 2.5. High resolution DEMs of logged areas around study sites at Robinson Forest Millseat (top left - RFMS), Forestry control (top right - FCA), and Field branch (bottom left - RFFB).

2.3.2 Robinson Forest Satellite Imagery and Sub-Basins

Satellite images from 2016 (Google Earth) were used to outline sub-basins for all sites. Satellite images from 1994 to 2016, taken at an altitude of approximately 15 miles, have been used to identify land scarring due to mining activity and overlaid on sub-basins to show how much of each was mined. The logged sites RFMS, RFFB, and FCA (Figure 2.6) are located within two separate sub-basins. RFMS and RFFB are located in the Clemons Fork sub-basin that encompasses an area of 4.20 km^2. One trench was excavated at each of the sites for a total of two sampling trenches within the Clemons Fork sub-basin (RFMS_17T, RFFB_18T). FCA is located in the Coles Fork sub-basin with an area of 17.20 km^2. A single trench was excavated at FCA for the Coles Fork sub-basin (FCA_15).

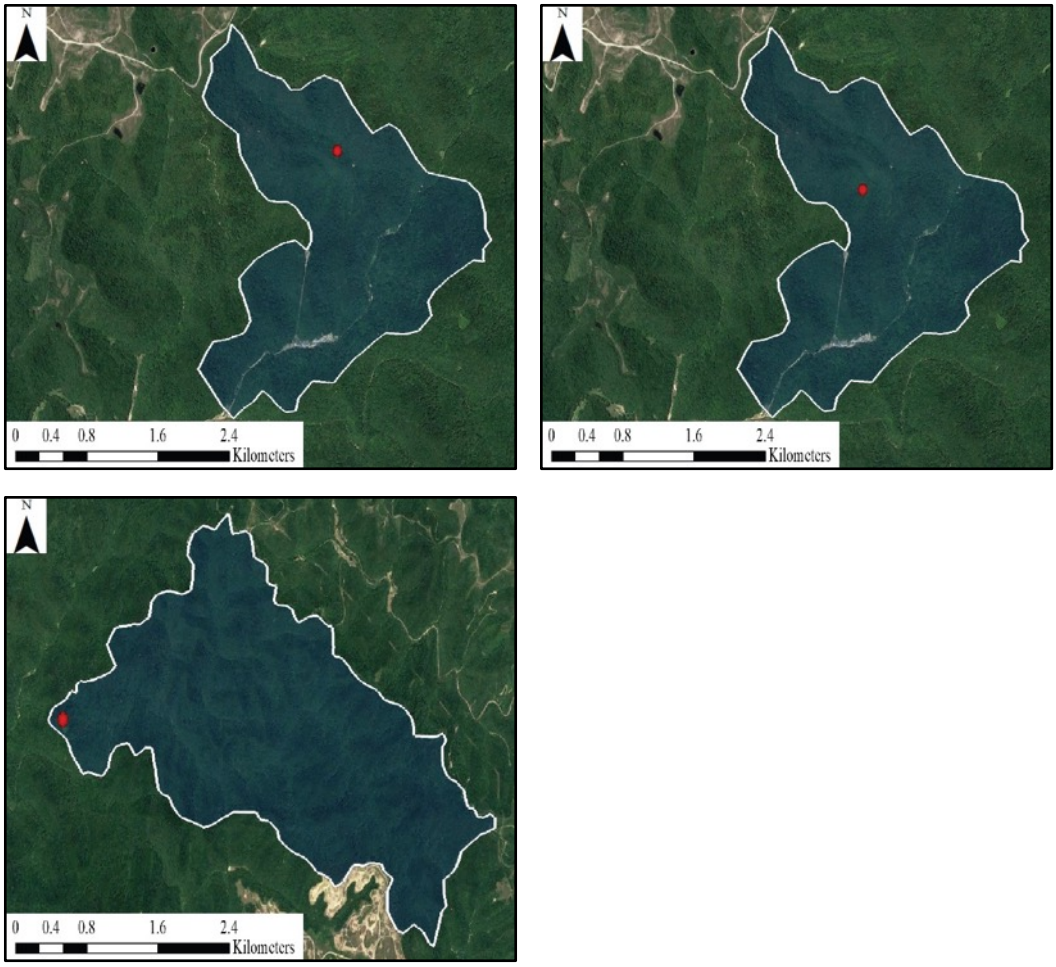

Figure 2.6. Satellite imagery (2016) showing the locations of previously logged sites (red) and the sub-basins (blue) within which they are located. RFMS (top left) and RFFB (top right) are both located within the Clemons Fork sub-basin. FCA (bottom left) is located within the Coles Fork sub-basin.

The mined site RFGC (Figure 2.7) is located within the Laurel Fork sub-basin that covers an area of 6.56 km^2. In 1994, ≈4.28 km^2 of the Laurel Fork sub-basin (65%) showed land scarring due to mining activity. By 1998, active mining decreased slightly to an area of 4.21 km^2 (64%). In 1998, RFGC was reclaimed as pastureland. RFGC was disturbed in 2008, and then reclaimed using the FRA. In images examined from 2008, and from 2016, no land scarring from mining was evident within the Laurel Fork sub-basin. Changes in mined area for the Laurel Fork sub-basin are shown in Figure 2.8. One trench and two push cores were collected from the Laurel Fork sub-basin of RFGC (RFGC_17T, RFGC_17PC_A, RFGC_17PC_B).

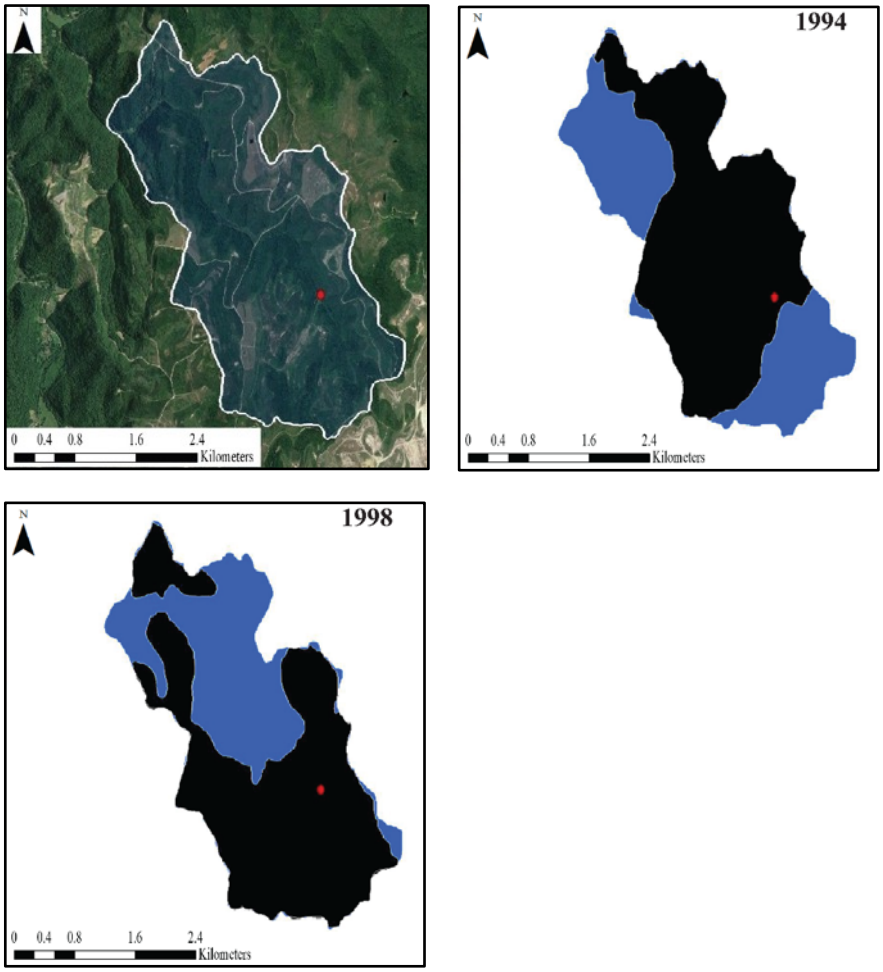

Figure 2.7. Satellite imagery (2016) showing RFGC (red) and its location within the Laurel Fork sub-basin (blue). Barren areas of the sub-basin (black) are shown for 1994, and 1998.

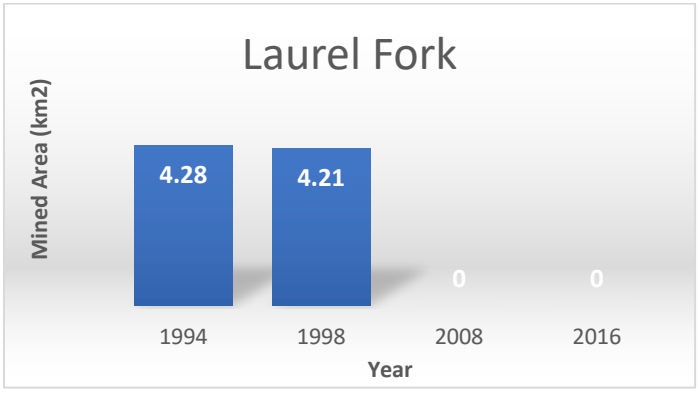

Figure 2.8. Changes in mining activity for the Laurel Fork sub-basin from 1994-2016.

The mined site SFMC (Figure 2.9) is located within the Long Fork sub-basin that covers an area of 10.80 km^2. In 1994, 1.10 km^2 of the Long Fork sub-basin (10%) had been mined. In 1997, SFMC was reclaimed using the FRA, but mining within the Long Fork sub-basin continued. By 1998, mining had increased to cover an area of 3.34 km^2 (31%). In 2008, mining decreased to an area of 3.13 km^2 (29%), and by 2016, it had increased to its maximum extent, covering 4.34 km^2 (40%). Changes in land scarring from mining are shown in Figure 2.10. A single sampling trench was excavated from SFMC within the Long Fork sub-basin (SFMC_15).

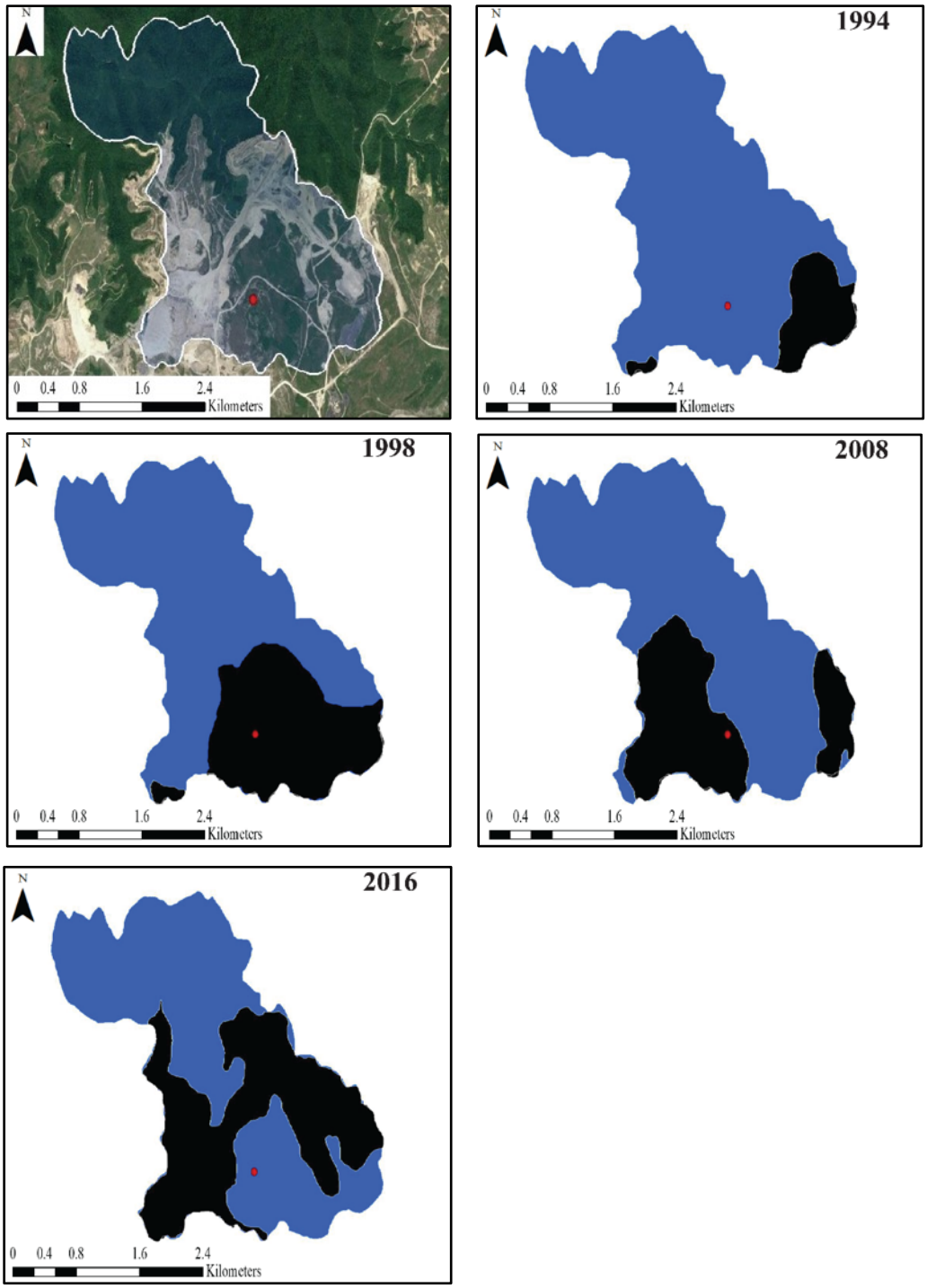

Figure 2.9. Satellite imagery (2016) showing SFMC (red) and its location within the Long Fork sub-basin (blue). Barren areas of the sub-basin (black) are shown for 1994, 1998, 2008, and 2016.

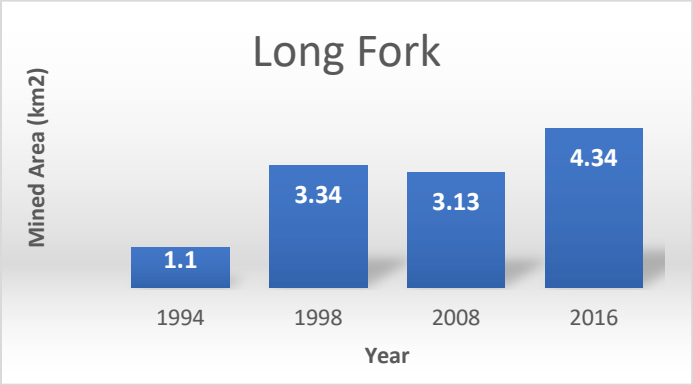

Figure 2.2. Changes in mining activity for the Long Fork sub basin from 1994-2016.

VFWB (Figure 2.11) is located in the Troublesome Creek sub-basin that encompasses an area of 8.17 km^2. In 1994, there was no land scarring from mining within the sub-basin. In 1998, 0.11 km^2 of the Troublesome Creek sub-basin (1%) had been mined, and this increased to its maximum extent of 2.51 km^2 (31%) in 2008. In 2013, VFWB was reclaimed as pastureland, and by 2016, mining activity decreased to an area of 0.88 km^2 (11%). Changes in mining activity for VFWB are shown in Figure 2.12. One push core was sampled from VFWB within the Troublesome Creek sub-basin (VFWB_17PC_A).

2.3.3 Bent Mountain Satellite Imagery and Sub-Basins

The mined site at BM (Figure 2.13) is located in the Brush Fork sub-basin that covers an area of 28.40 km^2. In 1994, mining covered ≈1.92 km^2 of the sub-basin (7%). In 1998, land scarring decreased to 1.22 km^2 (4%). In 2004, the site was reclaimed using the FRA, but mining within the sub-basin continued. By 2008, the mining area increased to its maximum extent at 3.79 km^2 (13%). By 2016, land scarring decreased to an area of 1.74 km^2 (6%). Changes in land scarring from mining activity for BM are shown in Figure 2.14. One sampling trench was excavated from the Bent Mountain mines within the Brush Fork sub-basin (BM_07).

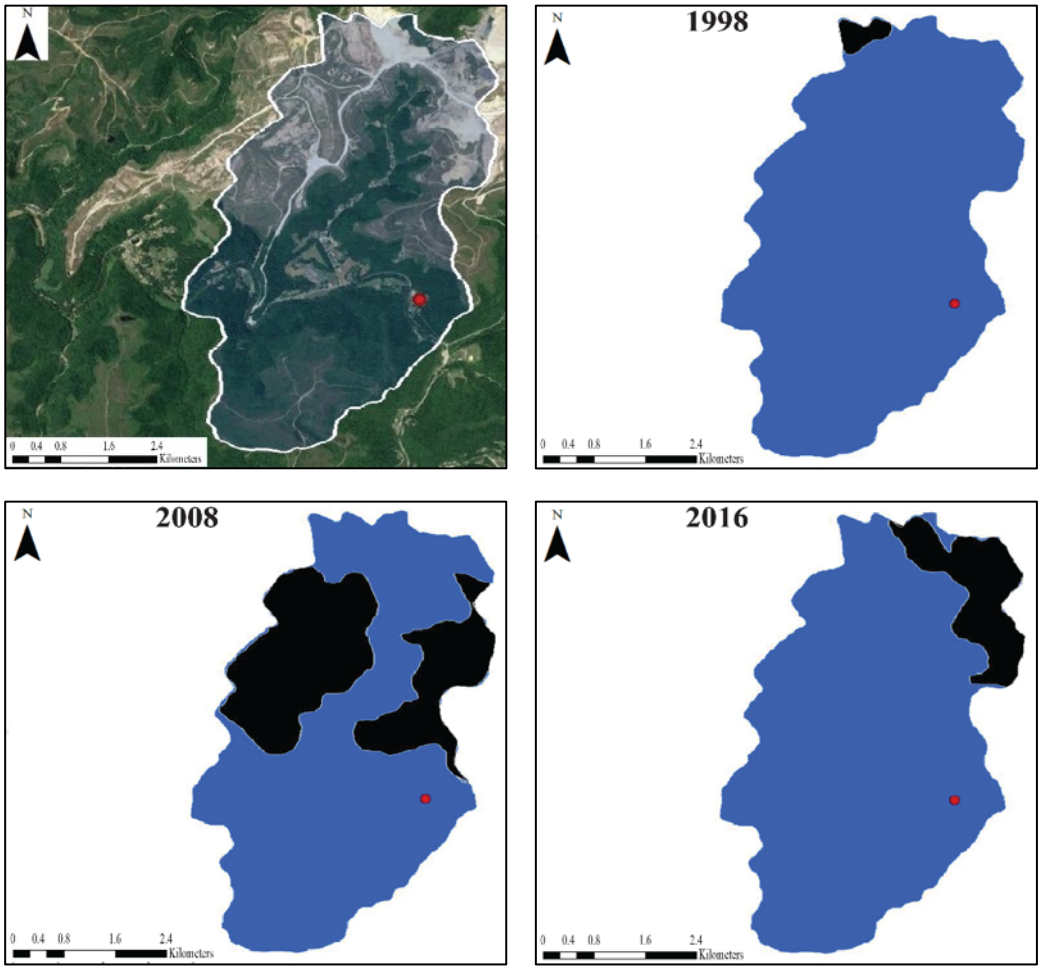

Figure 2.11. Satellite imagery (2016) showing VFWB (red) and its location within the Troublesome Creek sub-basin (blue). Barren areas of the sub-basin (black) are shown for 1998, 2008, and 2016.

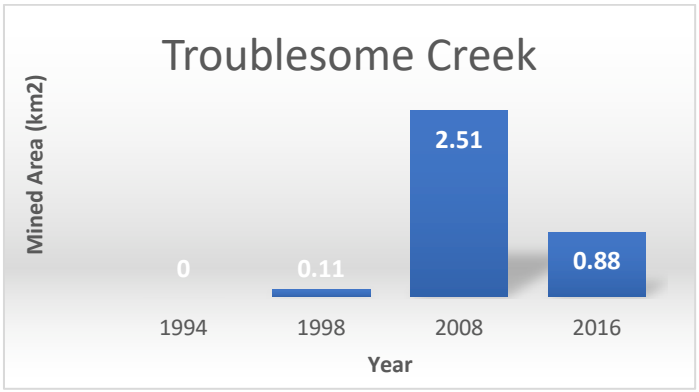

Figure 2.3. Changes in mining activity for the Troublesome Creek sub basin from 1994-2016.

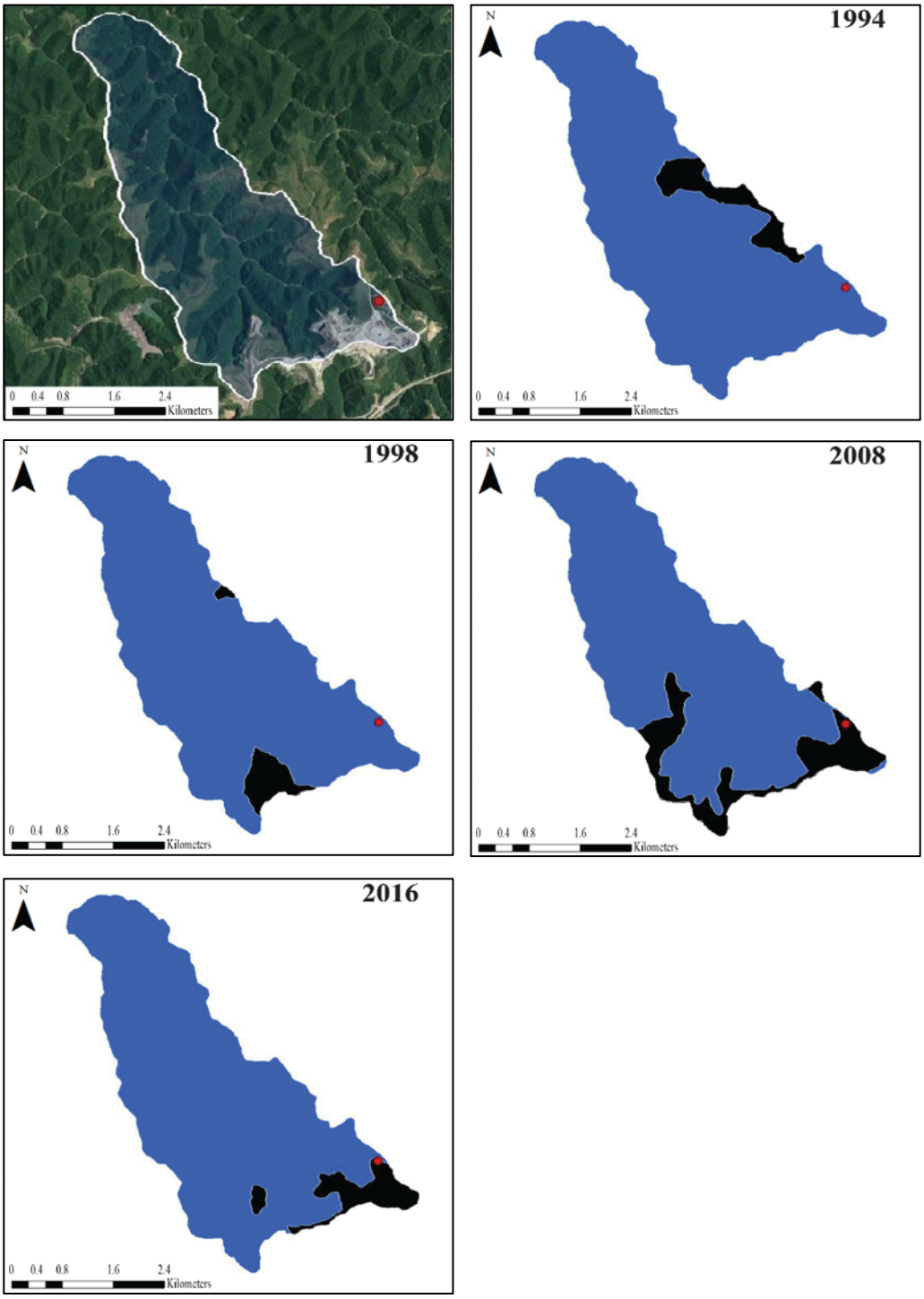

Figure 2.4. Satellite imagery (2016) showing BM (red) and its location within the Brush Fork sub-basin (blue). Barren areas of the sub-basin (black) are shown for 1994, 1998, 2008, and 2016.

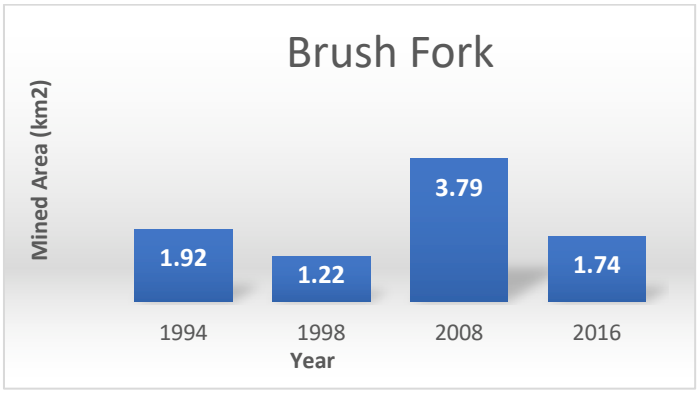

Figure 2.14. Changes in mining activity for the Brush Fork sub-basin from 1994-2016.

2.3.4 Grain Size Distributions

The control site trenches at the naturally regenerated riparian (RFMS _17T) and drainage divide (FCA_15) sites (Figure 2.15) were analyzed to a depth of 50 cm. RFMS _17T was sampled at 2-cm intervals over its entire depth, whereas FCA _15 was sampled at 2-cm intervals to 20 cm depth, and then at 5-cm intervals over the remaining depth. RFMS_17T sediments are predominantly sands (43-69%), then silts (20-46%), gravels (4-22%), and minor amounts of clay sized particles (0.9-5%). This trench does have a fining upward sequence from 0-16 cm. Data below 16 cm are more erratic, with a large spike in gravel at 36 cm (33%). FCA _15 is dominated by silts from 10-50 cm (39-57%), and contains a low percentage of clay-sized particles (2-14%). The upper 10 cm of the trench shows a noticeably higher amount of gravels (36-75%). There is an overall fining downward sequence at FCA_15.

RFGC_17T and RFFB_18T were sampled to depths of 26 cm and 22 cm, respectively (Figure 2.16), and both were sampled at 2-cm intervals over these depths. RFGC_17T sediments are predominantly silts (50-63%), and then sands (25-44%) from 0-10 cm. From 10-26 cm sands are prevalent (50-60%), while silts decrease (31-43%). Small amounts of clay-sized particles (5-11%), and minor gravels (0.5-4%) are present throughout the entire sampled depth and show a fining upward sequence. The dominant particle size throughout all of RFFB_18T is sand (40-63%). Gravels and silts show similar values (~20-30%) over the entire sampled depth, with minor amounts of clay-sized particles (1-2%).

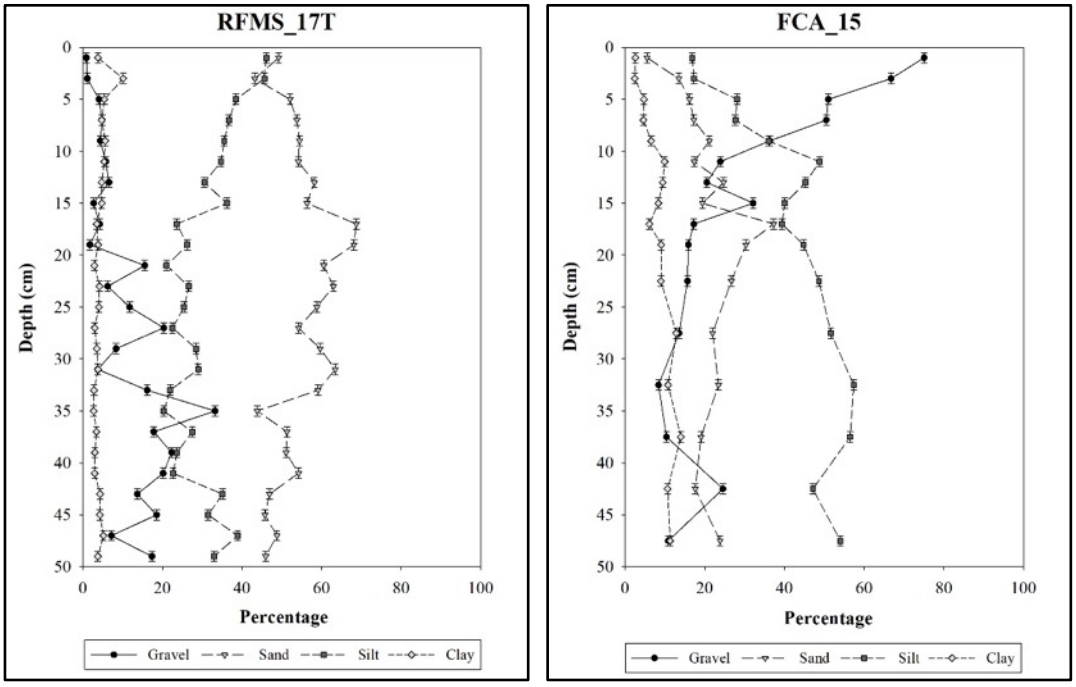

Figure 2.15. Grain size distributions vs. depth for natural regeneration trenches RFMS_17T (left) and FCA_15 (right). RFMS_17T is located in a floodplain of a naturally regenerated watershed, while FCA_15 is located in an upland location just below the watershed divide.

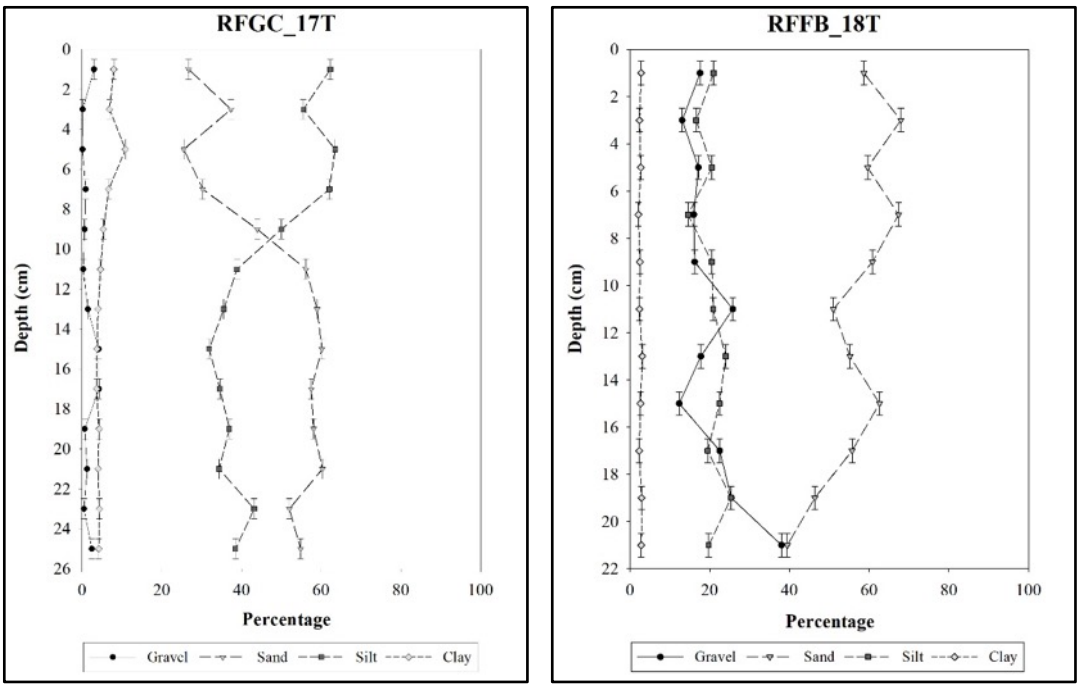

Figure 2.16. Grain size distributions vs. depth for trenches RFGC_17T (mined, left) and RFFB_18T (logged, right). Both samples were extracted from a trench in a floodplain above the confluence to a downstream tributary.

The two push cores RFGC_17PC_A and RFGC_17PC_B (Figure 2.17) were collected within 0.5 m of one another and reached depths of 96 cm and 98 cm, respectively. The top 18 cm of both cores fine upward, with increasing amounts of silts and clay-sized particles towards the surface. Below 18 cm, both cores exhibit a dominant mixture of sands and silts over the remaining section (with RFGC_17PC_B having more sand at depth), and both show an increase in gravels after ~70 cm.

Trenches SFMC_15 and BM_07_16 (Figure 2.18) were both sampled to depths of 50 cm and sectioned at 2 cm intervals for 20 cm, and then at 5 cm intervals over the remainder of the sections. These two sites show large differences in particle size distributions. SFMC_15 is the only site with gravel as the dominant particle size throughout the entire profile, with values ranging from 40-90%. After gravel, silts (8-40%), and sands (4-15%) make up the dominant size classes, with little clay sized particles present (0.5-3.7%). BM_07_16 is dominated by sands and gravel over the whole section, with some silts (~20%), and minor clay-sized particles (< 5%). The VFWB_17PC_A core (Figure 2.19) was sampled to a depth of 68 cm. The top 6 cm are dominated by silts (44-70%) with smaller amounts of sand (20-28%). Gravels (0.4-27%) and clay-sized particle (5-12%) fractions are low thoughout the core. From 6-68 cm, the particle size distribution becomes more erratic, with sands and silts dominating, with appreciable gravel over many depth intervals, and lesser amounts (typically ~10% or less) of clay-sized particles.

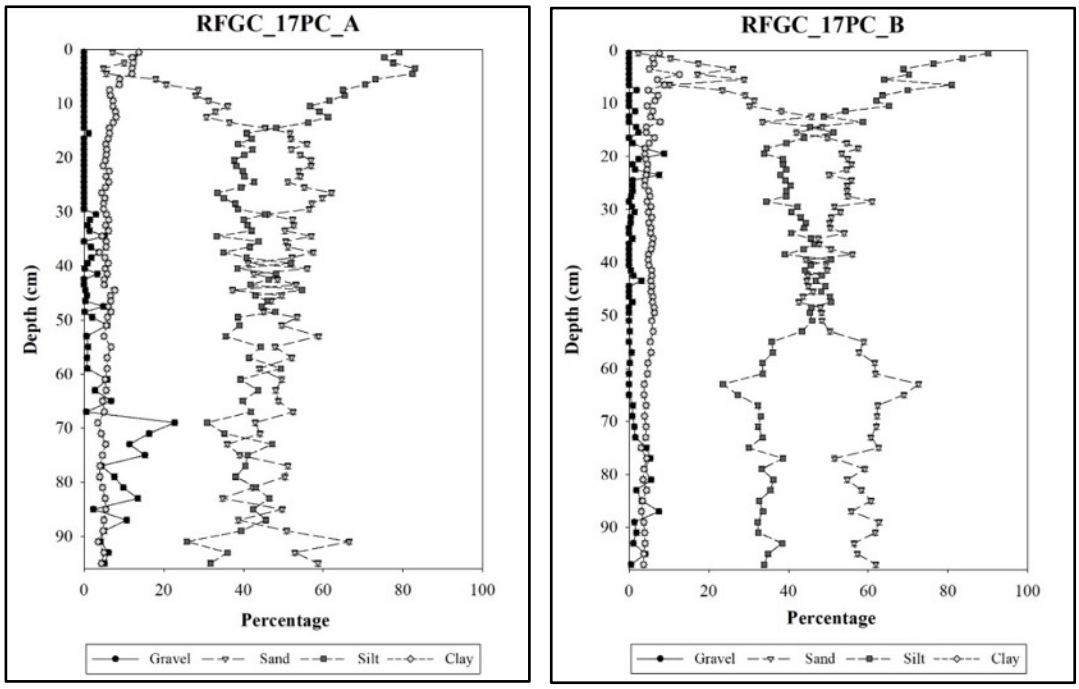

Figure 2.17. Grain size distributions vs. depth for push cores RFGC_17PC_A (left) and RFGC_17PC_B (right). Both cores were extracted from a floodplain at the terminus of the watershed above the confluence to a downstream tributary.

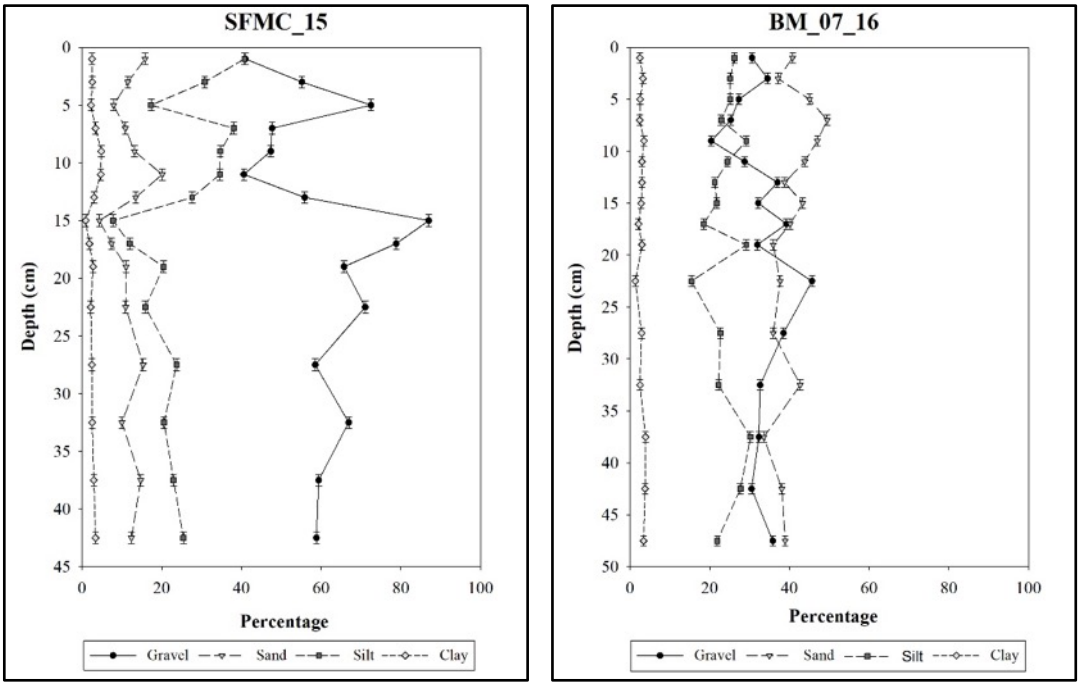

Figure 2.18. Grain size distributions vs. depth for trenches SFMC_15 (left) and BM_07_16 (right). Both sites were reclaimed using end dumped FRA.

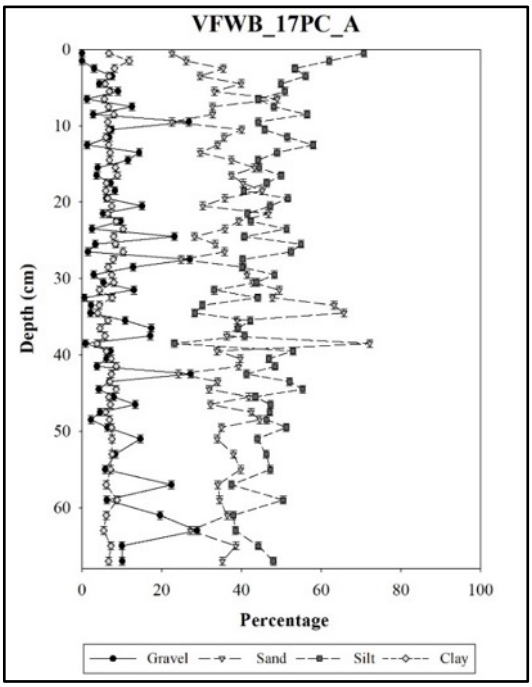

Figure 2.19. Grain size distribution vs. depth for push core VFWB_17PC_A.

2.3.5 Radiochemistry

2.3.5.1 Gamma Spectroscopy

^{7}Be was resolved at four of the six trenches sampled, but was not detected in the three push cores. ^{137}Cs activity concentration profiles were constructed for three trenches and two push cores. Inventories of ^{137}Cs and ^{7}Be are compared in Table 2.2, along with the expected ^{137}Cs inventory from atmospheric deposition alone. By comparing actual ^{137}Cs inventories to those expected from atmospheric deposition alone, a sedimentation ratio can be calculated. Sedimentation ratio values < 1 indicate that the site is net erosional, values > 1 indicate that net deposition has occurred, while values ~1 indicates that erosion and deposition have been roughly equal to one another, or that no deposition (hiatus) has occurred at that site during the period of record. Based on ^{137}Cs sedimentation ratios, all sites with measurable ^{137}Cs are net depositional with the exception of RFGC_17T. This site appears to be a depositional environment, but the ^{137}Cs profile is incomplete. ^{137}Cs linear (LAR) and mass (MAR) accumulation rates for 1952 and 1963 are compared in Table 2.3.

Table 2.2. ^{137}Cs and ^{7}Be inventories for all trenches and cores. *Indicates incomplete ^{137}Cs profile.

Core/Trench	^{137}Cs Inventory (mBq cm^{-2})	^{7}Be Inventory (mBq cm^{-2})	Sedimentation Ratio
Atmospheric	135.20	N/A	--
RFFB_18T	0	N.D.	--
RFMS_17T	288.23	13.12	2.13
FCA_15	472.01	28.30	3.49
RFGC_17T*	155.84	5.04	1.15
RFGC_17PC_A	336.64	N.D.	2.49
RFGC_17PC_B	393.36	N.D.	2.91
VFWB_17PC_A	0	N.D.	--
SFMC_15	0	18.72	--
BM_07_16	0	N.D.	--

N.D. = not detected.

Table 2.3. Linear and Mass Accumulation Rates from 1952 and 1963.

Core/Trench	^{137}Cs LAR (1963) (cm yr^{-1})	^{137}Cs LAR (1952) (cm yr^{-1})	^{137}Cs MAR (1963) (g cm^{-2} yr^{-1})	^{137}Cs MAR (1952) (g cm^{-2} yr^{-1})	Mean LAR (cm yr^{-1})	Mean MAR (g cm^{-2} yr^{-1})
RFMS_17T	N.D.	0.23 ± 0.03	N.D.	0.36 ± 0.07	--	--
FCA_15	N.D.	0.37 ± 0.03	N.D.	0.51 ± 0.10	--	--
RFGC_17T	N.D.	N.D.	N.D.	N.D.	--	--
RFGC_17PC_A	0.55 ± 0.02	0.68 ± 0.02	0.73 ± 0.15	0.95 ± 0.19	0.62 ± 0.02	0.79 ± 0.17
RFGC_17PC_B	0.55 ± 0.02	0.65 ± 0.02	0.76 ± 0.15	0.96 ± 0.19	0.60 ± 0.02	0.86 ± 0.17

^{7}Be is present in the uppermost interval (0-2 cm) at site RFMS_17T (Figure 2.20), indicating that some limited physical or biological mixing has taken place here recently ($\leq$ 1 year) because ^{7}Be adsorbs to surface material as it is delivered in new precipitation events. ^{137}Cs appears at 17 cm and its activity concentration increases moving towards the surface, however there is no clear peak in ^{137}Cs activity. This could be due to flooding that occurred within the watershed in 2009. This led to a change in the stream bed and multiple landslides. The first appearance of ^{137}Cs can be taken to represent the year 1952, from which mass and linear accumulation rates of 0.36 (g cm^{-2} yr^{-1}) and 0.23 (cm yr^{-1}) were derived.

^{7}Be and ^{137}Cs activity concentration profiles at the drainage divide site (FCA_15; Figure 2.21) were similar to those at RFMS_17T. ^{7}Be is present in the uppermost interval (0-2 cm) at this site, indicating that some limited physical or biological mixing has taken place here recently ($\leq$ 1 year). ^{137}Cs appears at 19 cm and its activity concentration generally increases moving towards the surface; however, there is no clear peak in ^{137}Cs activity. The first appearance of ^{137}Cs can be taken to represent the year 1952, from which mass and linear accumulations rates of 0.51 (g cm^{-2} yr^{-1}) and 0.37 (cm yr^{-1}) were derived. Notably, the appearance of ^{137}Cs is at a similar depth to when the abundance of gravel in the profile levels off, suggesting that colluviation from upslope bedrock exposure. Given its landscape position, it may also be possible that particles are being redistributed in the profile due to bioturbation or up gradient tree throw.

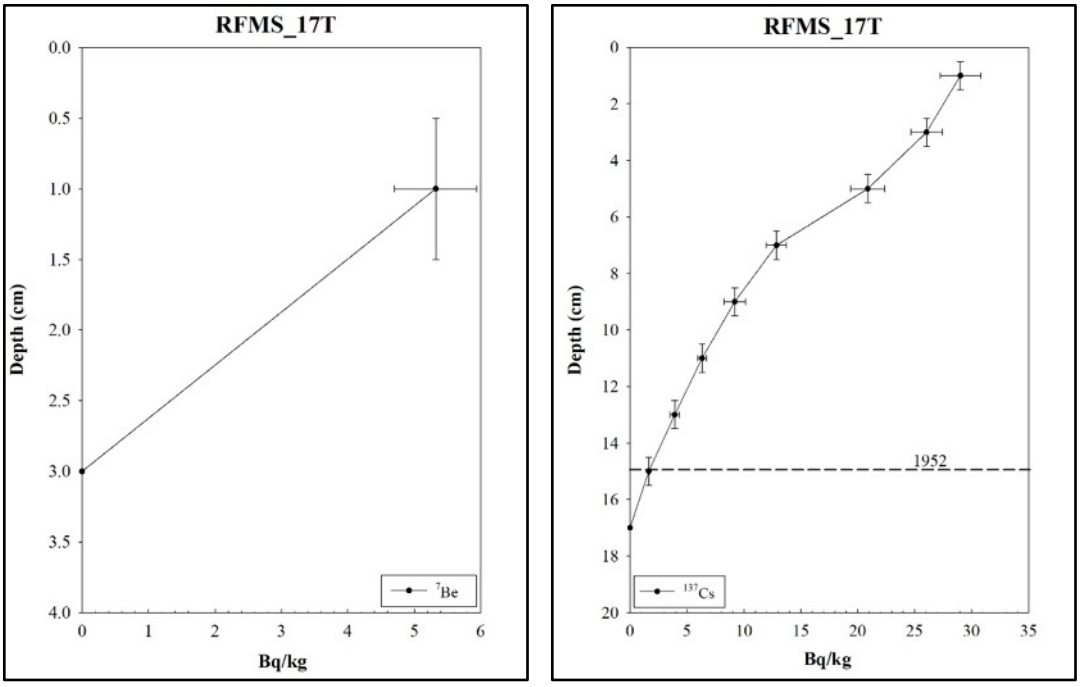

Figure 2.5. ^{7}Be (left) and ^{137}Cs (right) activity concentration profiles for trench RFMS_17T. The dashed line denotes the year 1952.

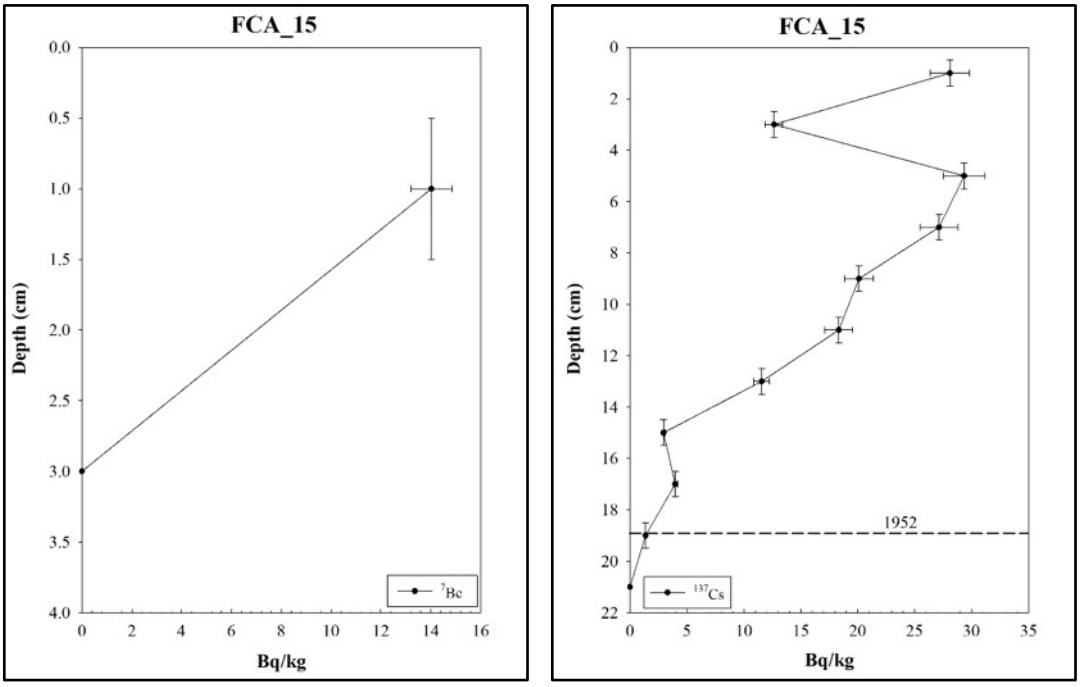

Figure 2.6. ^{7}Be (left) and ^{137}Cs (right) activity concentration profiles for trench FCA_15. The dashed line denotes the year 1952.

^{7}Be is present in the uppermost interval (0-2 cm) at site RFGC_17T (Figure 2.22), indicating that some limited physical or biological mixing has taken place here recently ($\leq$ 1 year). The ^{137}Cs activity concentration profile appears to be truncated, and does not include the first appearance of ^{137}Cs, nor a clear peak in activity (both likely due to the shallow depth of this section), making the determination of sediment accumulation rates using ^{137}Cs impossible. The two cores taken from this area, RFGC_17PC_A and RFGC_17PC_B (Figure 2.23), show no ^{7}Be activity, but do provide much more complete ^{137}Cs profiles. The absence of ^{7}Be suggests either no recent mixing ($\leq$ 1 year) or that ongoing colluviation disturbs the surface. In both of these cores, ^{137}Cs activity begins around 45 cm (1952) and maximum activity occurs around 30 cm (1963), more than 10 cm deeper than either of the drainage-divide sites. From 1952, RFGC_17PC_A has a mass accumulation rate of 0.95 (g cm^{-2} yr^{-1}), and a linear accumulation rate of 0.68 (cm yr^{-1}). From 1963, both the mass and linear accumulation rates decrease to 0.73 (g cm^{-2} yr^{-1}) and 0.55 (cm yr^{-1}), respectively. The mean mass and linear accumulation rates based on ^{137}Cs for RFGC_17PC_A are 0.79 (g cm^{-2} yr^{-1}) and 0.62 (cm yr^{-1}), respectively. From 1952, RFGC_17PC_B has a mass accumulation rate of 0.96 (g cm^{-2} yr^{-1}) and a linear accumulation rate of 0.65 (cm yr^{-1}). From 1963, these rates decreased to 0.76 (g cm^{-2} yr^{-1}) and 0.55 (cm yr^{-1}), respectively. The mean mass and linear accumulation rates based on ^{137}Cs for RFGC_17PC_B are 0.86 (g cm^{-2} yr^{-1}) and 0.60 (cm yr^{-1}), respectively.

SFMC_15 shows no ^{137}Cs activity in the depth sampled, but ^{7}Be is present within the upper 2 cm at this site, indicating that some limited physical or biological mixing has taken place here recently ($\leq$ 1 year) (Figure 24). The absence of ^{137}Cs is likely due to the surface mining that has taken place at the Starfire site and the recent reclamation (18 yr.), all of which post-dates the ^{137}Cs source. ^{137}Cs and ^{7}Be are similarly not detectable at sites VFWB_17PC_A and BM_07_16, both of which were reclamated since 2000. A lack of these radionuclides at RFFB_18T, which was harvested in 1982 and underwent natural reforestation, may be due to the high proportion of sand sized particles (>50%) in the top 20 cm (Figure 2.16); sand has a lower surface area than finer grained particles and generally adsorb fewer charged particles (Mabit et al. 2008; He and Walling 1996; Matisoff et al. 2002). ^{137}Cs-based sediment accumulation rates for all sites are presented in Figure 2.25.

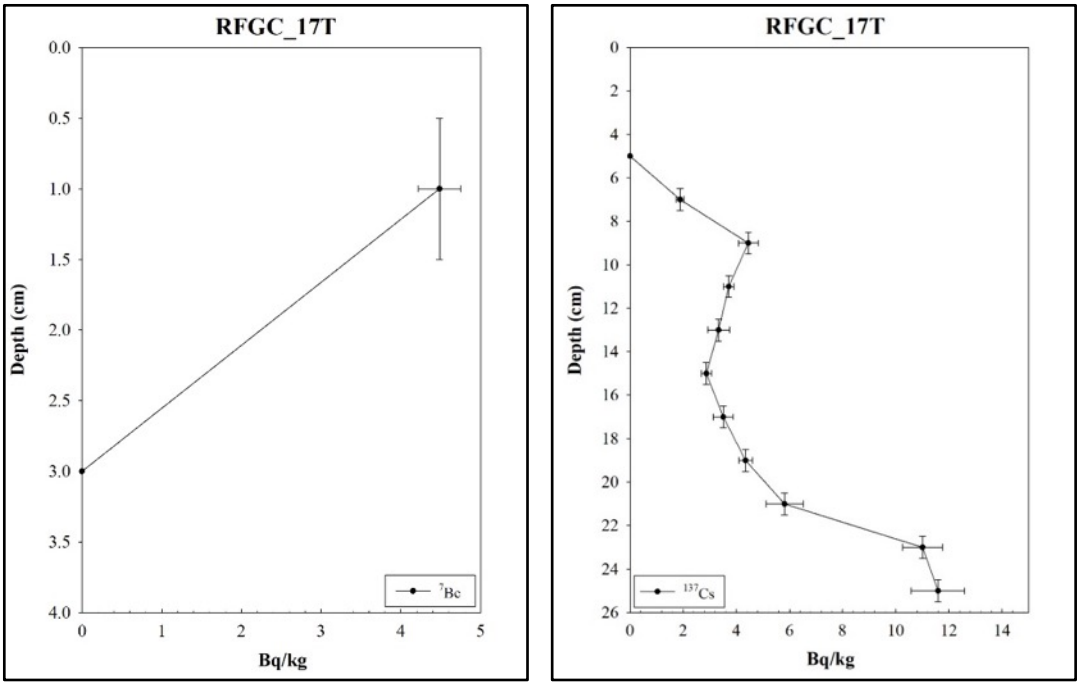

Figure 2.7. ^{7}Be (left) and ^{137}Cs (right) activity profiles for trench RFGC_17T.

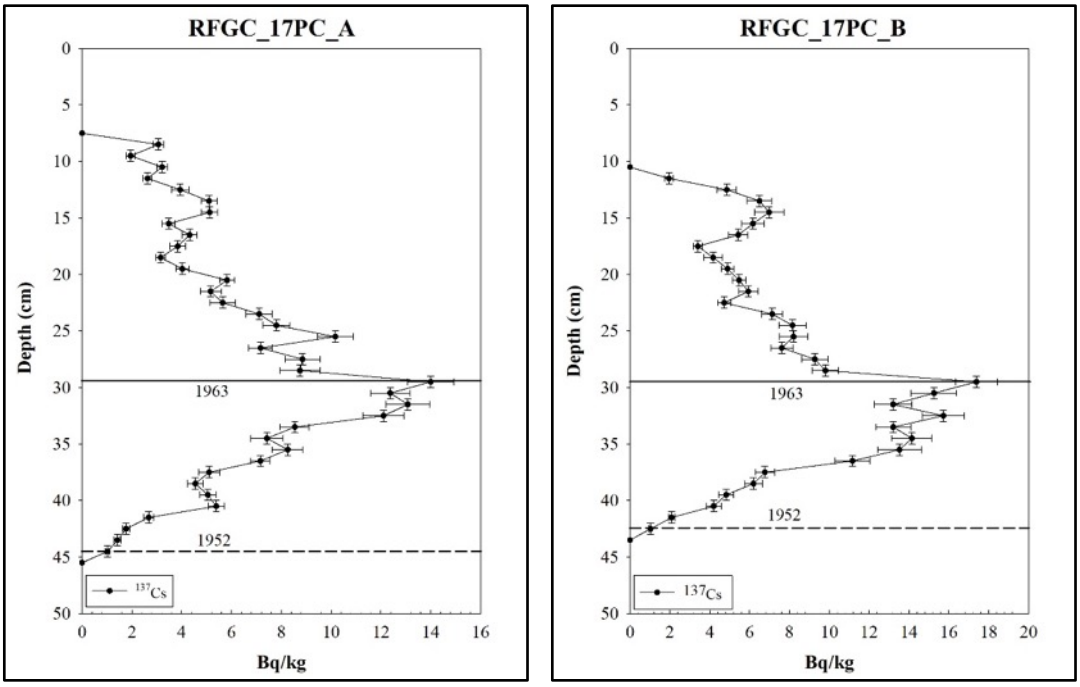

Figure 2.8. ^{137}Cs activity concentration profiles for push cores RFGC_17PC_A (left) and RFGC_17PC_B (right). The dashed and solid lines denote the years 1952, and 1963, respectively.

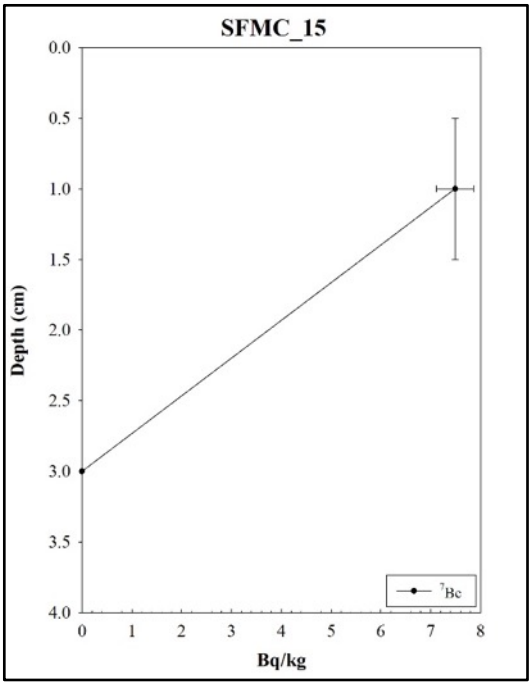

Figure 2.9. ^{7}Be activity profile for trench SFMC_15.

2.3.5.2 Alpha Spectroscopy and Sediment Accumulation Rates

Alpha spectrometry was performed on five of the six trenches and all three push cores sampled. The only site that did not yield $^{210}Pb_{ex}$ or ^{137}Cs was RFFB_18T, the sandy site where forest regeneration began after 1982 harvesting. The mined sites SFMC and BM had no detectable ^{137}Cs in the depth sampled, but do show $^{210}Pb_{ex}$. Grain size is similar for these three sites with very little clay present, but higher amounts of sands and gravel. Radionuclides readily absorb onto smaller grain size particles like clay and silt, but not sands or gravel (Mabit et al. 2008; He and Walling 1996; Matisoff et al. 2002). However, RFFB shows very low amounts of POC compared to SFMC and BM. The higher amounts of POC could explain the presence of $^{210}Pb_{ex}$ within the mined sites, but not at RFFB.

The inventories of $^{210}Pb_{ex}$ are listed in Table 2.4, along with the $^{210}Pb_{ex}$ inventory expected from atmospheric deposition alone, and sedimentation ratios based on $^{210}Pb_{ex}$. Sedimentation ratios indicate that RFGC_17T, VFWB, SFMC, and BM_07 show net erosion over the last century. RFMS and FCA cores suggest net deposition over the last century, since natural regeneration began. At the site where FRA was done after grassland (RFGC), both cores indicate net deposition since reclamation. MARs and LARs are listed in Table 2.5.

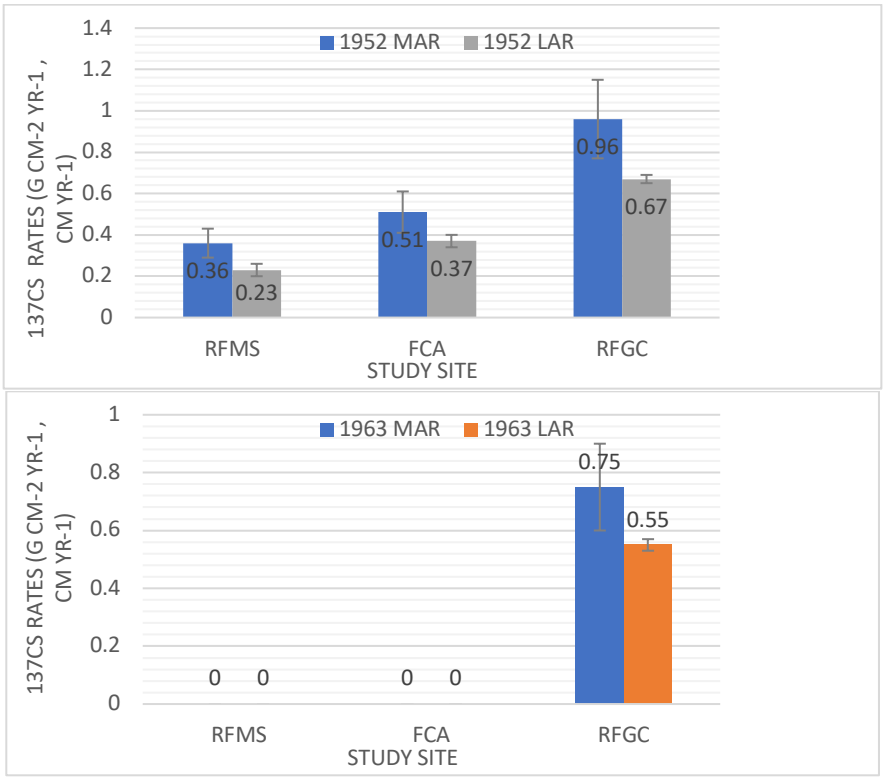

Figure 2.10. ^{137}Cs-based sediment accumulation rates based on the 1952 (top) and 1963 (bottom) time markers for RFMS, FCA, and RFGC. Values for RFGC are based on mean values for the two push cores taken at the site. Uncertainties reported at one standard deviation.

Table 2.4. $^{210}Pb_{ex}$ inventories for all cores compared against inventories expected from atmospheric deposition alone, and sedimentation ratios.

Trench/Core	$^{210}Pb_{ex}$ Inventory (mBq cm^{-2})	Sedimentation Ratio
Atmospheric	537.42	-
RFMS_17T	711.98	1.32
FCA_15	1,393.15	2.59
RFGC_17T	306.66	0.57
RFGC_17PC_A	1,032.33	1.92
RFGC_17PC_B	2,094.61	3.89
VFWB_17PC_A	52.92	0.09
SFMC_15	410.43	0.76
BM_07_16	9.55	0.02

Table 2.5. Comparison of average $^{210}Pb_{xs}$ Linear and Mass Accumulation Rates. All uncertainties reported at one sigma.

Trench/Core	$^{210}Pb_{ex}$ MAR (g cm^{-2} y^{-1})	$^{210}Pb_{ex}$ LAR (cm y^{-1})
RFMS_17T	0.20 ± 0.05	0.14 ± 0.04
FCA_15	0.58 ± 0.63	N.D.
RFGC_17T	0.14 ± 0.09	0.13 ± 0.08
RFGC_17PC_A	0.22 ± 0.15	0.23 ± 0.15
RFGC_17PC_B	1.11 ± 1.00	0.85 ± 0.76
SFMC_15	0.60 ± 0.33	N.D.
BM_07_16	N.D.	N.D.

Analysis of RFMS_17T (Figure 2.26) provides mass and linear accumulation rates determined using $^{210}Pb_{ex}$. Accumulation rates are the lowest around 80 years BP with values at 0.11 (g cm^{-2} yr^{-1}) and 0.08 (cm yr^{-1}) – this closely corresponds to the time period of logging. From 80 to 50 years BP rates increase to 0.23 (g cm^{-2} yr^{-1}) and 0.17 (cm yr^{-1}), as natural regeneration of the forest began. After this, rates remain between 0.20 to 0.24 (g cm^{-2} yr^{-1}) and 0.15 to 0.17 (cm yr^{-1}). The relatively strong linear regression fit for linear and mass accumulation rates (R^2 = 0.72; p = 0.03) indicates that sediment accumulation rates have steadily increased over time at this site.

Analysis of the drainage divide site (FCA_15) provides MAR data determined using $^{210}Pb_{ex}$ (Figure 2.27), spanning the last ~120 years BP. There is no LAR data for this site due to a lack of measured bulk density. The highest rates are seen at 101 years BP at 2.40 (g cm^{-2} yr^{-1}). This very high rate is likely due to logging activity that occurred up until 90 years BP around this site. Rates show a sharp decline from 100 to 80 years BP, corresponding to the period of natural regeneration. A strong exponential regression fit (R^2 = 0.77; p = 0.01) from 60 years BP to the present shows that accumulation rates have rapidly decreased within that 60-yr time period as the forest stand matured.

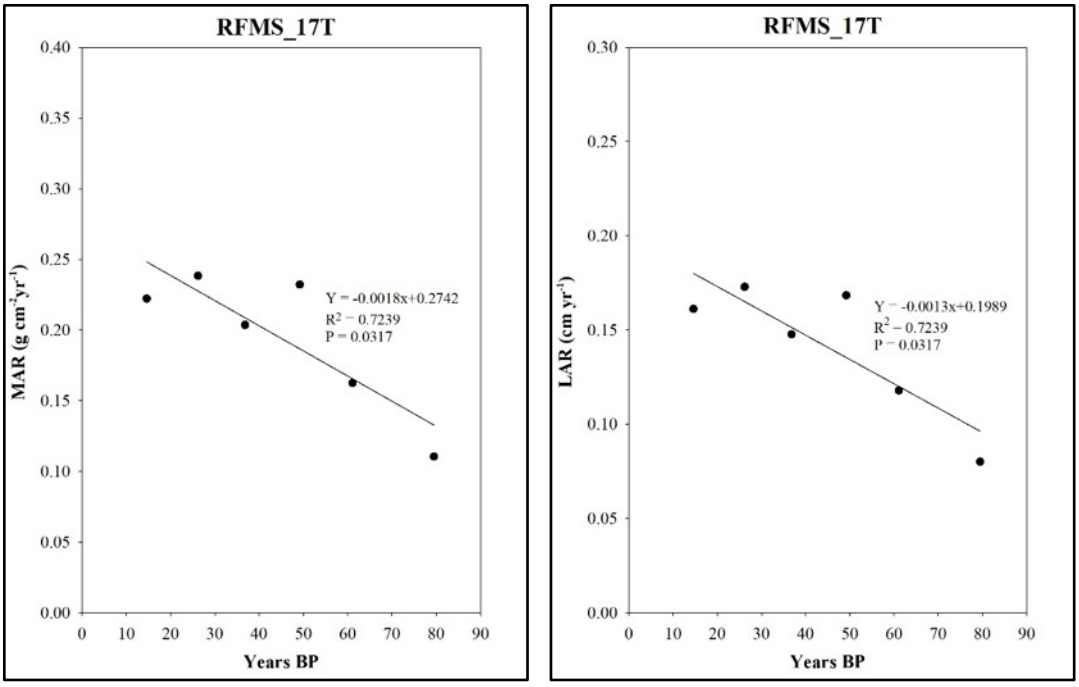

Figure 2.11. Sediment mass accumulation rates (left) and linear accumulation rates (right) for trench RFMS_17T.

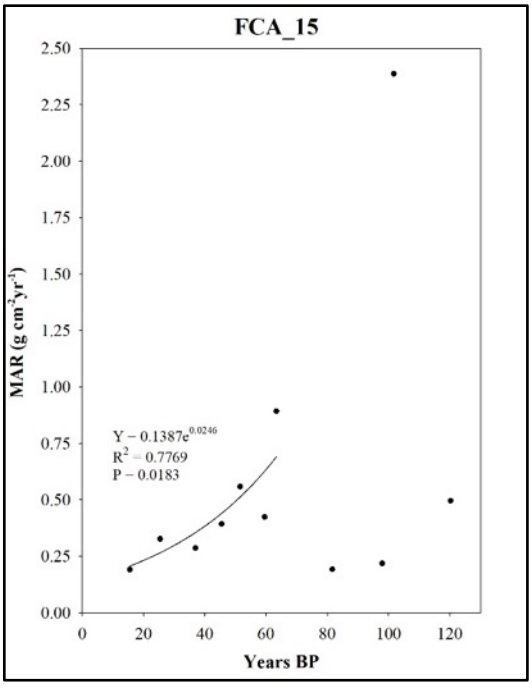

Figure 2.12. Sediment mass accumulation rates for trench FCA_15. Exponential regression is shown for data spanning 60 years BP to the present.

Analysis of the RFGC samples begins to shed light on the effects of FRA on erosion and sedimentation. The RFGC_17T (Figure 2.28) sample has few data points, so is difficult to interpret. The entire period of record has low MAR and LAR values (<0.27 g cm^{-2} yr^{-1} and cm yr^{-1}). Sediment MAR and LAR are measured up to 50 years BP, and the strong exponential regression fits (R^2 = 0.98; p = 0.01) indicate progressively increasing rates between 50 years BP and present. Because of the distribution of the data points, it is difficult to pinpoint sediment change due to the mining or reclamation. At 5 years BP, MAR is 0.27 g cm^{-2} yr^{-1} and LAR is 0.24cm yr^{-1}, which is equivalent to levels observed in the non-mined, naturally regenerating forest.

The $^{210}Pb_{xs}$ data from the two push cores collected in RFGC provide much better resolution than the trench site at RFGC_17T. RFGC_17PC_A (Figure 2.29) and RFGC_17PC_B (Figure 2.30) exhibit large differences in both sediment MARs and LARs, but exhibit similar trends in response to mining and reclamation. Sediment accumulation rates for RFGC_17PC_A are measured up to 110 years BP. Twenty years ago, when the site was reclaimed using grassland reclamation, the rates were 0.13 (g cm^{-2} yr^{-1}, and cm yr^{-1}). At 10 years BP, the FRA was implemented and an increase in MAR and LAR to 0.18 (g cm^{-2} yr^{-1}, and cm yr^{-1}) were observed in response to the disturbance. As the forest grew MAR and LAR dropped to about 0.15 (g cm^{-2} yr^{-1}, and cm yr^{-1}) 5 years BP, which is lower than the non-mined, naturally regenerating forest.

The average rates for RFGC_17PC_B are high when compared with all other sampling trenches and push cores. This push core did show the most robust $^{210}Pb_{ex}$
profile of all sampled sites. These highly elevated results are likely due to heterogeneity over small spatial scales; i.e., processes captured in the record at one core site were not captured at a second core site. There are strong exponential regression fits (R^2 = 0.85, P < 0.01) for both sediment LAR and MAR from 100 to 40 years BP, indicating that sediment accumulation rates rapidly increased during this period. From 40 years BP to the present, there is another set of strong exponential regression fits (R^2 = 0.72, P < 0.01) for both sediment LAR and MAR, indicating that sediment accumulation rates rapidly decreased during this period. Between 30 and 20 years BP, when the site was being mined, MAR and LAR rates more than double due to the disturbance. At 20 years BP the site was reclaimed as pasture, and MAR and LAR decrease to 0.55 (g cm^{-2} yr^{-1}) and 0.43 (cm yr^{-1}), respectively. After this, soils likely stabilized due to reclamation, and then sediment accumulation rates decreased further to 0.48 (g cm^{-2} yr^{-1}) and 0.37 (cm yr^{-1}). The site was again disturbed 10 years BP using the FRA, and sediment accumulation rates increased again to 0.67 (g cm^{-2} yr^{-1}) and 0.51 (cm yr^{-1}). In subsequent years, MAR and LAR decrease to 0.24 (g cm^{-2} yr^{-1}) and 0.21 (cm yr^{-1}), respectively. The most current levels are the lowest observed in 100 years, likely since the site was logged in the 1920's.

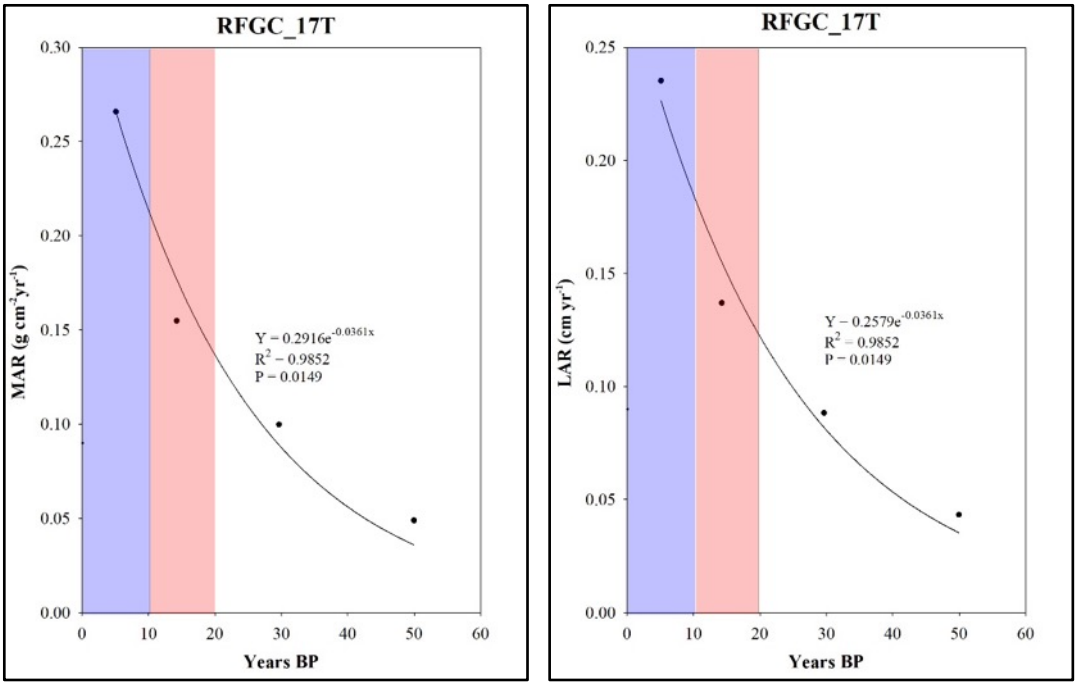

Figure 2.13. Sediment mass accumulation rates (left) and linear accumulation rates (right) for trench RFGC_17T. Shaded sections provide the timing of grassland reclamation (red) and the FRA (blue).

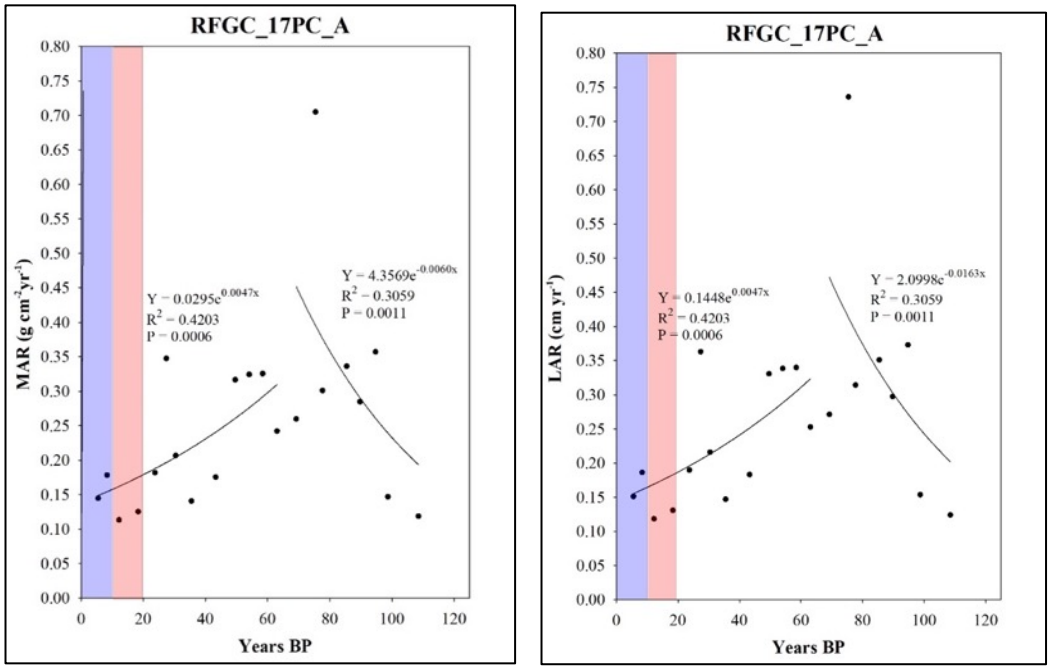

Figure 2.14. Sediment mass accumulation rates (left) and linear accumulation rates (right) for push core RFGC_17PC_A. Shaded sections provide the timing of grassland reclamation (red) and the FRA (blue).

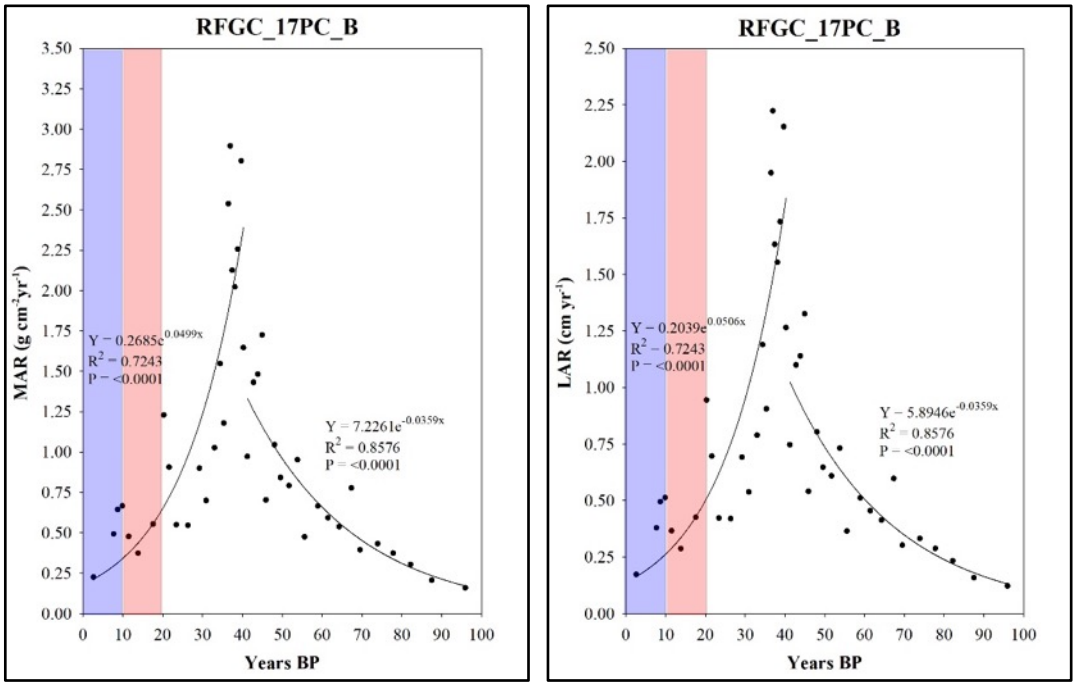

Figure 2.15. Sediment mass accumulation rates (left) and linear accumulation rates (right) for push core RFGC_17PC_B. Shaded sections provide the timing of grassland reclamation (red) and the FRA (blue). Exponential regression fits for 40 years BP to present are shown (left, both plots), as are fits from 40 to 100 years BP (right, both plots).

Both RFGC_17PC_A and 17PC_B exhibited an increase in MAR and LAR from 100 years BP to around 50 years BP. This is likely a response to logging that occurred in the area in the 1920's. Since these cores were taken near the outlet of the watershed, accumulation of eroded sediment from the logging disturbance would be expected.

VFWB SFMC_15 and BM_07 did not yield any useful ^{210}Pb data. This is likely due to the relatively young age of these reclaimed mine sites (5, 12 and 18 yrs., respectively) and the fact that all three sites were comprised of fill material (topsoil substitute or end dumped spoil). In contrast, RFGC was sampled in an intact floodplain just below the toe of the valley fill in the unmined riparian corridor.

2.3.6 Particulate Organic Carbon and Stable Isotopes

2.3.6.1 Particulate organic carbon and bulk density

The POC concentrations were determined for samples from all six trenches and the three push cores. Bulk density was calculated for all sampling sites with the exceptions of the drainage divide (FCA_15), SFMC_15 and BM_07_16. All cores and trench data show, as expected, an inverse relationship between POC and bulk density, with bulk density increasing with depth

while POC concentrations decrease. At all sites, POC is enriched at the surface (as expected). POC inventories over the top 10 cm, and POC fluxes (determined using $^{210}Pb_{ex}$-based rates) are listed in Table 2.6. Inventory and flux values are depicted in Figure 2.31. POC inventories are also compared with $^{210}Pb_{ex}$ based mass accumulation rates in Figure 2.32.

Table 2.6. POC inventories (1-10 cm), and surface (0-2 cm for trenches; and mean value of 1-2 cm for push cores) POC fluxes for all cores and trenches. POC fluxes are calculated using mean $^{210}Pb_{ex}$-derived sediment accumulation rates.

Trench/Core	POC Inventories (g cm^{-2})	POC Flux (g cm^{-2} y^{-1})
RFMS_17T	0.157	0.004
FCA_15	0.831	0.120
RFFB_18T	0.032	N.D.
RFGC_17T	0.204	0.003
RFGC_17PC_A	0.251	0.018
RFGC_17PC_B	0.772	0.203
VFWB_17PC_A	0.229	N.D.
SFMC_15	0.369	0.019
BM_07_16	0.369	N.D.

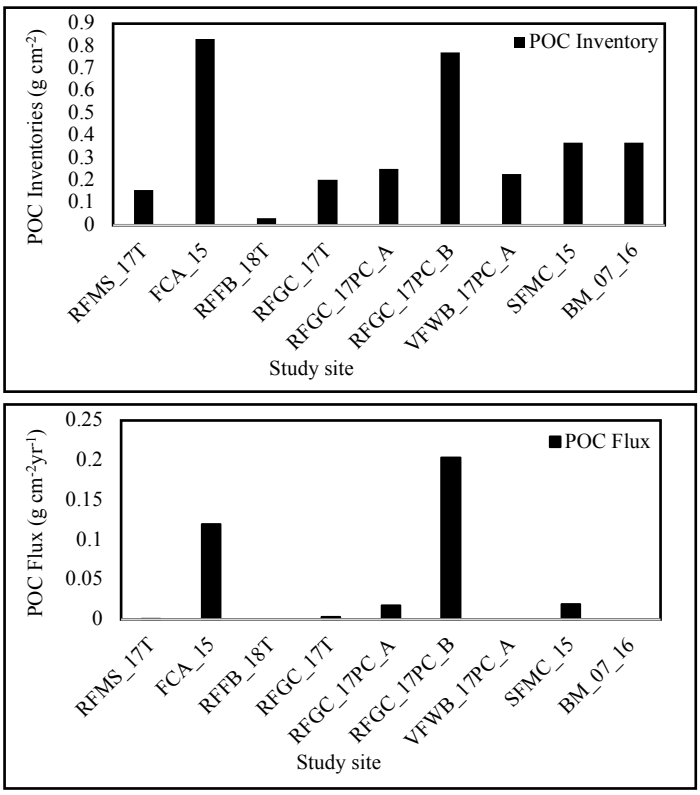

Figure 2.16. POC inventory (1-10 cm) (top), and POC flux (bottom) for all study sites.

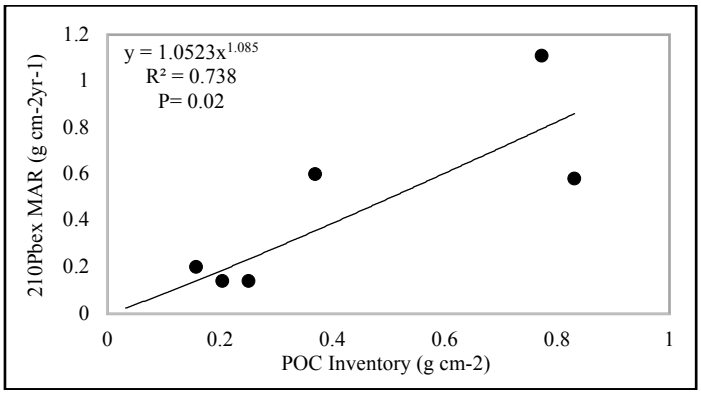

Figure 2.17. Comparison of $^{210}Pb_{ex}$ mass accumulation rates and POC inventories for all sites.

The two control sites, the naturally regenerated riparian (RFMS_17T) and ridgeline (FCA_15) sites (Figure 2.33), both show similar trends in POC concentrations with depth. In both trenches, POC concentrations are highest near the surface and decreases with depth with the exception of slight increases at 14 and 32 cm for the riparian area (RFMS_17T), that may result

from the buried channel before logging. The two push cores RFGC_17PC_A and RFGC_17PC_B (Figure 2.35), together with RFGC_17T, show similar trends to the control sites, but with increases in POC at depth that may reflect different stages in the mining, grassland reclamation, and FRA reclamation. RFGC_17PC_A and RFGC_17PC_B show almost identical POC concentration profiles, with RFGC_17PC_B having much higher maximum POC concentrations.

The trenches from the reclaimed mine lands at SFMC_15 and BM_07_16, as well as the more recently timbered RFFB_18T, show minimal changes in POC with depth – reflecting the recency of reclamation. The push core from the traditional grassland reclamation (VFWB_17PC_A) site (Figure 2.37) shows a 5% POC in the top 2 cm, suggesting the incorporation of POC as a result of the dense root network under a grassed surface.

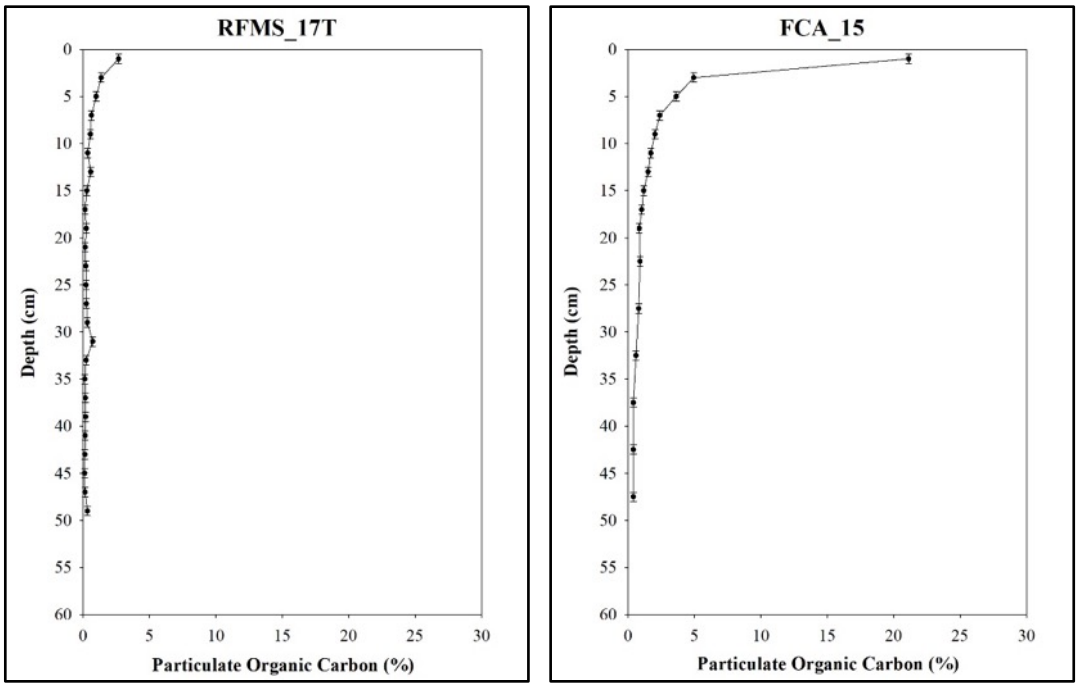

Figure 2.33. Particulate organic carbon (POC) concentration profiles for trenches control site trenches at the naturally regenerated riparian (RFMS_17T - left) and drainage divide (FCA_15 - right).

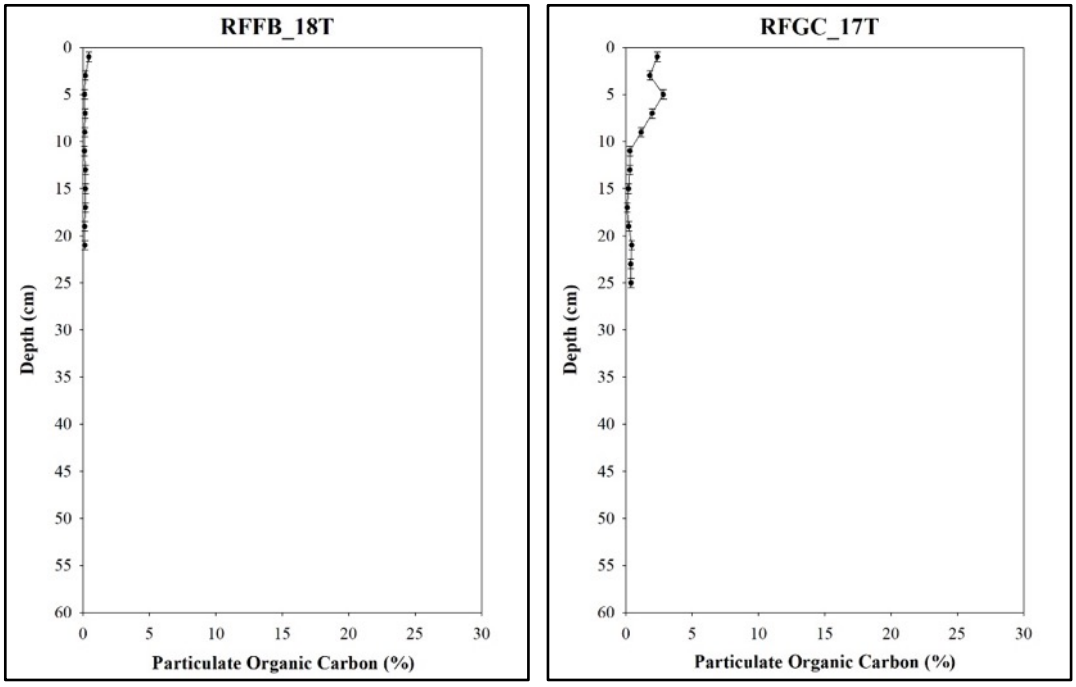

Figure 2.34. Particulate organic carbon (POC) concentration profiles for trenches RFFB_18T (left) and RFGC_17T (right).

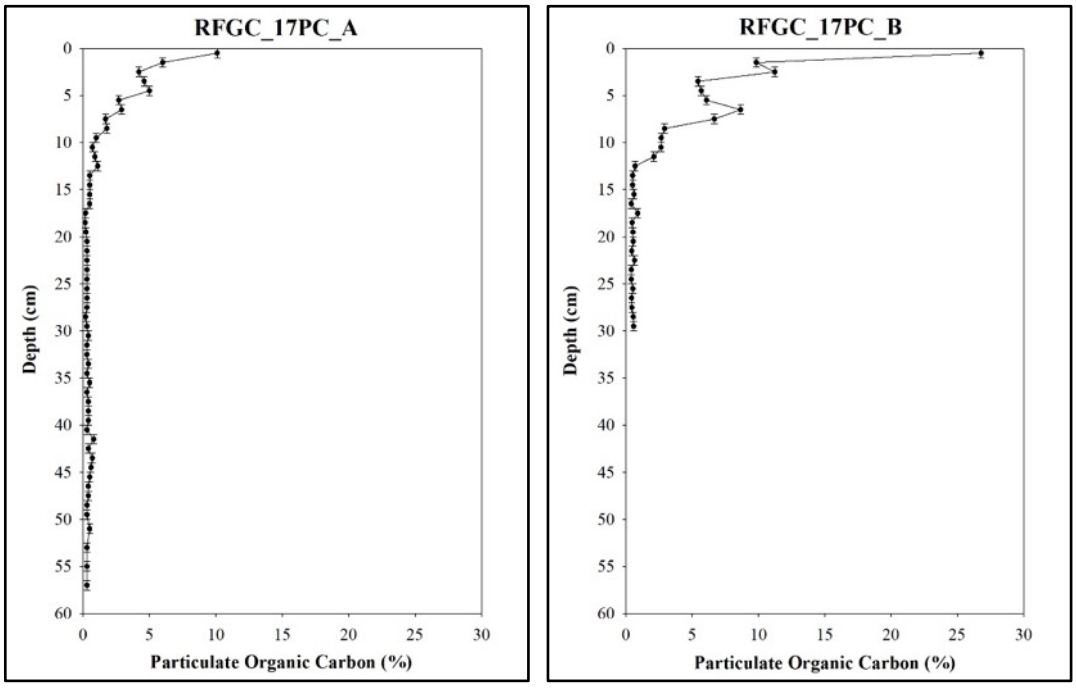

Figure 2.35. Particulate organic carbon (POC) concentration profiles for push core RFGC_17PC_A (left) and RFGC_17PC_B (right).

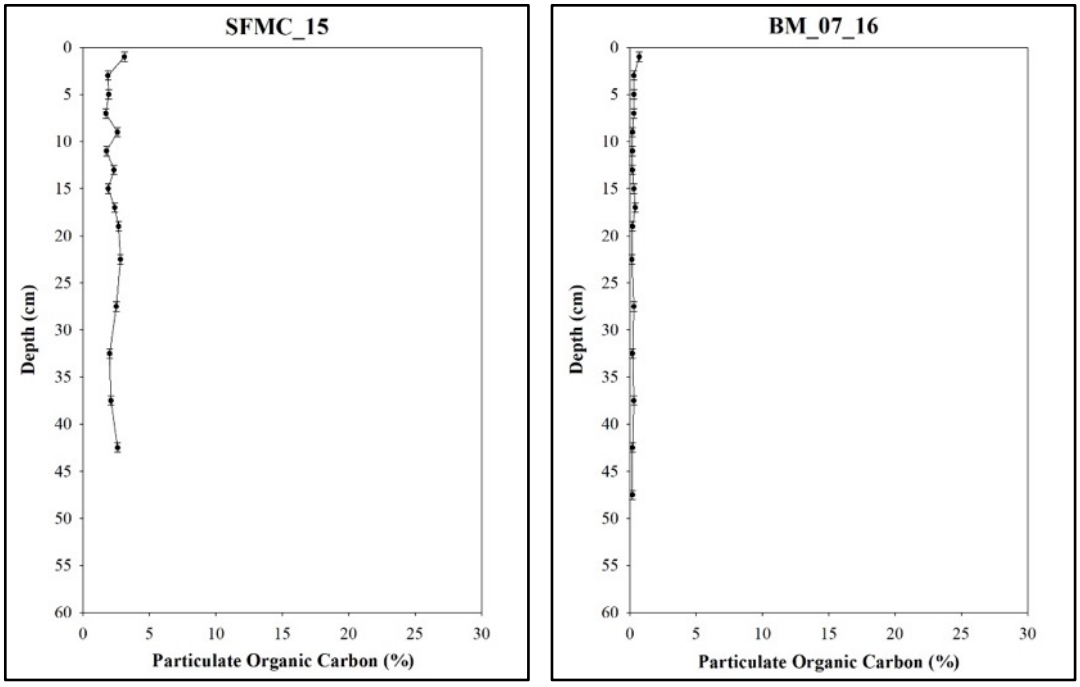

Figure 2.36. Particulate organic carbon (POC) concentration profiles for trenches SFMC_15 (left) and BM_07_16 (right).

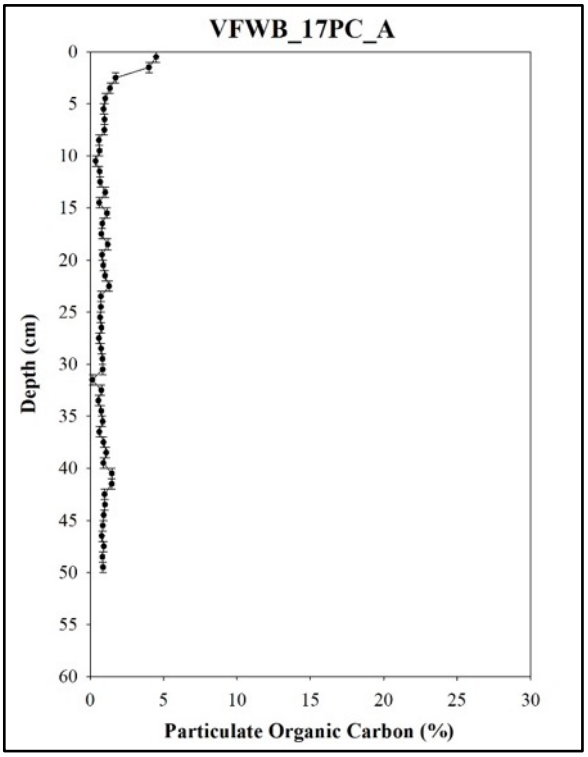

Figure 2.37. Particulate organic carbon (POC) concentration profile for push core VFWB_17PC_A.

2.3.6.2 Stable Carbon Isotopes

Stable carbon isotope data were compiled for five trenches and the three push cores. Gaps in $\delta^{13}C$ profiles are due to carbon isotope values that did not fall within acceptable detection limits. All $\delta^{13}C$ profiles fall within values associated with forested landscapes and a C3 pathway (-20‰ to -35‰). Trenches at the riparian (RFMS_17T) and drainage-divide (FCA_15) control sites are depicted in Figure 2.38. The values at RFMS_17T fall between -25‰ to -29‰. $\delta^{13}C$ data for FCA_15 range from -28‰ to -26.1‰, and show an enrichment in ^{13}C (less negative numbers) in the top 5-10 cm.

Among the reclaimed sites, many show a similar enrichment in ^{13}C between the surface and approximately 10 cm depth. The push core from RFGC_17PC_A (Figure 2.40) similarly exhibits enrichment in ^{13}C with within the top 5-10 cm, with $\delta^{13}C$ values range from -31‰ to -25.5‰, followed by a depletion that is mirrored in RFGC_17PC_B. $\delta^{13}C$ values for RFGC_17T similarly range from -26.8‰ to -29‰, but several samples, including the surface did not have enough material for successful analysis. The BM_07_16 and SFMC_15 (Figure 2.41) both show a slight shift to more positive $\delta^{13}C$ values as depth increases. SFMC_15 values range from -26.9‰ to -25.2‰ and shift to more positive values with increasing depth. BM_07_16 shows a slight enrichment with increased depth with values ranging from -27.6‰ to -25‰. The values for VFWB_17PC_A range from -28‰ to -25.5‰ with an overall enrichment in ^{13}C with increasing depth, with the exception of a depletion of ^{13}C at 23 cm, it is notable that although this site had been in grassland for 5 years when sampled, the $\delta^{13}C$ still reflects a forested community.

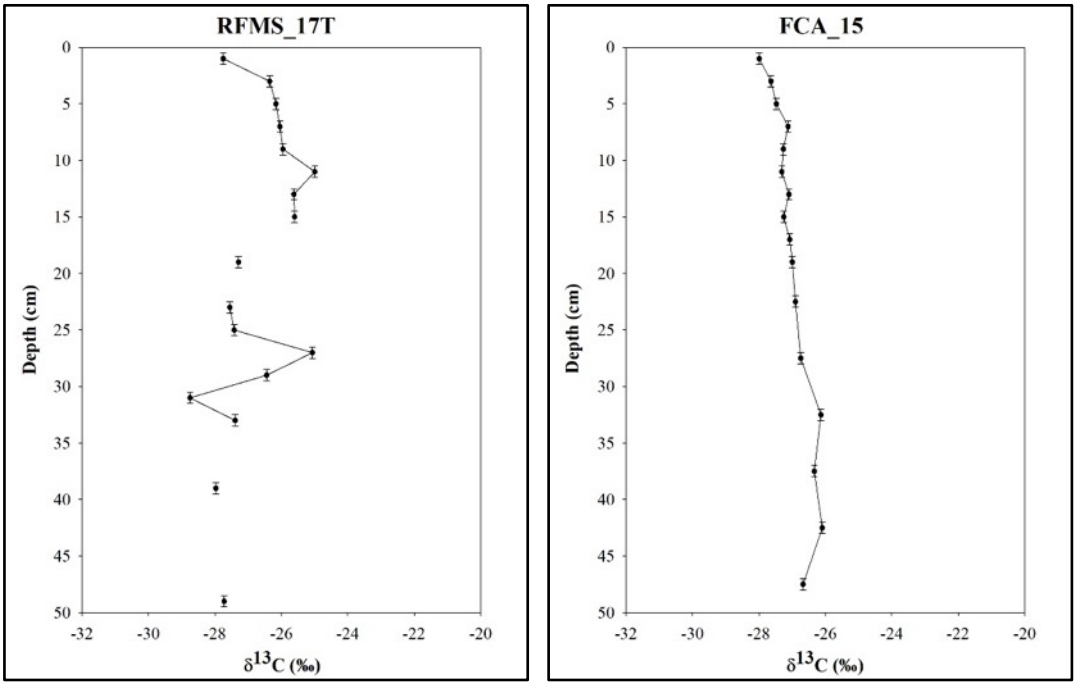

Figure 2.38. $\delta^{13}C$ profiles for trenches RFMS_17T (left) and FCA_15 (right).

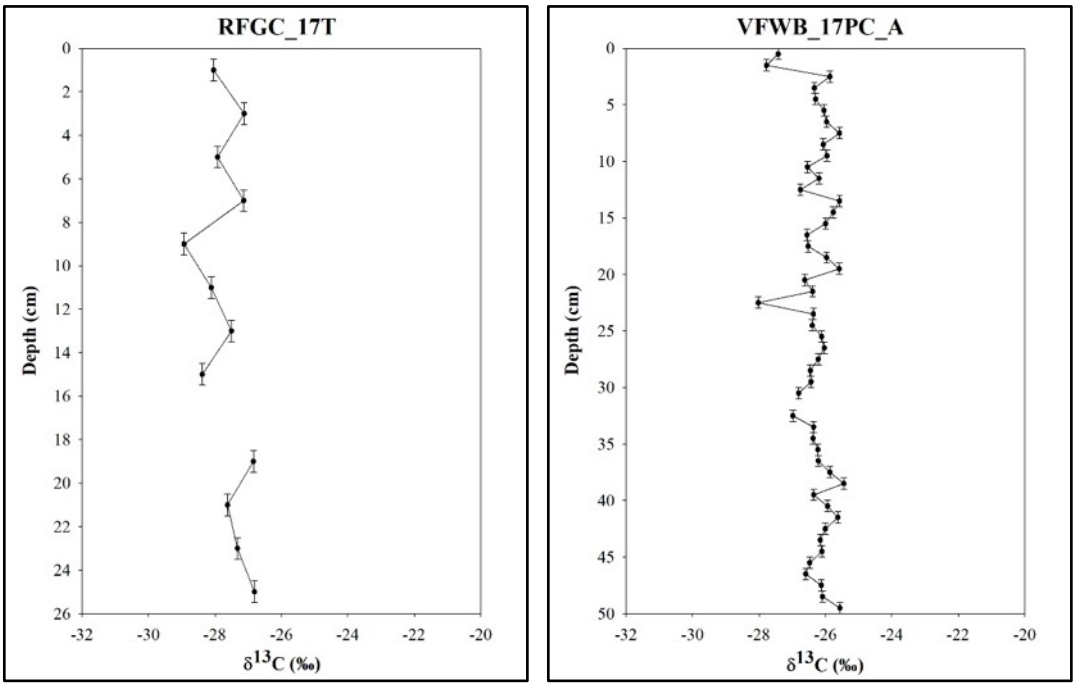

Figure 2.39. $\delta^{13}C$ profiles for trench RFGC_17T (left) and push core VFWB_17PC_A (right).

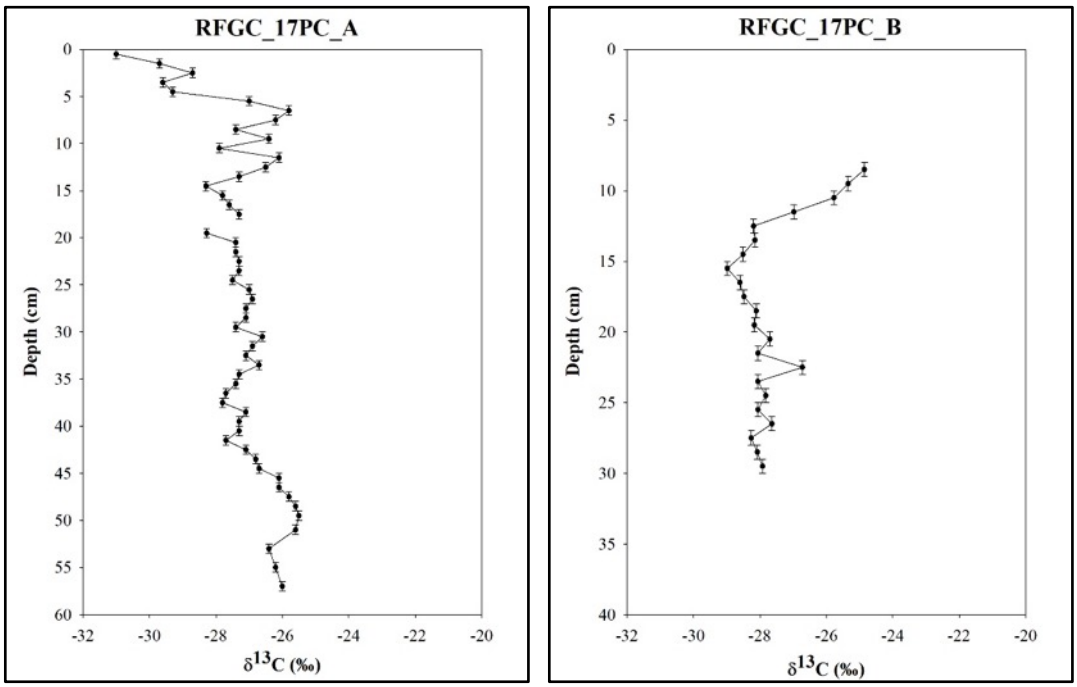

Figure 2.40. $\delta^{13}C$ profiles for push cores RFGC_17PC_A (left) and RFGC_17PC_B (right).

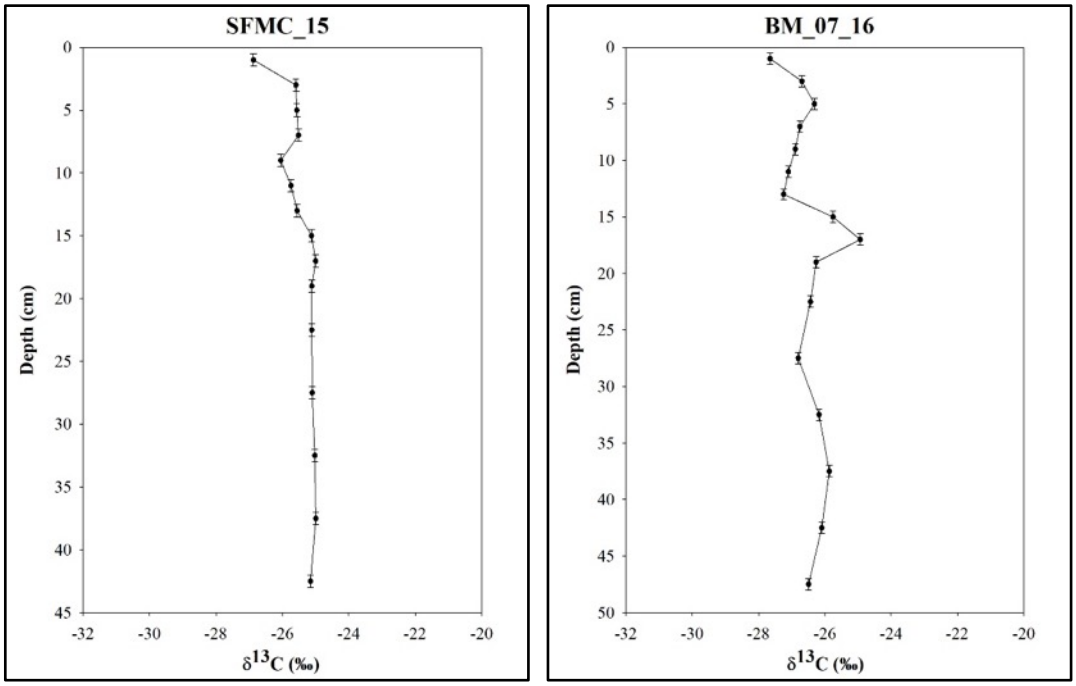

Figure 2.41. $\delta^{13}C$ profiles for trenches SFMC_15 (left) and BM_07_16 (right).

2.5 DISCUSSION

Little work has been done to measure sediment accumulation rates, and bulk changes in sedimentary organic matter in reclaimed mine lands and formerly logged areas. The findings of this study could potentially aid in the recovery of native hardwood forests that have been adversely impacted by the effects of strip mining and logging, in Kentucky and elsewhere.

The riparian control site (RFMS_17T) had similar proportions of silt and sand in the top 5 cm, and then became more sandy at depth, reflecting the parent material (Figure 2.14; ~50% over the whole section), with no erratic variations in particle size distribution within the fining upward sequence of the top 16 cm. The changes in grain size from 20 cm to the 50-cm depth of the core may indicate an increase in the energy of the depositional environment. Due to this site's close proximity to a stream, this could be a result of flooding events in 2009, since mining did not occur at this site. Radionuclide data (see below) suggests that sediments deeper than ~20 cm likely represent the period during or immediately following active logging in this sub-basin, which is in congruence with the presence of appreciable gravel (20-40%) and less silt between 20 cm and the end of the section. POC concentrations and inventory for the site (Figure 2.33) do not show any irregularities, but there is less organic carbon at this site compared to the other control site at FCA (POC inventories are lower than FCA by more than a factor of 4). This is likely due to the location where sampling occurred (virtually no surface vegetation) and the potential for removal of organic matter from scouring events.

Neither ^{137}Cs (Figure 2.19) nor $^{210}Pb_{ex}$ are found below 15 cm in RFMS_17T, suggesting that sediments below this depth represent ~100 years BP or more (during or immediately following active logging). The relatively strong linear regression fit for $^{210}Pb_{ex}$ sediment accumulation rates (Figure 2.25) show a gradual increase over the last century. Given that this site was located in a floodplain of a steep sloping watershed, sediment accumulation is anticipated. The increase in sedimentation could also be due to an overall increase in stream power. Both logged and undisturbed watersheds have shown increases in sedimentation with higher stream power (Rice et al. 1979). Periods with decreased streamflow could have been caused by large influxes of woody debris to streams from logging activity. Typically, undisturbed logged watersheds do not transport large amounts of woody debris (Benda 2005), so higher amounts of woody material could create dams that slow stream flow. The ^{137}Cs-based sediment accumulation rates from 1952 are a bit higher than the average $^{210}Pb_{ex}$ accumulation rates (Tables 2.3 and 2.5), but compare reasonably well. Both radionuclides do indicate that over the last century the site has shown net deposition (Tables 2.2 and 2.4).

The trench grain size profile at the upland control site FCA_15 (Figure 2.14) shows a coarsening upwards sequence from ~20 cm to the surface (increasing gravel and decreasing silt) with no erratic changes in particle size distribution over the section. This does not appear to be out of the ordinary due to the site's location at a ridgetop. In this setting, very fine-grained sediments are either not deposited, or can be eroded by wind and rain, or localized events (Foufoula-Georgiou et al. 2010). The upper 10 cm of this site are dominated by gravel likely from colluvium, with the rest dominated by silt-sized particles (20-40%) with some sand (5-30%) and minor clay (5-10%). The POC concentrations, inventory and flux for this site are all much higher than the other two logged sites in the study (Figure 2.33). This is very likely due to its location, presence of a mature hardwood forest and lack of recent disturbance.

The FCA_15 site saw ^{137}Cs extending to 19 cm (Figure 2.20) and $^{210}Pb_{ex}$ to 27 cm, suggesting that sediments below this depth (27 cm) represent more than 100 years BP. As such, one or both of these radionuclides record the period during which this area was logged. $^{210}Pb_{ex}$ based sediment accumulation rates from ~120-70 years BP are erratic (Figure 2.26), but capture the highest resolved sediment accumulation rate (~2.49 g cm^{-2} y^{-1}) of any site, at ~100 years BP, when this area was actively logged. A strong exponential regression fit for $^{210}Pb_{ex}$ (Figure 2.26) shows that rates sharply declined from 60 BP to the present. This is likely due to the regrowth of forests in the area.

The two push cores collected from Guy Cove, RFGC_17PC_A and RFGC_17PC_B, show many similarities to one another, as expected. Both grain size profiles (Figure 2.16) exhibit fining upward sequences from ~20 cm to the surface. This same trend (from ~12 cm to the surface) is seen within the trench collected from this site. In both cores, the sections below 20 cm are dominated by sands (50-80%), with appreciable gravel appearing below 70 cm in core A (up to ~20%). These coarser sediments could reflect a higher energy setting and a different, and dominantly coarser, supply of sediment than in recent time, both likely due to mining. Another explanation for the courser sediments is that it represents and older stream bed that was buried. POC concentrations, inventories and fluxes for both sites show the same trends, but RFGC_17PC_B shows the highest POC flux, and second highest POC inventory (after control site FCA) of all stations (Figure 2.35). The differences observed between the two cores and one trench sampled at this site reflect heterogeneities over small spatial scales.

The ^{137}Cs-based sediment accumulation rates for RFGC_17PC_A and RFGC_17PC_B are similar to one another, as expected. Both cores show that rates decreased from 1952 to 1963 (Table 3). Strong exponential regression fits to $^{210}Pb_{ex}$ derived sediment accumulation rates from RFGC_17PC_B (Figure 2.29) show that accumulation rates rapidly increased from ~100 years to

~40 years BP, and then rapidly decreased from ~40 years BP to the present, with some fluctuations over the last ~30 years BP.

This large spike in accumulation rates at RFGC_17PC_B occurred before mining began around this site in the late 1980s. The increase in accumulation rates around 30 years BP are likely from the surface mining that occurred within the watershed. No sediment control structures were place below the valley fill, so sediment discharge was likely. As such, the site was net depositional, which is supported by both ^{137}Cs and $^{210}Pb_{ex}$ sedimentation ratios (Tables 2.2 and 2.4). The site was reclaimed using grassland reclamation 20 years BP, and was then re-disturbed 10 years later to implement the FRA. After implementation of the FRA, accumulation rates initially increased likely due to the disturbance. Approximately 115,000 cubic meters of material were dug out of the fill and redistributed as "end-dumped" FRA during the restoration project (Agouridis et al. 2018). The site was planted with 30,000 trees and exhibited a stem density of 1,539 stems per hectare after five years. The growth of the planted trees likely contributed to the quick reversal of the sediment accumulation and to the low MAR and LAR levels observed in the most recent date (Figure 2.29). Increased canopy interception (as discussed in Chapter 1) will reduce the erosive power of rainfall and likely decrease streamflow in the RFGC system, thereby reducing the sediment discharge from the watershed.

The grain size distribution for trench SFMC_15 (Figure 2.17) shows that this is the only site dominated by gravel sized particles over the entire section, with the highest value at 90%, and average value at ~60%. This is to be expected as the site was reclaimed using end-dumped FRA and the soil was composed entirely of weathered and unweathered spoil. Similarly, the grain size profile for BM_07_16 (Figure 2.17) shows high quantities of sands and gravels, with moderate amounts of silt (~20-30%) and little clay (~5%). As with SFMC, the BM site was reclaimed using end-dump FRA with no salvaged topsoil used in its creation. There was no ^{137}Cs present at SFMC_15 and BM_07_16 because the sites were created out of overburden and interburden that had not been exposed to fallout until the mining was initiated (18 and 12 years, respectively).

The grain size distribution for VFWB_17PC_A (Figure 2.18) is dominated by silts and sands, and appears fairly consistent over the entire section. Gravels are present throughout much of the section, comprising as much as 20% in places, with lesser amounts of clay-sized particles (~$\leq$10%). These results should be expected due to the very young age (5 years) of this reclaimed mining site. This explains the lack of ^{137}Cs, and very limited $^{210}Pb_{ex}$ data. Any sediments deposited here prior to mining were likely either eroded, or deeply buried during mining due to subsequent valley fill operations with sediments lacking either of these radionuclides. POC concentration data for this site follows the normal trend seen with other sites but is slightly

irregular at the surface (Figure 2.37), likely due to the presence of a wetland below the valley fill.

The recently harvested (1982) and naturally regenerating riparian site (RFFB_18T) was the most difficult to characterize using the included methods among study sites, likely as a combination of the small basin size (9 ha) and recent flooding. This soil is sandy (>50% sand), with appreciable gravel (~20% throughout), with little variability in the profile and rock at 20 cm depth. The larger amount of gravel at the base of the trench (~40%) could indicate a change in the energy of the depositional system. The presence of more sand at this site is likely the reason that radionuclides are absent. However, the site is adjacent to a stream and sediments with radionuclides could have also been removed during scouring events from floods that occurred within the watershed in 2009. POC concentrations and inventory for this site (Figure 2.34) are the lowest of all study sites. These low quantities of POC could also be an indicator of scouring at the study site. Logging ceased in this area over 36 years ago, but the site shows less organic carbon than the other two logging sites and the most recently reclaimed mining sites at VFWB and BM_07.

2.6 CONCLUSION

The grain size and radionuclide data from this study are valuable tools for understanding the complex erosion, sediment transport and depositional processes following coal mine reclamation in eastern Kentucky and other parts of the world. The results for RFGC are a good indicator of increased sediment loading due to valley fill operations, as seen by the increase in sediment accumulation during the active mining phase, and subsequent decrease in accumulation rates through the various reclamation phases.

POC data was useful for showing increasing carbon in the surface of the reclaimed sites and was influenced by time since reclaimed. As described by Maharaj et al. (2007) and Sena et al. (2018), carbon accumulation in the upper soil horizon (top 5-cm) begins to increase as the trees mature and the canopy closes. Ample litter fall and root turnover allow for decomposition to occur and enrichment of organic carbon in the soil profile. As the trees mature, soil deeper in the profile will become more enriched.

The ^{7}Be data present in this study could be a potential tool for observing soil weathering or short-term bioturbation (Sharma et al. 1987) at the reclaimed mines and regenerated watersheds. ^{7}Be is only present at older sites (RFMS, FCA, RFGC_17T, and SFMC) and not the RFFB where POC was limiting. The presence of ^{7}Be at the older mine sites supports the rapid spoil genesis on FRA sites as described by Miller et al. (2012) and Sena et al. (2018).

3. EVALUATING THE INFLUENCE OF THE FORESTRY RECLAMATION APPROACH ON WATER QUALITY

3.1 INTRODUCTION

Between 60 and 80% of the cumulative channel length in mountainous areas, such as eastern Kentucky, is comprised of headwater streams (Shreve 1969). These headwater streams are vital components of the landscape and to the overall function of aquatic ecosystems. Headwater streams serve as the primary pathways for water, sediment and organic matter transport to higher-order stream systems (May and Gresswell 2003). Gomi et al. (2002) noted that headwater regions receive and mediate the majority of surface runoff in mountainous watersheds, thereby serving as regulators of flow intensity (e.g., flooding) for lower gradient regions. Additionally, headwater streams support large populations of macroinvertebrates, amphibians, and fish thus effectively increasing biodiversity as well as providing habitat for rare and endangered species (Petranka and Murray 2001; Lowe and Likens 2005; Meyer et al. 2007; Clark et al. 2008; Brannon and Purvis 2008).

Surface mining, and in particular mountaintop mining with its associated valley fills, poses a significant environmental risk to aquatic and terrestrial life through the direct conversion of headwater streams to uplands and the associated degradation of downstream receiving waters. Among the potential consequences to downstream waters are increased sedimentation, elevated specific conductance, and substantial changes in pH (Pond et al. 2008; USEPA 2011). With regards to water chemistry, one of the largest impacts of mountaintop mining and valley fills involves dramatic increases in specific conductance or total dissolved solids (Pond 2004; Hartman et al. 2005; Pond et al. 2008). In one study, the average specific conductance among reference streams in Kentucky's Eastern Coal Fields (ECF) was 63 µS cm^{-1}, whereas the average of streams draining valley fills was 1,096 µS cm^{-1} (Pond 2004). Biota in forested headwater streams of the ECF are accustomed to an aquatic environment with low dissolved solids. Pond et al. (2008) and Green et al. (2000) found significantly fewer taxa and lower percentage of individuals belonging to the insect orders Ephemeroptera, Plecoptera and Trichoptera (EPT taxa) when specific conductance was greater than 500 µS cm^{-1}. From a food web perspective, these effects trickle through individual predator-prey relationships thus impacting a multitude of species that utilized the habitat prior to mining.

In light of the importance of headwater streams, development of practical stream restoration techniques for mined lands is crucial in order to restore impacted headwater stream systems. Stream restoration efforts are predominately focused on waterways in agricultural and urban

settings (Bernhardt et al. 2005) with a relatively limited number of projects on mined lands (Palmer and Hondula 2014). Often employing natural channel design (NCD) techniques, stream restoration practitioners utilize reference reaches to design new channels with the appropriate dimensions, patterns and profiles (Rosgen 1998; Hey 2006). The crux of the NCD approach is the ability of the designer to locate appropriate reference reaches, ones with similar hydrogeological characteristics (e.g., watershed area, valley type, geology, soils, and climate) to the impacted reach. Mined lands, particularly valley fills, present a unique challenge to stream restoration designers in that the valley configuration is notably altered from its prior natural state, the geologic age of the material in the structure itself is relatively young as buried strata are now exposed meaning the weathering process is new, and the water table is now located tens to hundreds of meters below the reclaimed ground surface.

Furthermore, modifications to vegetative communities (e.g., the conversion of forests to grasslands) result in altered hydrology, water chemistry, and habitat (Bosch and Hewlett 1982; Zipper et al. 2011). Efforts to restore forested communities on mined lands in Appalachia have resulted in the Forestry Reclamation Approach (FRA), which consists of five steps: (1) selecting the best available growth medium, (2) minimizing compaction during placement of the rooting medium, (3) selecting appropriate tree species based on approved post-mining land use and site specific characteristics, (4) using tree compatible ground cover, and (5) using proper tree planting techniques (Burger et al. 2005; Zipper et al. 2011). Research surrounding the FRA has documented successful regrowth of hardwood forests (Torbert and Burger 1994; Graves et al. 2000; Sena et al. 2015) while mimicking pre-mining hydrologic conditions (Taylor et al. 2009a; Taylor et al. 2009b; Sena et al. 2014).

With regards to the use of FRA on water chemistry, findings indicate that following an initial flush in fines during the first few years, a rapid decrease followed by stabilization occurs with many water quality constituents, including specific conductance, following the first few years of spoil placement (Agouridis et al. 2012; Sena et al. 2014). However, these finding were done at the plot level (1-acre FRA end dump cells) and water quality effects at the watershed scale have not been reported. In an effort to replace lost headwater stream form and function, improve water quality, and enhance aquatic and terrestrial habitat, researchers at the University of Kentucky recreated a headwater stream system on a valley fill in 2008 utilizing NCD techniques and the FRA. The project resulted in the creation and enhancement of 1,450 m of ephemeral, intermittent and perennial streams, 0.1 ha of vernal pools, and 16.2 ha of hardwood forest. After ten years, the site is fully forested and canopy closure is evident throughout much of the watershed. As shown in Chapter 1, we expect many of the forest hydrologic function with regards to canopy interception and throughfall to be similar to that of an unmined young forest. What effect that will have on water chemistry will be examined in this Chapter.

3.2 METHODS

3.2.1 Site Description

The project was located at the University of Kentucky's Robinson Forest, which is an over 6,000 ha experimental forest located in southeastern Kentucky. Robinson Forest is comprised of eight discontinuous properties, with the main block comprising over 4,100 ha. Research, extension and education activities conducted at the forest are largely performed on the main block. The forest sits within the rugged eastern section of the Cumberland Plateau, and its landscape consists of long, rectilinear side slopes cut into a horizontally-bedded substrate of sandstone, shale, siltstone and coal (Smalley 1984). The vegetation is typical of the mixed mesophytic forest region and ranges from xeric oak-pine dominated stands to rich mesic cove hardwoods (Braun 1950; Carpenter and Rumsey 1976). The climate is humid and temperate with an average annual rainfall of 123 cm and mean monthly temperatures ranging from about 2°C in January to about 24°C in July (USDC 2002).

The University of Kentucky acquired Robinson Forest in 1923 after extensive logging. As such, the majority of the forest is comprised of 90+ year old second growth. During the early to mid-1990s, a portion of Robinson Forest was mined for coal resulting in the creation of several valley fills. In the valley that was once known as Guy Cove, over 1.8 million m^3 of spoil was placed over the top of a headwater stream system. The Guy Cove valley fill (Figure 3.1) consisted of a crown, which was designed to slope away from the face toward the back of the fill at a slope of 1%, a face which was constructed of three 15.2 m tall benches each with a 3% back-slope and a 2:1 (H:V) drop, two groin drains (rock-lined) along both sides of the face, and an underdrain (approximately 5 m x 2.5 m in size). The presence of ponded water (approximately 0.2 ha) at the back of the crown indicated that the underdrain was experiencing some level of clogging. Valley side slopes, along the crown, were regular and steep (2:1 H:V) with ephemeral gullies interspersed throughout. A sediment-laden pond was located at the toe of the valley fill. Because a lesser amount of coal was present than anticipated (e.g., the coal seam ended before reaching the valley ridgetop), Guy Cove was not completely surface mined. Instead, a 9 ha section at the most upgradient portion (ridgetop) of the valley experienced some clearing and grubbing (e.g., removal of trees) only. A small spring-fed channel flows nearly year-round (average baseflow of 55 m^3 d^{-1}) from this unmined section. This streamflow was directed into the underdrain at the interface with the mined section. The Guy Cove watershed is 44 ha in size, and prior to restoration, had a drainage density of 0.0034 m m^{-2}.

3.2.2 Pre-Restoration Water Quality and Vegetation

Movement of water through the unconsolidated fill has resulted in poor water quality for the watershed and downstream environments (Table 3.1). Examination of water samples collected on a monthly basis starting in June 2004 indicated that specific conductance, chloride, sulfate, calcium, magnesium, potassium and sodium concentrations in Guy Cove were well above that observed from a nearby unmined reference watershed, Little Millseat (LMS) (Mastin et al. 2011). The concentrations observed reflect a problem that is prevalent throughout surface mining areas of central Appalachia. Of particular concern was specific conductance and manganese levels, which were both above discharge water quality standards for active mine sites (Code of Federal Regulations 1996). Evidence of erosion and deposition was common throughout Guy Cove. Fine grain sands had accumulated in low gradient areas and had resulted in a notable level of embeddedness in receiving waters. An iron rich flocculent was observable in waters emanating from the underdrain, which indicated the presence and oxidation of pyrite (FeS_2). Low pH values were typically observed where iron precipitation was present; however, buffering from high dissolved solid concentrations and subsequent alkalinity production had maintained a neutral pH and limited trace element mobility from the overburden. Analyses were below detection for arsenic (As), selenium (Se), lead (Pb), mercury (Hg), cadmium (Cd), and chromium (Cr) in water samples obtained from Guy Cove.

Table 3.1: Average pre-construction water quality characteristics from a nonmined reference reach (LMS), an upgradient stream that drained into the fill (seep), and a stream channel below the valley fill (Guy Cove).

Site[1]	pH	EC	Cl	SO_4	NO_3	Ca	Fe	Mn
		$\mu S\ cm^{-1}$	----------mg L^{-1}----------					
LMS (30 yr)[2]	6.5	46	0.6	10	0.13	2.3	na[4]	na
Seep[3]	7.9	478	1.3	225	0.09	47	0.3	4.0
Guy Cove[3]	7.0	1723	2.3	1293	0.01	137	0.7	21.4

[1]LMS = Little Millseat reference watershed; Seep = natural seepage from unmined upgradient area; Guy Cove=downstream of the fill and underdrain.
[2]Average from weekly samples collected over a thirty-year period.
[3]Samples collected monthly from June 2004 to June 2008.
[4]na = not analyzed.

The regenerated forest located in the 9 ha unmined section of Guy Cove was comprised primarily of yellow poplar (*Liriodendron tulipifera*), white oak (*Quercus alba*), sweet birch (*Betula lenta*), American beech (*Fagus grandifolia*), red maple (*Acer rubrum*), black walnut (*Juglans nigra*), and American sycamore (*Platanus occidentalis*) (Maupin 2012; Blackburn-

Lynch 2015). Along the crown, face and on 50% of the side-slopes adjacent to the crown, vegetation was predominately herbaceous consisting of ground cover species that were seeded during the initial reclamation (Figure 3.1).

Figure 3.1. The Guy Cove valley fill in 2007, prior to creation of a headwater stream system. Note: forested section in the top center of the picture is an area that was not mined and where a small stream channel remained relatively intact.

3.2.3 Restoration Design

Valley fills result in unnatural topography, particularly with respect to valley widths and slopes. Intermittent and perennial stream reaches in LMS have valley slopes of about 12 and 6%, respectively (Villines et al. 2015). Lower slopes, such as the one present on the crown prior to construction, encourage sediment deposition in mined lands. As this project was a retrofit of a valley fill, economic limits were present regarding the amount spoil we could move to reshape the width and slope of Guy Cove's valley. The design incorporated the use of multiple valley slopes along the crown starting with 1% at the most upgradient section of the project transitioning to a maximum slope of 5.5% before decreasing to a slope of 3% prior to transitioning to the face of the valley fill. The new valley slope resulted in the elimination of the uppermost bench along the face of the valley fill. To achieve a cut-fill balance within Guy Cove, all excavated spoil was used to create a narrower valley (Figure 8.6). Spoil was backfilled along the lower portion of the valley side walls and compacted resulting in an average final grade of 3:1 (H:V). Following compaction, additional spoil was placed along the side slopes in accordance

with the FRA (Burger et al. 2005). Along these slopes, spoil was dumped in piles that closely abutted each other with an approximate height of 2.5 m. Using an excavator, the tops of the piles were struck-off (see Chapter 7) to level the surface while minimizing mechanical compaction. The resulting surface was rocky and loosely compacted. Approximately 115,000 m^3 of spoil were moved to reconfigure the valley.

To promote the surface expression of waters (e.g., reduce infiltration into the fill), the crown was compacted during valley reconfiguration. Loaded dump trucks were repeatedly driven over the crown to increase compaction. Spoil was placed at the interface of the unmined and mined sections (i.e., entrance to the underdrain) and compacted in a similar manner. Along the face of the valley fill, the right groin drain, when facing down valley, was removed and the benches were regraded to improve the ability of water to flow from the benches into the left groin drain. Large boulders along the left groin drain, which were blocking overland flow from the benches, were removed. Woody debris was also added to improve habitat conditions. These modifications were done so that the main channel on the crown of the valley fill would flow into a single groin drain (e.g., single channel).

The main channel consists of a 760-m section along the crown, nearly 120-m section along the face, and a nearly 140-m section below the toe of the valley fill. For the sections along the crown and below the toe, the stream was created. The typical design bankfull dimensions for the riffle cross-sections along the main channel, excluding the face of the valley fill, were as follows: area= 1.4-1.5 m^2, width=2.4-2.7 m, and mean depth=0.2 m. Typical design bankfull dimensions for a pool cross-section, excluding the face of the fill, were as follows: area= 1.8-3.4 m^2, width=2.7-3.4 m, and mean depth=0.2-0.4 m. As previously noted, for the portion of the main channel on the crown, slopes ranged between 1 and 5.5% while values for sinuosity (distance along stream between two points ÷ straight line distance between the two points) ranged between 1.0 and 1.2 along the crown. Along the face, the slope was 25.5% with a sinuosity of 1.0. For the portion of the channel below the toe of the valley fill, slopes ranged between 2 and 4% with a sinuosity of 1.02.

Instream structures within the main channel predominately consisted of cross-vanes, steps, and constructed riffles. Due to the remoteness of the project site coupled with the prevalence of a nearby forest, the cross-vanes and steps were constructed of logs and anchored in place using boulders. Because of the long distance to a rock quarry, it was cost-prohibitive to haul in rock for instream structures or riffles. As such, a Powerscreen (Dungannon, Ireland, UK) was used to sort spoil into four size classes of which the largest class (large gravel to cobble size material) was used to construct the riffles in the main channel.

Ephemeral channels convey water from the side slopes to the main channel during runoff producing rain events. While ephemeral channels transport water for short periods of time, these streams are important to headwater ecosystems (McDonough et al. 2011). Four ephemeral channels, (totaling 435 m in length) were constructed with their placement guided by the development of pre-existing gulleys (i.e., the presence of gulleys at a particular location indicated overland flow had channelized at that point, hence a preferential flow path existed). Ephemeral channels were designed in the field largely on the basis of local slopes and available construction material (e.g., rock and logs). Due to the steepness of the ephemeral channels (typically >20%), these streams predominately exhibited a step-pool morphology.

Reforestation of the watershed was performed separately for riparian (adjacent to the created stream) and upland areas. The riparian corridor was divided into two zones paralleling the main channel. The inner zone (Zone 1), extending 5 m on either side of the stream, was densely stocked (1 x 1 m centers) with shrubs and trees adapted to occasional flooding and frequent disturbance. One-year old bare-root American sycamore, American beech, green ash (*Fraxinus pennsylvanica var. subintegerrima*), swamp chestnut oak (*Quercus michauxii*), and dogwood (*Cornus sp.*) seedlings, all common in riparian zones of mixed mesophytic forests, were used in this first riparian zone. A second zone (Zone 2) extending 10 m beyond the inner, streambank zone was planted with additional trees and shrubs species (2 x 2 m centers) that are accustomed to occasional flooding and saturated soils. Additional species included: white oak, silver maple (*Acer saccharinum*) and river birch. Black willow (*Salix nigra*) stakes were densely planted (0.5 x 0.5 m centers) in areas that were susceptible to bank erosion (intersections of ephemeral and main channels).

The remaining watershed to which FRA was applied (Zone 3) was planted with mixed mesophytic hardwoods typical of eastern Kentucky and the Cumberland Plateau. Yellow poplar, white oak, northern red oak (*Quercus rubra*), chestnut oak (*Quercus prinus*), white ash (*Fraxinus americana*), sugar maple (*Acer saccharum*), eastern white pine (*Pinus strobus*), black locust (*Robinia pseudoacacia*), dogwood and redbud (*Cercis Canadensis*) seedlings were planted on 3 x 3 m centers and mixed throughout the entire midslope and ridge top regions.
In all three zones combined, over 30,000 seedlings were planted.

3.2.4 Monitoring

Post restoration water quality was monitored only on the main channel immediately upstream of the project site (GC01), at the crest or transition point from the crown to the face of the valley fill (GC02), and just downstream of the confluence of the new channel and the underdrain (GC03) (Figure 3.2). Water samples were collected from GC01, GC02, GC03, LMS,

and Wharton Branch (WtB) (unrestored valley fill) on a bi-weekly basis from 2004-2013. In 2017, monitoring was reinitiated in GC02 and GC03 and a newly reclaimed traditional grassland site at Williams Branch (VFWB).

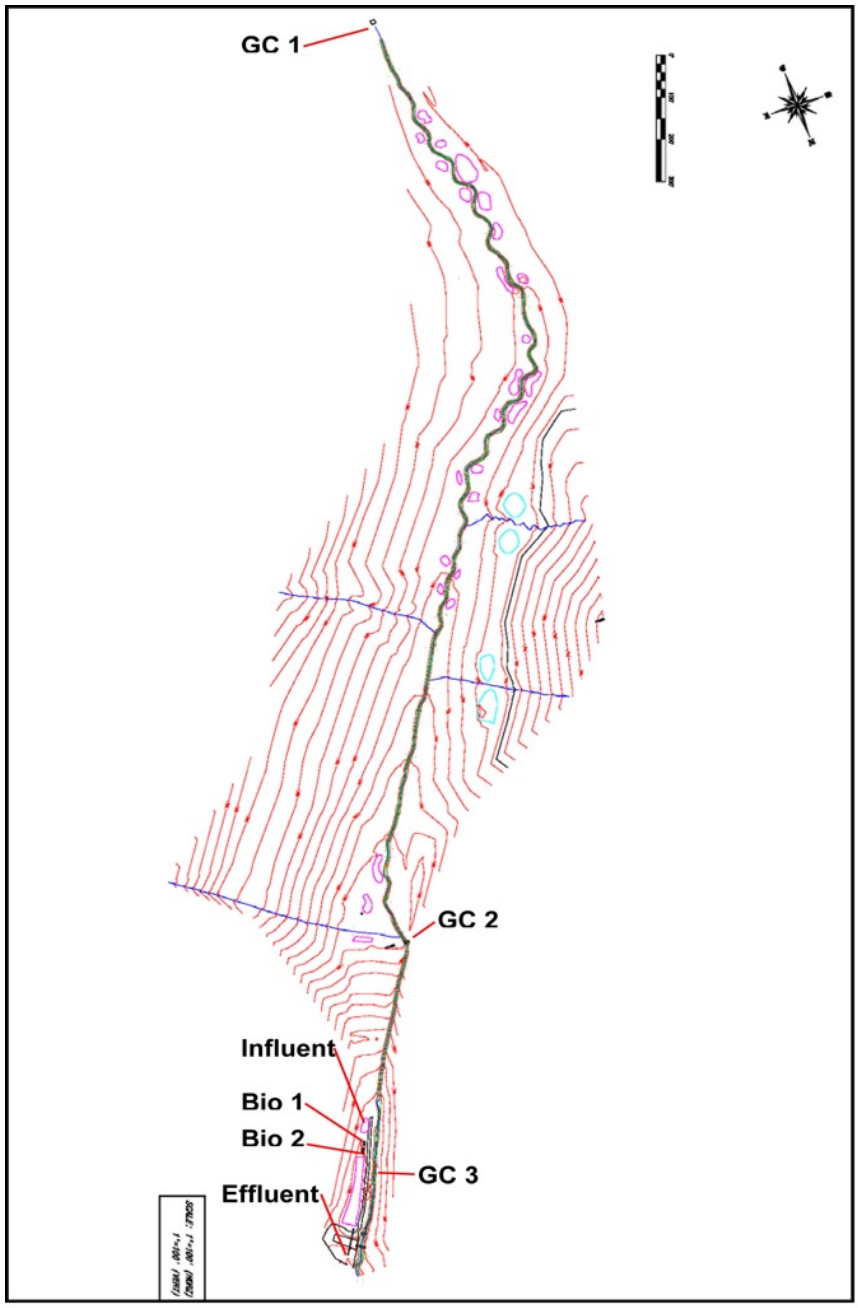

Figure 3.2. Location of water sample monitoring points at Guy Cove.

Sampling, preservation and analytic protocols were performed in accordance to standard procedures (Greenberg et al. 1992). Water quality parameters such as pH and specific conductance (EC) were monitored in the field using a Yellow Springs Instrument (Yellow

Springs, Ohio) 556 multi-probe monitor. Water samples were collected in plastic bottles and immediately stored in ice chests. Field collected water samples were transferred to a refrigerator at 4°C as soon as feasible. All samples remained refrigerated until they were processed. Samples were filtered through 0.45 µm syringe filters prior to analysis. Sulfate was analyzed on a Dionex ion chromatograph system 2500 (ISC 2500). The set-up contained an AS50 auto sampler, IS25 chromatograph, LC25 chromato-oven, and an EG50 eluent generator. Nitrate was analyzed with a Braun:Luebbe Auto Analyzer 3 using the Colorimetric procedure. An ICP-OES - Varian Vista-Pro CCD Simultaneous (Varian Instruments, CA, USA) was used to measure dissolved iron (Fe) and manganese (Mn). Laboratory control standards and blanks were run for accuracy, and duplicates were run for precision.

3.3 RESULTS AND DISCUSSION

3.3.1 Vegetation

An extensive survey of the vegetation was performed in 2013, five years after planting. Despite several setbacks with regards to plant loss and damage from animal browse and in some cases human activities (one plot in riparian Zone 1 was lost), the reforestation effort was quite successful. In 2013, browse was observed on 44% of trees in riparian sample plots and on 11% of those in the upland plots. Although browse appears have a significant effect on height growth, survival of the planted seedlings does not appear to have suffered. Browse was initially attributed primarily to elk, but excrement from deer, cattle and horses were observed on the site. By 2013 much of the herbaceous vegetation established for erosion control was replaced by other naturally seeded species such as bulrush, spiked rush, cattails and many forbs.

Table 3.2 contains height growth data for Year 1 and height growth and survival data for Year 5 in plots from Zones 1 and 2. For all species, survival was 75% and ranged from 42% for silver maple to 100% for five species. Within the plots, tree density was calculated at 2,805 trees ha^{-1}. Height growth over the five-year period was observed, but damage from browse resulted in unusual growth patterns for the planted species (not linear as would be expected). Black locust, green ash, silver maple, and river birch exhibited extensive browse (> 80%). Natural colonization of several species was observed in the study plots. European alder (*Alnus glutinosa), and* Virginia pine (*Pinus virginiana*) were the most commonly observed.

Table 3.2. Year 1 (height) and 5 (height, survival and browse) data for primary riparian species planted in Zones 1 and 2[1].

	Year 1	Year 5		
Species	Height (m)	Height (m)	Survival (%)	Browse (%)
Green Ash	0.42	0.60	54	87
Beech	0.52	0.47	91	0
Sycamore	0.37	1.04	77	1
Swamp White Oak	0.57	0.83	90	48
Silver Maple	0.71	0.56	42	89
River Birch	0.62	0.83	96	80
Black Locust	0.36	1.70	100	83
Chestnut Oak	0.61	1.14	100	0
N Red Oak	0.52	0.89	78	21
White Oak[2]	0.53	1.64	100	0
White Pine[2]	0.31	1.28	100	0
Yellow Poplar[2]	0.55	0.45	100	50

[1]Year 1 = 2009; Year 5 = 2013.

[2]Year 5: Low number of survey trees in plot for these species (n < 5).

Sample plots were resurveyed in the mixed species upland planting areas (Zone 3) at the project site in Year 5 (Table 3.3). Survival was greater than 100% for sycamore and white pine due to natural colonization (population increased by over 100 specimens in the sample plots). Excluding sycamore and white pine, overall survival was ≥85% for 5 of the other 8 observed species. Within the plots, tree density was calculated at 1,539 trees per ha. Height growth was improved over that observed in the riparian zones and browse was much lower for most species. The reduction in browse may be attributable to the hummocky nature of the FRA which is less hospitable to large herbivores. The following naturally colonized tree and shrub species were observed in the upland sample plots: quaking aspen (*Populus tremuloides*), sweet birch (*Betula lenta*), river birch, red maple (*Acer rubrum*), black gum, European alder, Virginia pine, Sourwood (*Oxydendrum arboreum*), Tree-of-Heaven (*Ailanthus altissima*), Royal paulownia (*Paulownia tomentosa*), and Autumn olive (*Elaeagnus umbellate*). The last three, Tree-of-Heaven, Royal paulownia and Autumn olive, are exotic and invasive and efforts were undertaken in 2016 to remove them using herbicide.

Table 3.3. Year 1 (height) and 5 (height, survival and browse) data for primary species planted in low compacted spoil located in upland Zone 3.

Species	Year 1	Year 5		
	Height (m)	Height (m)	Survival (%)	Browse (%)
White Ash	0.54	0.95	66	66
White Oak	0.56	1.39	89	2
Chestnut Oak	0.67	0.93	100	0
Sycamore	0.53	2.00	>100[1]	0
N Red Oak	0.57	0.81	86	28
Sugar Maple	0.28	0.42	43	66
Yellow Poplar	0.40	1.63	100	0
Black Locust	0.67	2.72	85	33
White Pine	0.35	1.57	>100[1]	0
Red Bud	0.42	0.65	20	0

[1]2013 populations greater than 2009 population likely due to natural colonization.

Year 10 vegetation surveys were not performed, but vegetative growth has been closely monitored and photo documented each year. In 2017 drone imagery show that the uplands had achieved near canopy closure, but the riparian areas still had areas that were open (Figure 3.3). By 2019, tree growth had accelerated and very few canopy gaps existed in the watershed (Figure 3.4).

Figure 3.3. The Guy Cove valley fill in 2017, nine years after planted. Note: canopy openings in the riparian Zone 2 between the edges of the stream and upland.

Figure 3.4. The Guy Cove valley fill in 2019, eleven years after planted. Note: canopy openings in the riparian Zone 2 have largely closed.

3.3.2 Water Quality

Results from the post-construction monitoring period are presented in Table 3.4. Water quality in the constructed stream section located on the crown of the fill are better than those observed during the pre-restoration sampling period. One parameter of note is the EC level at GC02, which dropped from a mean concentration of 852 µS cm^{-1} in 2010 to a mean concentration of 471 µS cm^{-1} in 2013. The 2017 and 2018 EC levels have dropped further to about 400 uS cm^{-1}. This period of initially elevated EC levels followed by a decrease as finer material is flushed through the system mirrored the trend seen by Agouridis et al. (2012) and Sena et al. (2014) for FRA test plots. At that sampling point, approximately 40 hectares is draining to 0.7 km of created stream. Maintaining an EC below 500 µS cm^{-1} from 2013 to 2018 should be of benefit to stream macroinvertebrates (Pond et al. 2008) and will help restore the health of this disturbed system. Although water leaving the watershed (GC03) still has an EC slightly above 1,000 µS cm^{-1}, that level has dropped 49% since the restoration and incorporation of FRA was implemented.

Concentrations of sulfate exhibited a similar decreasing trend over the eight-year post-construction monitoring period at GC02 and GC03. Over the eight-year post restoration monitoring period, sulfate was reduced by 89 and 85.5% in GC02 and GC03, respectively. The concentration of Mn at GC02 and GC03 has gone down dramatically over the eight-year period. At GC02, Mn levels were below detection for the entire 2017 sampling year and the average for 2018 was 0.02 mg L^{-1}, which represents a 99% reduction from 2010 levels. Similarly, mean 2018 Mn levels at GC03 were 0.5 mg L^{-1}, which represents a 92% reduction from 2010 levels. The reduction of sulfate and Mn in the stream are likely due to a change in the redoximorphic chemistry of the fill material, which has slowed the oxidation of pyrite. This could be a function of less water coming in contact with buried pyrite since canopy interception has reduced the amount of throughfall actually making it to the forest floor and more water is leaving via evapotranspiration and runoff in the created stream. Alternatively, the readily dissolvable ions may have simply flushed from the system.

Concentrations of dissolved ions on the crown were lower than observed exiting the underdrain. Groundwater discharging from the underdrain continues to be a source of contamination to downstream reaches. Unfortunately, little is known about the hydrology of these underdrains and the long-term ramifications it may have on the environment. Wharton Branch (WtB), which was not initially reclaimed via FRA, continues to be a source of high dissolved ions in discharge water. Although data are not shown, we continue to monitor Wharton Branch for EC and pH on a quarterly basis. For 2017 and 2018, EC levels at Wharton

Branch remained above 2,500 µS cm^{-1}. Williams Branch (VFWB) was picked-up in the 2017 and 2018 monitoring to represent a non-FRA grassland site (parts of Wharton Branch were ripped and planted as part of FRA in 2015, making it no longer usable as a non-forested control). EC concentrations in Williams Branch were similar to those exhibited in pre-FRA Wharton Branch for 2010-2014. Guy Cove, on the other hand, has shown water quality improvements over time. We speculated that during the planning of the project that as the forest matured water chemistry would improve, simply because there would be less water available to infiltrate through the fill material. Additional work is needed to prove this, but the data presented here are encouraging.

Since water with high EC has been implicated as a potential driver of macroinvertebrate assemblage shifts (Pond et al. 2008), developing reclamation techniques that mitigate high EC concentrations is a priority. The creation of the stream on top of the valley fill allowed for freshwater, primarily from precipitation, to move through the watershed without extensive co-mingling with spoil buried in the fill. This limited contact time between water and readily dissolvable minerals and dissolved solid concentrations were reduced. Sulfate has been identified in previous studies (Kennedy et al. 2003, Lindberg et al. 2011, Hopkins et al. 2013) as a major contributor to the elevated EC and associated macroinvertebrate toxicity. On the crown, sulfate decreased from 871 to 99 mg L^{-1} during the post-construction period (89% reduction), which was encouraging. If the system remains at these levels, or continues to improve, water quality conditions should be sufficient to support sensitive macroinvertebrate species common to the region (Pond et al. 2008).

Table 3.4: Average post-construction water quality characteristics from Guy Cove, a non-mined reference stream (LMS) and a nearby traditionally constructed and reclaimed valley fill (WtB/VFWB).[1]

Sample ID[2]	**2010**	**2011**	**2012**	**2013**	**2017**	**2018**
	EC µS cm^{-1}					
LMS	52	43	45	42	39	39
GC01	479	457	526	447	na	na
GC02	852	827	598	471	384	404
GC03	1949	1724	1841	1598	1221	1191
WtB/*VFWB*	2343	2126	2397	1979	*2428*	*2618*
	SO_4 mg L^{-1}					
LMS	9	15	8	7	10	7
GC01	525	417	134	71	na	na
GC02	871	815	309	161	243	99
GC03	1470	1780	1310	715	399	213
WtB/*VFWB*	1884	2465	1826	960	*1662*	*830*
	Mn mg L^{-1}					
LMS	0.3	0.3	0.2	na[3]	na	na
GC01	0.1	0.2	0.1	0.1	na	na
GC02	3.2	5.3	0.4	0.2	BDL	0.02
GC03	6.2	3.6	4.9	1.9	0.9	0.5
WtB/*VFWB*	7.4	15.5	11.4	8.0	*0.5*	*0.4*
	pH					
LMS	5.8	6.6	6.2	5.5	5.2	5.3
GC01	7.5	7.8	7.2	7.4	na	na
GC02	6.0	6.3	6.3	6.9	6.1	6.7
GC03	6.2	6.6	6.2	6.6	6.2	6.5
WtB/*VFWB*	6.1	6.6	6.3	6.6	*7.6*	*7.8*

[1]Construction and planting activities occurred from July 2008 to July 2009.

[1]LMS = Little Millseat reference watershed; GC01 = confluence of existing upgradient stream and beginning of created stream; GC02= interface between crown and face of valley fill; GC03=downstream end of project reach; WtB=Wharton Branch reference impacted (valley fill) watershed analyzed 2010-2013; VFWB=Williams Branch reference impacted (valley fill) analyzed 2017-2018.

[2]na = not analyzed.

3.4 CONCLUSION

Following nearly four years of planning, the University of Kentucky, in a first of its kind project, utilized NCD techniques and knowledge gained by research on the FRA to create a headwater stream system on a valley fill at Guy Cove in 2008. This project was proof-of-concept in that it sought to answer questions on "how to" retrofit an existing valley fill in an effort to restore lost stream and watershed functions. During a six-month period, 1,450 m of headwater streams were created along with 0.1 ha of vernal pools, and 16.2 ha of hardwood forest. Results from the post-restoration monitoring period point to a number of successes. Tree growth and survival are quite good for most species, particularly in the uplands. By 2019, canopy closure was evident across the entire watershed. The state of the young forest should greatly influence the hydrology of the watershed through increased canopy interception and increased evapotranspiration. On the portion of the main channel located on the crown, water quality has improved greatly. Overall water quality in the watershed has also exhibited considerable improvement. Notably, the 760-m created stream on the crown did not exist after fill construction was completed and there was no surficial connection between the small headwater stream in the unmined portion of the watershed and the stream reach below the fill; now there is a continuous channel joining the small unmined headwater reach with the reconstructed stream valley. This project provided an opportunity to put back what was lost, reconnect the streams and, with improved water quality, restore lost habitat for wildlife. Salamanders, sensitive aquatic macroinvertebrates and even fish have been observed in the restored stream.

4. HYDROLOGIC MODELING TO EXAMINE THE INFLUENCE OF THE FRA AND CLIMATE CHANGE ON MINELAND HYDROLOGY

4.1 INTRODUCTION

Headwater stream systems are significantly impacted by surface mining. For example, surface mining results in the production of excess spoil or overburden, which is often placed in adjacent valleys resulting in the creation of valley fills. These valley fills bury headwater streams which in turn can negatively impact downstream ecosystems. Restoring headwater stream systems and their ecosystem services requires an understanding of the interconnectedness of hydrologic, geomorphic and ecological processes (Kauffman et al., 1997). As seen in the Stream Function Pyramid, restoration of aquatic communities occurs when the more basic functions of hydrology, hydraulics, geomorphology and the soil physiochemical properties have been restored (Harman et al., 2012). According to Harman et al. (2012), the foundation of restoring streams involves reestablishing hydrologic functions such as precipitation-runoff relationships and flow duration. Recent research on stream restoration on mined lands at the University of Kentucky's Guy Cove suggests that the FRA can play a vital role in reestablishing storm event hydrology (Blackburn-Lynch, 2015).

A hydrologic modeling approach that evaluated streamflow, soil-water storage, and streamflow permanence in headwater systems was developed for eastern Kentucky. The Cumberland Plateau was included in regional calibration of the Kentucky Water Availability Tool for Environmental Resources (WATER) decision support system (DSS). Robinson Forest was one of two Kentucky field sites used to simulate soil-water movement and storage (Williamson et al., 2015a,b). Other recent work integrated samples from the Natural Resources Conservation Service's (NRCS) National Rapid Carbon Assessment (RaCA) in order to extend this hydrologic modeling to a larger geographic area and frame the results in the context of agricultural resiliency for a 30-yr, normalized record centered on 2050. Work supported by the USGS Water Census (Williamson et al., 2015b) validated ET estimates for a mixed forest community using a mix of Ameriflux and Soil-Surface Energy Balance simulations (Senay et al., 2013) for the Delaware River Basin (DRB) with the intention of understanding water availability given projected changes in climate (Frumhoff et al., 2007). In each case, the hydrologic model is being used to understand the effects of climate and land-use change by integrating Coupled Model Intercomparison Project (CMIP) general circulation model (GCM) data using a change-factor approach for precipitation, temperature, and potential evapotranspiration (PET). This research will further improve our ability to simulate the water budget that controls streamflow in forested regions that provide drinking water to large portions of the U.S., including populations that are geographically isolated from alternative sources. The encapsulation of this

hydrologic modelling approach (WATER) in a DSS that is already used by regulators and resource managers in several states ensures transferability of this knowledge to objectively consider how land-use, and reforestation (FRA) might affect streamflow and water availability.

This particular project was designed to specifically address issues involving comprehensive ecosystem restoration and in particular: "*How does the Application of Forestry Reclamation Approach Attenuate Runoff Characteristics in Streams in Appalachia*." To answer this question, the following objectives were identified and tested:

1. Compare saturated hydraulic conductivity (Ksat) of soils that underwent a variety of surface mine reclamation strategies and with different times since reclamation in order to evaluate the influence of FRA on infiltration and water movement in the soil environment.
2. Simulate the resultant streamflow response as a function of differing soil properties that characterize reclaimed minelands.
3. Model actual evapotranspiration (AET) at the watershed scale as a function of differing soil properties that characterize reclaimed minelands and under projected climate conditions for 2050 (CMIP6).

4.2 METHODS

4.2.1 Site Descriptions

The Little Millseat basin is a 0.79 km^2 basin in Robinson Forest that has been left relatively undisturbed for approximately 100 years. This basin provides a control for evaluating the potential differences in hydrology as a function of mine-reclamation strategies that have been implemented throughout Appalachia. Four other study sites were chosen for comparison with this control basin in order to encompass a range of time since recovery after mine reclamation in addition to several different strategies, including the forestry reclamation approach (FRA), conventional grassland reclamation, and FRA implemented after other conventional strategies (Table 4.1). A daily record of precipitation and temperature is available for the basin extending back to the mid-1970s. For all simulations, the hydrologic model was driven by a composited daily record from three on-site locations (Camp Station, Little Millseat Basin, and Falling Rock ridgeline) of precipitation and mean-temperature that has been used previously in Robinson Forest research (Williamson et al., 2015). This record includes 3,717 days, from October 1 2002 thru September 30, 2012. One year of data was used to initialize the model, so results are discussed for the October 1, 2003 to September 30, 2012 time period, totaling 3,352 days. Previously published work (Williamson et al., 2015) used only the November 14, 2004 to December 16, 2006 time period because this was the longest continuous record of streamflow

observation. Consequently, visual and statistical comparisons of hydrology will focus on these two years (761 days).

Table 4.1. Study sites used for comparison of hydrology as a function of mine-reclamation strategy.

Site	Landscape Positions[1]	Treatment	Dates of Sampling	Number of Ksat Measurements (0-20 cm/20-40 cm)	Years since disturbed
Little Millseat (LMS)	D,SS,T	Control	Jun, Sep 2017	18 /14	94
Guy Cove (GC)	D,SS,T	FRA on mine soil	Sep, Oct 2017	18 / 18	9*
Williams Branch (WB)	D,SS,T	Grassland reclamation	Oct, Nov, 2017 Dec 2018	18 / 18	5
Starfire (ST)	Flat	Strikeoff FRA	Sep 2018	6 / 6	21
VanBooven (vB)	Flat	Ripped FRA	Oct 2018	6 / 6	14

[1]D = drainage divide/ridgetop; SS = side-slope; T = toeslope; Flat = top of mountain top mining bench.
*Guy Cove was originally reclaimed as grassland, then re-disturbed in 2008 to employ FRA and create a stream (see Chapter 3).

4.2.2 Field Work and Data Collection

Within each of the five study areas, soils were described and sampled in coordination with NRCS (Schoeneberger et al., 2012) beginning in June 2017 and ending in November 2018. Descriptions and sampling focused on three landscape positions (drainage divide, side-slope, and toeslope; D,SS,T) for the control site and the reclaimed valley fills. Starfire and VanBooven were only sampled on the upland mining bench or "top" of the reclaimed, mountaintop mining operation (Figure 4.1 and Table 1). Guy Cove FRA included strike-off and ripping FRA, Starfire was reclaimed using strike-off FRA and VanBooven was ripped only. See Adams (2017) for an explanation of the various FRA techniques. Williams Branch was reclaimed with "conventional" grassland techniques.

Within approximately 5 m of each described pedon, on the same landscape position, Ksat was measured in the field (four or more replicates at each of two depths – 0-20 cm and 20-40 cm) with a compact constant-head permeameter (CCHP; Amoozemeter) and calculated using the Glover solution (Amoozegar, 1992). The resulting dataset includes physically measured values of hydrologic properties for each study site, including field Ksat, bulk density (translatable to

total porosity) from a core, where possible, or a trench, and soil-water storage from pressure plates (field capacity, and wilting point).

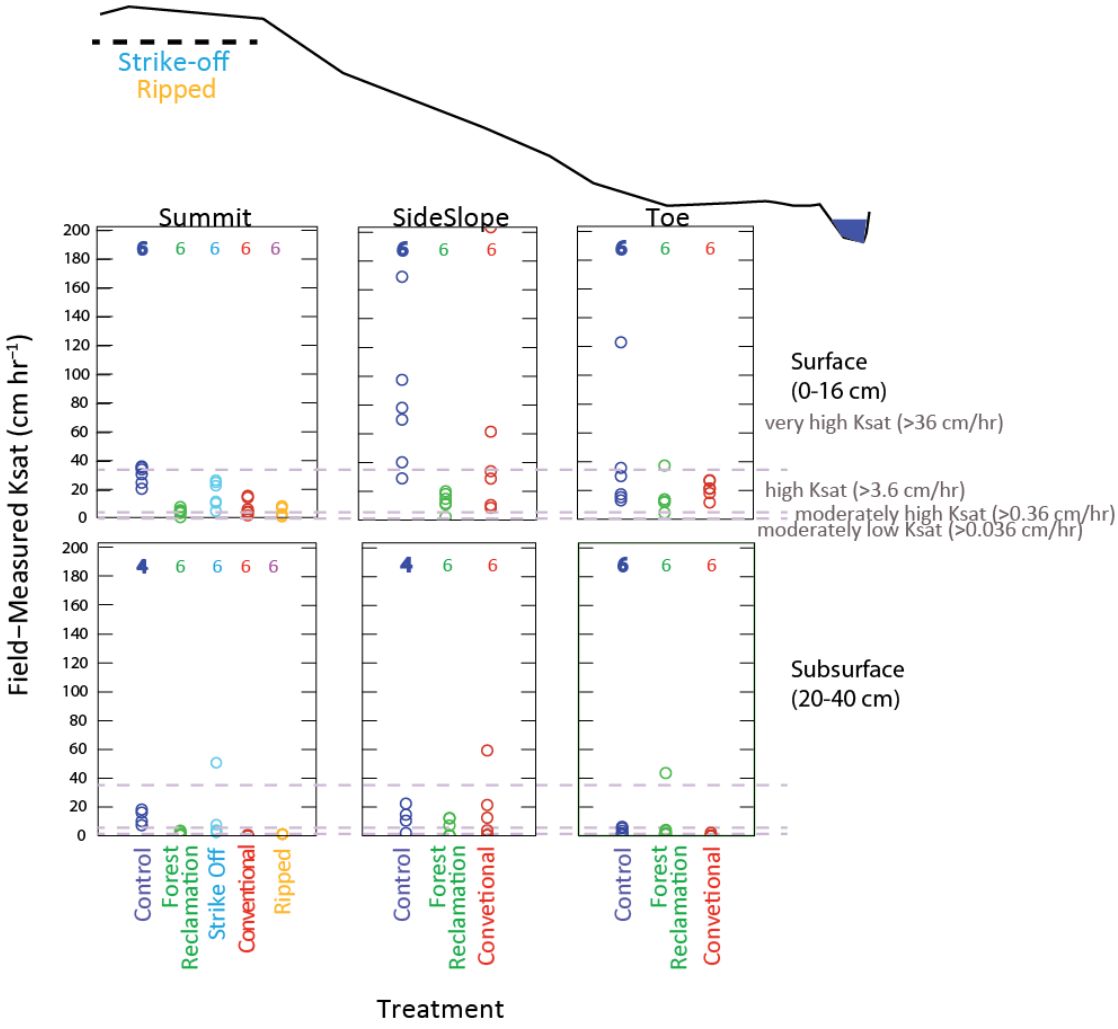

Figure 4.1. Conceptual diagram of landscape positions and field measured Ksat for each site. Note that only those soil layers with a moderately high or higher Ksat were used in hydrologic modeling. LMS=control (blue), GC=Forest Reclamation (green),ST = strikeOff (cyan),WB = Conventional (red), vB = Ripped (orange).

4.2.3 Processing of soils data and use in hydrologic simulations

Soil hydrologic properties were aggregated as surface and subsurface “layers” for each site. Only data from physical measurement of hydrologic soil properties collected as part of this project were used (Table 4.2) and, based on previous research with the hydrologic model showing that the daily hydrology was best characterized using those layers for which Ksat was >

1 micrometer per second (µm sec^{-1}; 86.4 mm per day or 0.36 cm per hour) (Williamson et al., 2014), depth-weighted means were calculated using only the soil layers identified as hydrologically active using the field-measured Ksat. Otherwise, all pedon descriptions were used to obtain a representative (mean) value for each soil property for each site (Table 4.2). Hydrologic simulations used the Water Availability Tool for Environmental Resources (WATER) that was developed for Kentucky, using parameterization that was refined for forested areas (Williamson and Claggett, 2019, Williamson et al., 2013) including a rooting depth that was 75% of the hydrologically-active soil thickness. However, no site-specific optimization of the hydrologic model was done. WATER uses TOPMODEL (Beven and Kirkby, 1979) to simulate the movement of water through pervious parts of the landscape. The conductivity multiplier and scaling parameter for TOPMODEL were both derived directly from the physically measured soil properties in order to quantify how Ksat changes between the surface and subsurface as well as how gravity drained porosity relates to this change; more detail on the hydrologic model and calculating these parameters is provided in (Williamson et al., 2013).

Table 4.2. Representative values of soil properties for each study site that were used in hydrologic model.

Site	Hydrologically-Active Soil Thickness	Total Porosity	Field Capacity	Water Holding Capacity	Ksat	Conductivity Multiplier	Scaling Parameter	Rooting Depth
	mm	----------	unitless	---------	mm d^{-1}	unitless	mm	mm
Little Millseat	850	0.48	0.32	0.14	4958	259.14	25.39	638
Guy Cove	367	0.43	0.20	0.09	1741	95.86	18.91	275
Williams Branch	290	0.31	0.27	0.13	3002	468.06	2.16	218
Starfire	280	0.48	0.14	0.09	3225	19.44	32.23	210
vanBooven	200	0.37	0.21	0.10	1378	5.51	18.44	150
LMS-SSURGO[a]	1166	0.33	0.20	0.12	2264	7330	109.59	300[b]

[a]Soil Survey Geographic Database (U.S. Department of Agriculture - Natural Resource Conservation Service [USDA-NRCS], 2010). This is the source of soils data in the previously published simulations of the Little Millseat Basin (Williamson et al., 2015).

A simulated hydrologic record using the local soil descriptions for the control basin was used as a baseline for evaluation of how hydrology could be expected to change as a result of soil properties associated with different methods of mine reclamation. Other physical aspects of the basin remained constant, including total area and the topographic wetness index, which digitally describes the topography of the basin (Beven and Kirkby, 1979). Only the soil properties changed.

4.2.4 Projected Climate Conditions

Coupled Intermodel Comparison Project (CMIP6; Eyring et al., 2016) datasets for both historical (1994-2014) and projected (2040-2060) time periods were downloaded between July 10-12 2019 from Lawrence Livermore National Laboratory data node (aims3.llnl.gov). All downloads were centered on Robinson Forest (37.48N, 83.18W). The fossil-fueled development scenario (SSP585; O'Neill et al., 2016) was used for the projected period; this is the only scenario that produces a radiative forcing of 8.5 W m^{-2} in 2100. All replicas and versions were downloaded for each of nine general circulation models (global climate models; GCMs – Table 4.3) which were selected based on those available for the complete set of necessary parameters in addition to those for which previous CMIP generations had been shown to perform well for this geographic region (Bock et al., 2018). For each GCM, monthly data (amon table) were downloaded for near-surface temperature (tas), precipitation (pr), surface upward latent heat flux (hfls), and surface upward sensible heat flux (hfss). Monthly change factors (deltas; δ) were calculated for mean daily temperature (addititive), precipitation (multiplicative), and radiation-based potential evapotranspiration (PET; multiplicative) after Williamson et al. (2016). This radiation-based δ -PET was compared to the mean monthly change using a temperature-derived PET (Hamon, 1963) that was calculated within the hydrologic model for a 3266 day record.

Table 4.3. Coupled Model Intercomparison Project Phase 6 (CMIP6) datasets used.

GCM	Historical	SSP585
IPSL-CM6A-LR	(Boucher et al., 2018)	(Boucher et al., 2019)
BCC-CSM2MR	(Beijing Climate Center, 2018)	(Beijing Climate Center, 2018)
UKESM1.0-LL	(Met Office Hadley Centre, 2018)	(Met Office Hadley Centre, 2018)
CNRM-ESM2-1	(Seferian, 2018)	(Centre National de Recherches Meteorologiques and Centre Europeen de Recherche et de Formation Avancee en Calcul Scientifique, 2018)
MRI-ESM2.0	(Yukimoto et al., 2019)	(Yukimoto et al., 2019)
CNRM-CM6-1	(Voldoire, 2018)	(Voldoire, 2019)
CanESM5	(Canadian Centre for Climate Modelling and Analysis, 2018)	(Canadian Centre for Climate Modelling and Analysis, 2018)
GFDL-CM4	(Guo et al., 2018)	(Guo et al., 2018)
MIROC6	(Tatebe and Watanabe, 2018)	(Shiogama et al., 2019)

4.3 RESULTS AND DISCUSSION

4.3.1 Variability of Soil Properties

Comparison of Ksat among landscape positions shows that surface Ksat is generally lowest on the drainage divide and sub-surface Ksat is generally lowest at the toeslope. When these data are aggregated by site, Ksat is highest for the control site (Little Millseat) and Ksat is lowest for the ripped FRA (vanBooven). Field measured Ksat for the control was approximately twice the

value obtained from SSURGO, which was used in previous simulations for this site (Williamson et al., 2015), resulting in similar differences in the conductivity multiplier and scaling parameter, although the field description showed the soil to be less a deep as defined by the use of soil layers with a Ksat > 1 μm sec^{-1}. Among the soils described for this study, the control soil was the thickest and had among the highest total porosity and water retention. The FRA soils generally had a more shallow soil thickness and lower total porosity, but generally higher water retention for plant use relative to the control, so less gravity-drainable pore space to prevent overland flow during storm events. The conventional grassland site (Williams Branch) soil dataset has the lowest total porosity, most of which retains water at field-capacity conditions, and the largest change in Ksat between the surface and base of the hydrologically active soil. Ksat at the surface is approximately 500 times that at the base of the soil (the conductivity multiplier), creating a hydrologic environment for the conventional grassland site in which water movement into the subsurface is impeded. Compounding this is that the gravity-drained porosity (total porosity – field capacity) is <5%, resulting in higher amounts of overland flow instead of precipitation recharging soil water and becoming baseflow in the stream. In contrast, the other reclaimed mine soils have gravity-drained porosity ranging from 16-34% and conductivity multipliers ranging from 6-96. This would suggest that the ripped FRA and strike-off FRA enables infiltration and limits overland flow. The reduction in Ksat with depth at the VanBooven ripped site would also suggest that water could infiltrate at a moderate rate at the surface, but then slow as it proceeds down the soil profile. Deep ripping at this site was performed with a Caterpillar D8 bulldozer equipped with a 1-m ripping shank. High fragmenting of the surface soil is achieved with this method, but its effectiveness is centralized on the upper part of the soil horizon which makes tree planting and success possible. Although the lower Ksat with depth isn't ideal, the lower permeability may create conditions for depression storage of water which could be utilized by the forest during dry weather conditions. A similar condition has been described for strike-off FRA (Sena et al., 2014).

4.3.2 Hydrologic Differences Resulting from Soil Characteristics

Previous hydrologic simulation using SSURGO derived soil properties for this basin showed it to be useful in understanding how water moves through the subsurface and towards the channel (Williamson et al., 2015). The Nash-Sutcliffe efficiency (Ef) of previous simulation was 0.58; for comparison, a perfectly simulated record will have an Ef of 1 (Nash and Sutcliffe, 1970). Using the physically measured soils data and forest parameterization for the hydrologic model, the Ef increased to 0.68 as a result of a more accurate quantification of baseflow conditions – a direct result of local characterization of the hydrologic properties.

Because the same climate record and basin topography were used for all simulations (Figure 4.2), differences in streamflow are a direct result of differences in soil properties and how they control water movement and storage in the soil (Figure 4.3). Simulated streamflow for the FRA in mine soil (Guy Cove), strikeoff FRA (Starfire), and ripped FRA (vanBooven) are relatively similar to the control dataset (Little Millseat), albeit with higher stormflow peaks, especially in

winter (Table 4.4). For the strikeoff- and ripped-FRA soils, where a thin soil profile combines with relatively consistent Ksat to maximize water movement to the stream through the sub-surface, streamflow magnitudes are relatively at low flow conditions relative to the control simulation. In contrast, the conventional grassland reclamation site (Williams Branch) is simulated to be flashy and ephemeral, with runoff only associated with rain events and a dry channel a majority of the time. This is another consequence of the low total and gravity drained porosity combined with a 500 times change in Ksat between the surface and 280 mm depth.

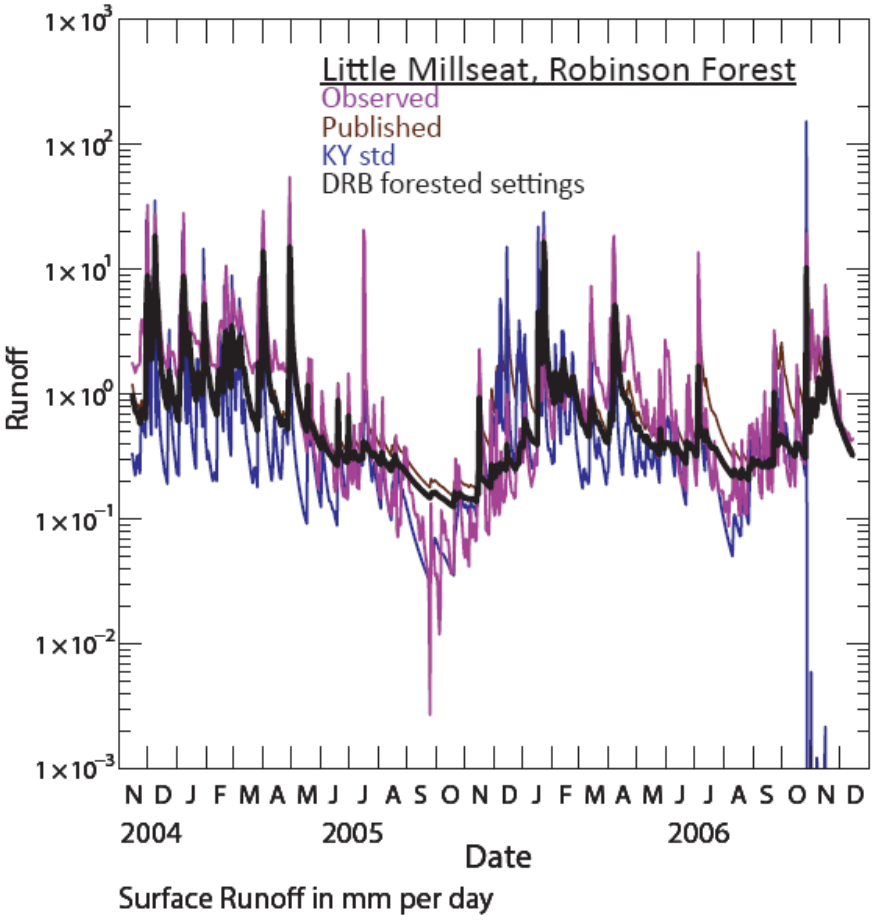

Figure 4.2. Daily streamflow observation and simulation for the Little Millseat basin.

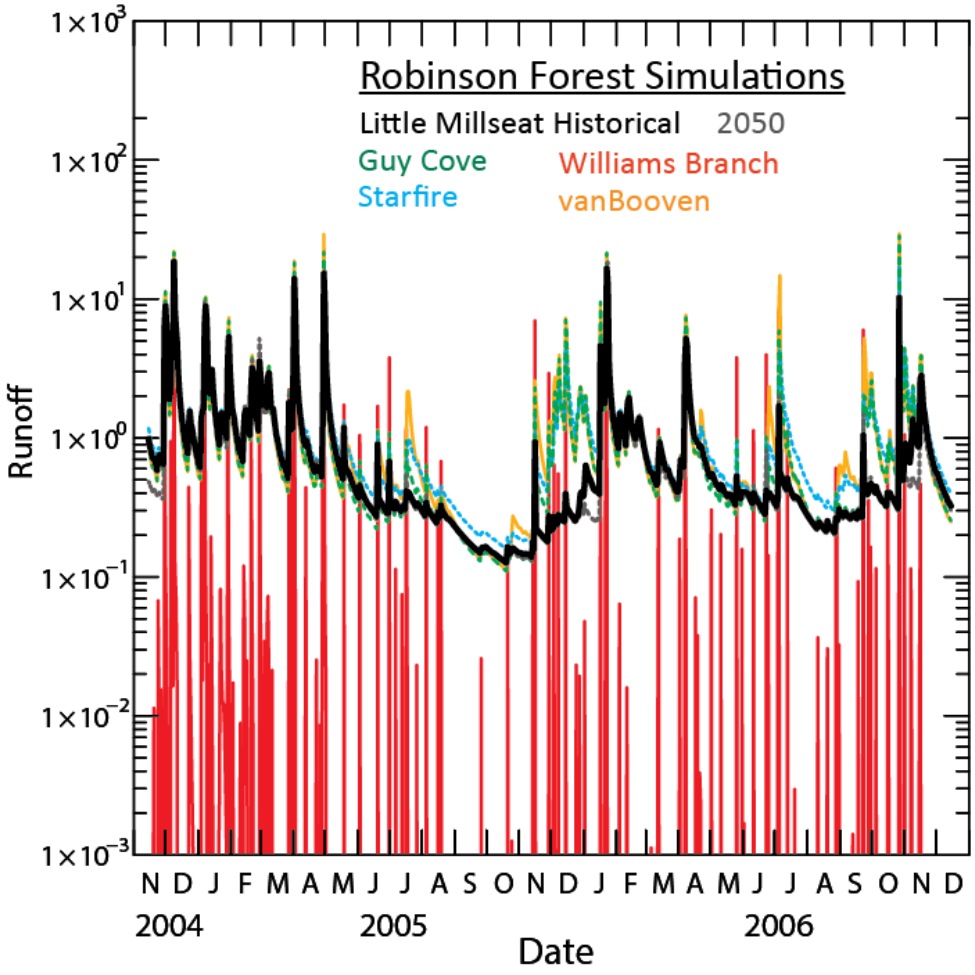

Figure 4.3. Daily streamflow simulation for the control site and four different reclamation methods.

Table 4.4. Flow exceedance probabilities for mine-reclamation simulations normalized to mm per day.

Soil Dataset	Site		Streamflow	Distribution	2004	To 2006		
		hi_99	hi_90	hi_75	med_50	lo_25	lo_10	lo_1
Observed Record	**Little**	**23.64**	**4.09**	**1.95**	**0.75**	**0.20**	**0.07**	**0.00**
Control Simulation	**Millseat**	8.76	1.93	0.95	0.42	0.27	0.20	0.13
FRA in mine soil	Guy Cove	11.82	2.45	1.17	0.51	0.28	0.19	0.12
Traditional	Williams Branch	6.04	0.05	0.00	0.00	0.00	0.00	0.00
Strikeoff FRA	Starfire	9.64	2.66	1.45	0.72	0.42	0.28	0.17
Ripped FRA	vanBooven	13.55	2.63	1.26	0.61	0.34	0.23	0.13
Projected 2050 for Control Basin	*Little Millseat*	*9.46*	*1.84*	*0.84*	*0.39*	*0.26*	*0.19*	*0.12*

Differences in actual evapotranspiration (AET) and water budget are also a direct effect of differences in the soil characteristics because precipitation and PET were the same among all simulations. The control basin shows that this environment becomes water limited during the summer, as early as June and extending into October, as the soil-water available for plant use is not enough to meet the potential evapotranspiration (PET) demand (Figure 4.4). Comparison of simulated AET among the four reclamation soil datasets shows that each reclaimed environment is water limited longer than the control and exceed that in the control basin for almost the entire growing period. The strike-off FRA (Starfire) and ripped FRA (vanBooven) environments become water limited as early as April, reflecting available-water storage of <10% for each of these soil datasets.

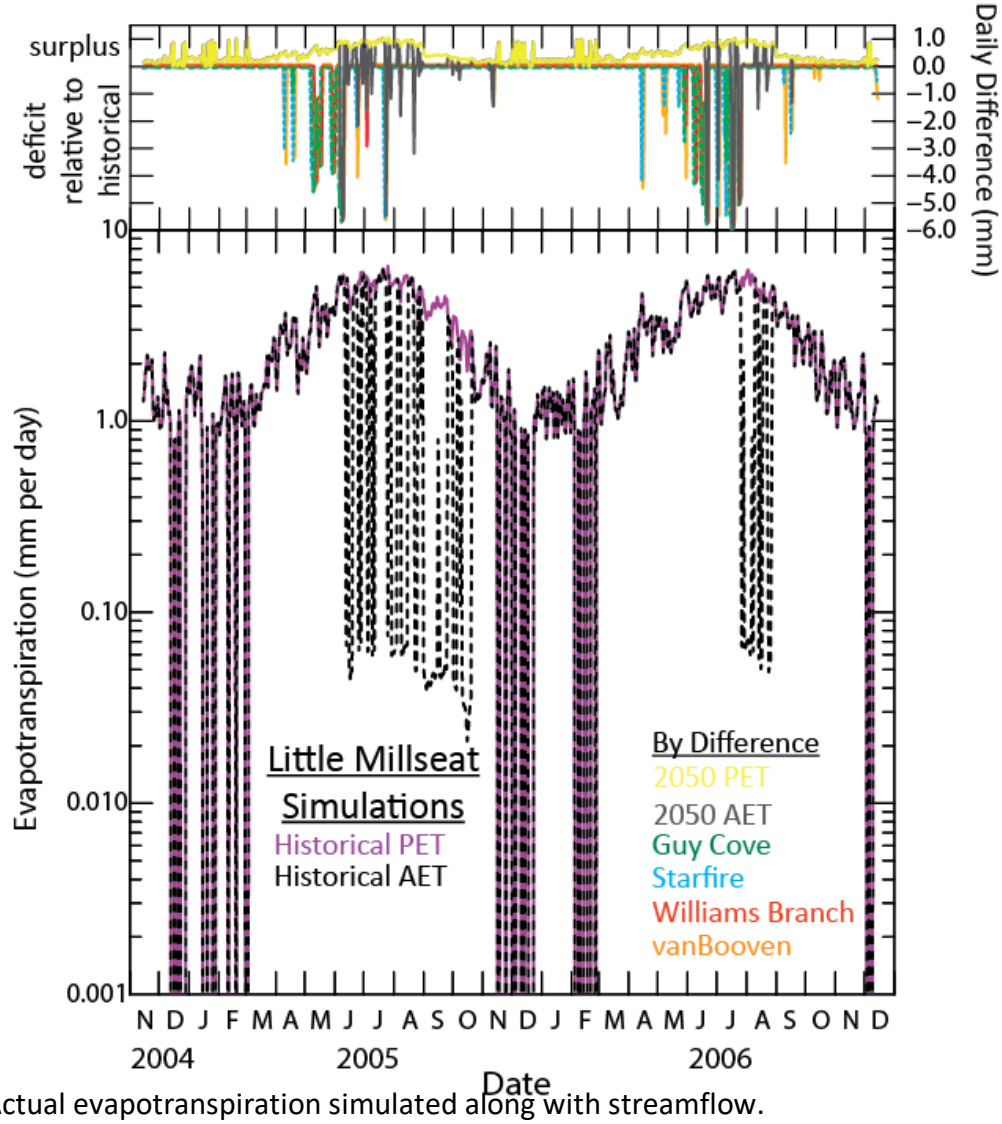

Figure 4.4. Actual evapotranspiration simulated along with streamflow.

4.3.3 Projected Mid-Century Climate Conditions

Given that each of the mine reclamation strategies results in a more water limited environment for plant growth and flashier streamflow, projected climate conditions were examined in order to understand if hydrologic changes from mine-reclamation might be exacerbated during the coming century. A projected weather record was made for the Little Millseat control basin by applying change factors for precipitation and temperature to the historical dataset. On average, daily temperature is projected to increase by 2.36 C, with the largest increase during August (Figure 4.5a). Precipitation is projected to increase by a factor of 1.05 (Figure 4.5b), with individual months increasing by a factor of 1.01 to 1.15 (a 15% increase in February that

amounts to 10.5 mm), except for October (δPPT = 0.92; an 8% decrease in October amounting to 5.5 mm). Notably, temperature is projected to increase the most during the summer months while the largest increases in precipitation are projected during December to March, with little increase ($\approx$1%) to a decrease for May, June, October, and November.

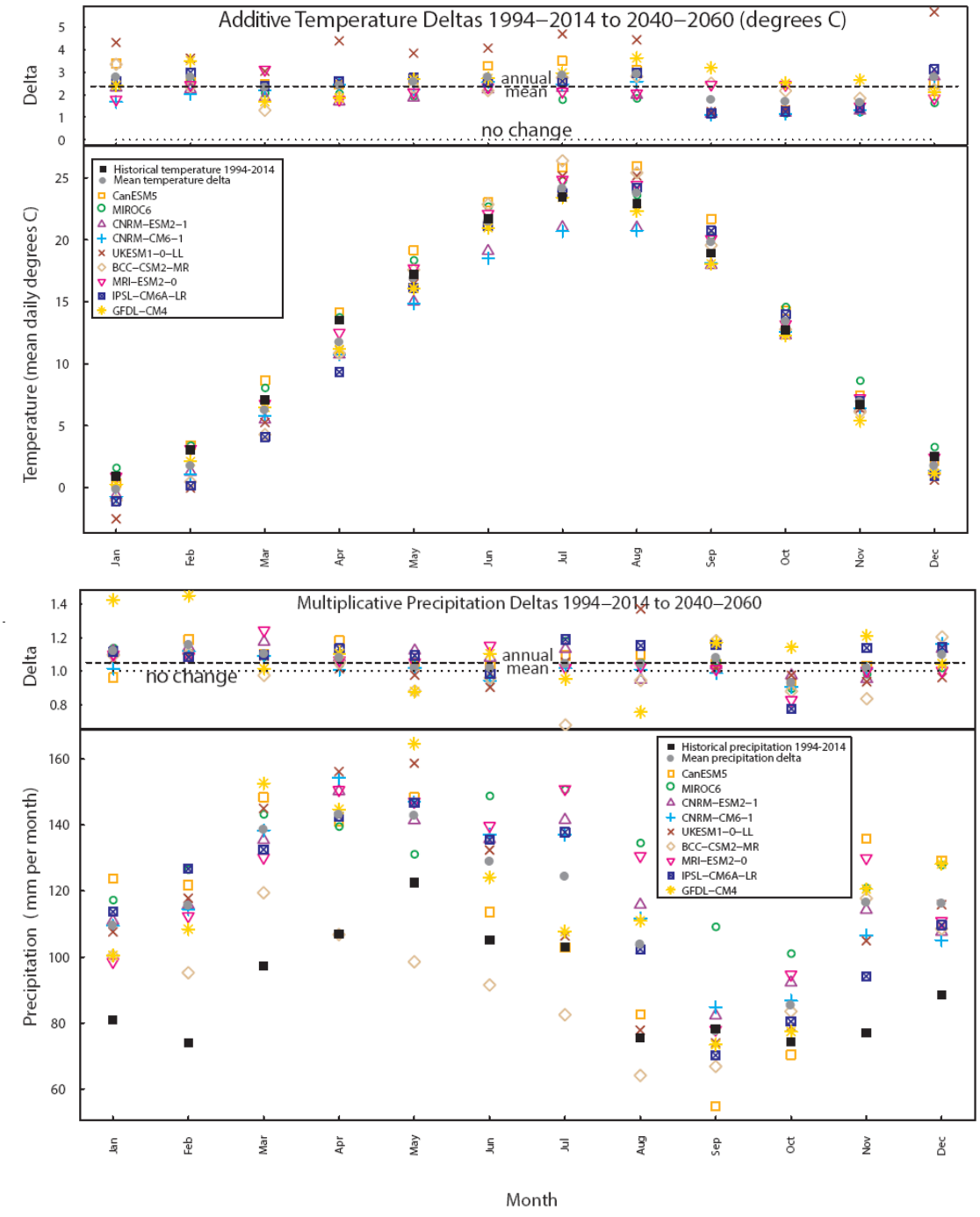

Figure 4.5. Projected change in temperature (a) and precipitation (b) between the 1994-2014 time period and 2040-2060 as derived from nine CMIP 6 datasets.

Hydrologic simulation using the projected record shows that projected streamflow is similar to the control dataset, although each streamflow probability is lower in magnitude. Evaluation of the AET for these simulations shows that the system becomes more water limited in June and extends into October and November (Figure 4.4). Notably, water limitation relative to the

control dataset is less during July and August, when precipitation is projected to increase by 3-4%, accounting for the higher temperature and exceeding the resultant PET demand.

PET is projected to increase by a factor of 1.15 (Figure 4.6) overall when evaluated as a function of the energy budget, with the largest change projected for December to February (≈19% increase) and the least in July (≈10% increase). When PET is estimated using projected temperature, the mean value of change is similar and the largest increase is during the winter months, however, the projected change during summer is approximately double that with the radiation-based change factor. Using the temperature-based method, mean annual PET is 0.5 mm per day higher and as much as 1 mm per day higher during the June to August period.

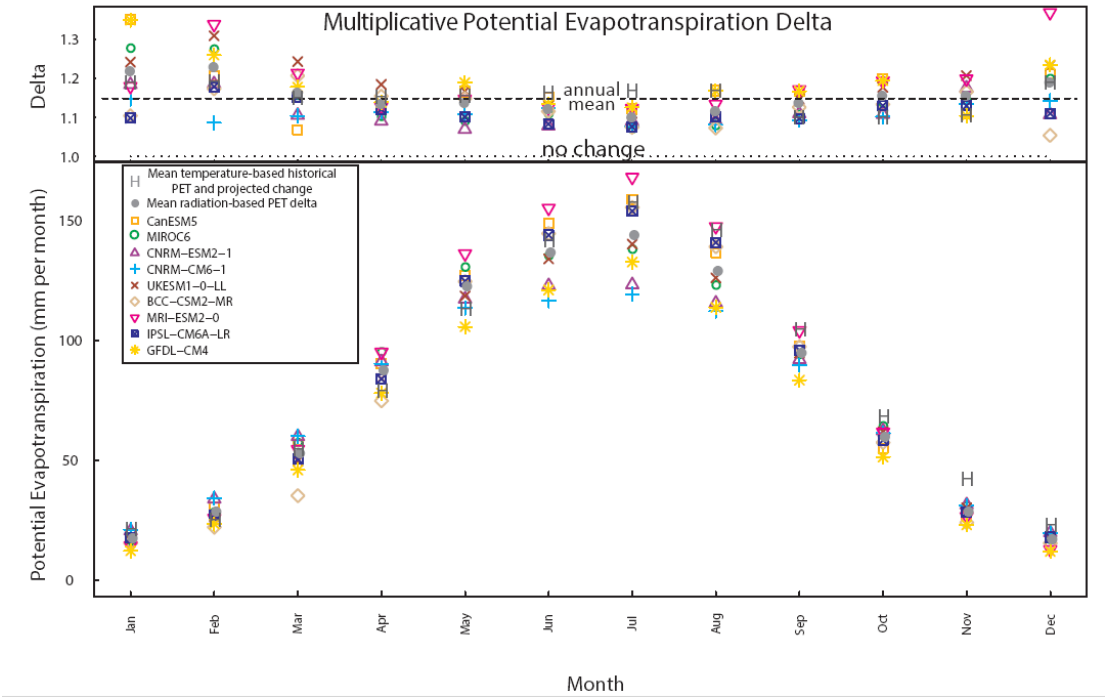

Figure 4.6. Projected PET using two different methods, an energy-based estimate of change and a change calculated from a temperature-based PET estimate as simulated in the hydrologic model.

4.4 SUMMARY

1. Generally lower porosity on FRA sites explains the higher peakflows relative to that simulated for the control soil – the reclaimed soils is more quickly saturated. During higher intensity summer events (Chapter 1) this lower porosity provides less space to replenish and relatively higher runoff for some FRA soils. So, although soils can store similar amount of plant available water, there is a decreased opportunity to store water

moving down the hillslope as near-surface flow because of the lower total porosity. So, new precipitation events are less effective at recharging soil relative to the control and less water is stored for plant use.

2. The conventionally reclaimed site (Williams Branch) combines the lowest total porosity (0.31) with a relatively high field capacity (0.27), resulting in a soil profile that cannot efficiently move water in the sub-surface during precipitation events. Further evidence of this condition is in the high conductivity multiplier and low scaling parameter –which quantify how water movement and porosity, respectively, change with depth in the soil. The result is that hydrology is simulated to be flashy – with little to no baseflow between storms.
3. Projected water limitations overlap with the months during which the reclaimed soils become more water limited relative to the control simulation. This indicates that land-use and climate change will cause hydrologic change in the same direction, amplifying the independent effects of either. Consequently, streamflow and plant survival in these areas would be expected to decrease as projected climate combines with reclaimed soils.
4. The projected soil-water deficit in June, July, and August may be an overestimate because these simulations used a temperature-based PET for projected conditions. However, the late-season soil-water deficit, in September and October reflects higher PET projections that are consistent, regardless of method. This suggests that the time period when streamflow is already lowest and plant-available water is least will become more extreme as a result of the combined increased temperature during this time period, changing energy balance, and decreased October precipitation.

5. REFERENCES

5.1 Executive Summary

Adams, Mary Beth, ed. 2017. The Forestry Reclamation Approach: Guide to Successful Reforestation of Mined Lands. Gen. Tech. Rep. NRS-169. Newtown Square, PA: U.S. Department of Agriculture, Forest Service, Northern Research Station: 1-7.

Baker, T.J., Williamson, T.N., Lee, B.D. 2015. Translating soil properties to simulated soil-water availability under forecasted climate. Soil Science Society of America Annual Meeting, Minneapolis, MN.

Bernhardt, E.S., Lutz, B.D., King, R.S., Fay, J.P., Carter, C.E., Helton, A.M., Campagna, D., Amos, J., 2012. How many mountains can we mine? Assessing the regional degradation of central Appalachian rivers by surface coal mining. *Environmental Science and Technology*, 46: 8,115-8,122.

Blackburn-Lynch, W. 2015. Development of techniques for assessing and restoring streams on surface mines. University of Kentucky Libraries. Ph.D Dissertation 822 pages.

Burger, J.A., C.E. Zipper , P.N. Angel, N. Hall, J.G. Skousen, C.D. Barton, S. Eggerud. 2013. Establishing native trees on legacy surface mines. U.S. Office of Surface Mining. Forest Reclamation Advisory Number 11. 10 p. http://arri.osmre.gov/fra.htm.

Burger J, Graves D, Angel P, Davis V, Zipper C ., 2005. The forestry reclamation approach. Appalachian Regional Reforestation Initiative, US Office of Surface Mining.

Carroll, C., Merton, I., Burger, P., 2000. Impact of vegetative cover and slope on runoff, erosion, and water quality for field plots on a range of soil and spoil materials on central Queensland coal mines. *J. of Soil Research*, 38: 313-327.

Espigares, T., Moreno de las Heras, M., Nicolau, J.M., 2011. Performance of vegetation in reclaimed slopes affected by soil erosion. *Restoration Ecology*, 19: 35-44.

Frumhoff P.C., McCarthy J.J., Melillo J.M., Moser S.C., Wuebbles D.J. 2007. Confronting Climate Change in the U.S. Northeast: Science, Impacts, and Solutions Northeast Climate Impacts Assessment, Cambridge, MA.

Harman, W., R. Starr, M. Carter, K. Tweedy, M. Clemmons, K. Suggs, C. Miller. 2012. *A Function-Based Framework for Stream Assessment and Restoration Projects.* US Environmental Protection Agency, Office of Wetlands, Oceans, and Watersheds, Washington, DC EPA 843-K-12-006.

Helvey, J.D., Patric, J.H., 1965. Canopy and litter interception of rainfall by hardwoods of eastern United States. *Water Resources Research*, 1: 193-206.

Hopkins, R. L., Altier, B. M., Haselman, D., Merry, A. D., & White, J. J. (2013). Exploring the legacy effects of surface coal mining on stream chemistry. Hydrobiologia, 713, 87–95.

Hornbeck, J. W., Pierce, R. S., & Federer, C. A. (1970). Streamflow changes after forest clearing in New England. Water Resources Research, 6, 1124–1132.

Kauffman, J.B., Beschta, R.L., Otting, N., Lytjen, D. 1997. An ecological perspective of riparian and stream restoration in the western United States. Fisheries. 22:12-24.

Kinnell, P.I.A., 2005. Why the universal soil loss equation and the revised version of it do not predict event erosion well. *Hydrological Processes*, 18: 3,191-3,194.

Kinnell, P.I.A., 2008. Sediment delivery from hillslopes and the Universal Soil Loss Equation: Some perceptions and misconceptions. *Hydrological Processes*, 22(16): 3,168-3,175.

Lindberg, T., Bernhardt, E.S., Bier, R., Helton, A.M., Merola, R.B., Vengosh, A., Di Giulio, R.T., 2011. Cumulative impacts of mountaintop mining on an Appalachian watershed. *Proceedings of the National Academy of Sciences*, 108: 20,929-20,934.

Loch, R.J., 2000. Effects of vegetation cover on runoff and erosion under simulated rain and overland flow on a rehabilitated site on the Meandu Mine, Tarong, Queensland. *Australian J. of Soil Research*, 38(2): 299-312.

McIntosh, J.E., Barnhisel, R.I., 1993. Erodibility and sediment yield by natural rainfall from reconstructed mine spoils. *J. of Soil Science*, 156: 118–126.

Miller, A.J., Zegre, N.P., 2014. Mountaintop removal mining and catchment hydrology. Water. 6:472-499.

Muncy, Brenee' L., Steven J. Price, Simon J. Bonner, Christopher D. Barton. 2014. Mountaintop removal mining reduces stream salamander occupancy and richness in southeastern Kentucky (USA). Biological Conservation. 180: 115-121.

Neary, D.G., Ice, G.G., Jackson, C.R., 2009. Linkages between forest soils and water quality and quantity. *Forest Ecology and Management*, 258: 2,269-2,281.

Negley, T. L., Eshleman, K.N., 2006. Comparison of stormflow responses of surface-mined and forested watersheds in the Appalachian Mountains, USA. *Hydrological Processes*, 20: 3,467-3,483.

Orndorff, Z. W., Daniels, W. L., Zipper, C. E., Eick, M.,Beck M., 2015. A column evaluation of Appalachian coal mine spoils' temporal leaching behavior. Environmental Pollution 204:39-47.

Parsons, A.J., Wainwright, J., Brazier, R.E., Powell, D.M., 2006. Is sediment delivery a fallacy? *Earth Surface Processes*, 31: 1,325-1,328.

Pond, G. J. 2011. Biodiversity loss in Appalachian headwater streams (Kentucky, USA): Plecoptera and Trichoptera communities. Hydrobiologia, 679, 97–117.

Pond, G.J., 2010. Patterns of Ephemeroptera taxa loss in Appalachian headwater streams (Kentucky, USA). *Hydrobiologia*, 641: 185-201.

Pond, G.J., Passmore, M.E., Borsuk, F.A., Reynolds, L., Rose, C.J., 2008. Downstream effects of mountaintop coal mining: Comparing biological conditions using family-and genus-level macroinvertebrate bioassessment tools. *J. of the North American Benthological Society*, 27: 717-737.

Porto, P., Walling, D.E., Callegari, G., 2011. Using Cs-137 measurements to establish catchment sediment budgets and explore scale effects. *Hydrological Processes*, 25(6): 886-900.

Porto, P., Walling, D.E., Callegari, G., Capra, A., 2009. Using caesium-137 and unsupported lead-210 measurements to explore the relationship between sediment mobilization, sediment delivery and sediment yield for a Calabrian catchment. *Marine and Freshwater Research*, 60(7): 680-689.

Ritter, J. B., & Gardner, T. W. (1993). Hydrologic evolution of drainage basins disturbed by Surface mining, central Pennsylvania. Geological Society of America Bulletin, 105, 101–115.

Sena, K., Barton, C., Angel, P., Agouridis, C., Warner R., 2014. Influence of spoil type on chemistry and hydrology of interflow on a surface coal mine in the eastern US coalfield. Water, Air, and Soil Pollution 225:2171.

Senay G.B., Bohms S., Singh R.K., Gowda P.H., Velpuri N.M., Alemu H., Verdin J.P. 2013. Operational Evapotranspiration Mapping Using Remote Sensing and Weather Datasets: A New Parameterization for the SSEB Approach. JAWRA Journal of the American Water Resources Association 49:577-591. DOI: 10.1111/jawr.12057.

Sheoran, V., Sheoran, A.S., Poonia, P., 2010. Soil reclamation of abandoned mine land by revegetation: A review. *International J. of Soil, Sediment and Water*, 3(2): Art. 13.

Smucker, N. J., & Vis, M. L. (2011). Acid mine drainage affects the development and function of Epilithic biofilms in streams. Journal of the North American Benthological Society, 30, 728–738.

Taylor, T.J., Agouridis, C.T., Warner, R.C., Barton, C.D., 2009. Runoff curve numbers for loose-dumped spoil in the Cumberland Plateau of eastern Kentucky. *International J. of Mining, Reclamation and Environment*, 23: 103-120.

Toy, T.J., 1989. An assessment of surface-mine reclamation based upon sheetwash erosion rates at the Glenrock Coal Company, Glenrock, Wyoming. *Earth Surface Processes and Landforms*, 14(4): 289-302.

Toy, T.J., Foster, G.R., Renard, K.G., 1999. RUSLE for mining, construction and reclamation lands. *J. of Soil and Water Conservation*, 54: 462–467.

Walling, D.E., 1999. Linking land use, erosion and sediment yields in river basins. Hydrobiologia, 410: 223-240.

Walter, I.A., R.G. Allen, R. Elliott, M.E. Jensen, D. Itenfisu, B. Mecham, T.A. Howell, R. Snyder, P. Brown, S. Echings, T. Spofford, M. Hattendorf, R.H. Cuenca, J.L. Wright, D. Martin. 2000. ASCE's Standardized Reference Evapotranspiration Equation. Proc. of the Watershed Management 2000 Conference, June 2000, Ft. Collins, CO, American Society of Civil Engineers, St. Joseph, MI.

Wickham, J., Wood, P.B., Nicholson, M.C., Jenkins, W., Druckenbrod, D., Suter, G.W., Strager, M.P., Mazzarella, C., Galloway, W.,Amos, J., 2013. The overlooked terrestrial impacts of mountaintop mining. *BioScience*, 63: 335-348.

Wilkinson, S.N., Wallbrink, P.J., Hancock, G.J., Blake, W.H., Shakesby, R.A., Doerr, S.H., 2009. Fallout radionuclide tracers to identify a switch in sediment sources and transport-limited sediment yield following wildfire in a eucalypt forest. *Geomorphology*, 110(3-4): 140-151.

Williamson T.N., Agouridis C.T., Barton C.D., Villines J.A., Lant J.G. 2015a. Classification of ephemeral, intermittent, and perennial stream reaches using a TOPMODEL-based approach. Journal of the American Water Resources Association in press. DOI: 10.1111/1752-1688.12352

Williamson T.N., Lant J.G., Claggett P., Nystrom E., Milly P.C.D., Nelson H., Hoffman S., Colarullo S., Fischer J. 2015b. Summary of hydrologic modeling for the Delaware River Basin using the Water Availability Tool for Environmental Resources (WATER), Scientific Investigations Report, U.S. Geological Survey, Reston, VA. http://dx.doi.org/10.3133/sir2015/5143.

Witt, Emma, Christopher Barton, Jeffrey Stringer, Alex Cherry and Randall Kolka. 2015. Influence of variable streamside management zones configurations on water quality following forest harvest. Journal of Forestry.

Zipper, C.E., Burger, J.A., Skousen, J.G., Angel, P.N., Barton, C.D., Davis, V., Franklin, J.A., 2011. Restoring forests and associated ecosystem services on Appalachian coal surface mines. *Environmental Management*, 47(5): 751-765.

5.2 Chapter 1

American Geological Institute [AGI]. 2006. Coal and the Environment. AGI Environmental Awarenes series 10. Eds. S.F Greb, C.F. Eble, D.C. Peters, and A.R. Papp.

Agouridis, C.T., P.N. Angel, T.J. Taylor, C.D. Barton, R.C. Warner, X. Yu, and C. Wood. 2012. Water Quality Characteristics of Discharge from Reforested Loose-Dumped Mine Spoil in Eastern Kentucky. Journal of Environmental Quality 41: 454-468.

Angel, P., V. Davis, J. Burger, D. Graves, and C. Zipper. 2005. The Appalachian Regional Reforestation Initiative. Forest Reclamation Advisory No. 1. U.S. Office of Surface Mining.

Angel, P.A., D.H. Graves, C. Barton, R.C. Warner, P.W. Conrad, R.J. Sweigard, and C. Agouridis. 2006. Surface Mine Reforestation Research: Evaluation of Tree Response to Low Compaction Reclamation Techniques. Ed. R.I. Barnheisel. American Society of Mining and Reclamation, 7th International Conference on Acid Rock Drainage (ICARD). St. Louis, MO, March 26-30.Appalachian Regional Commission [ARC]. 2019. The Appalachian Region. Available at https://www.arc.gov/appalachian_region/MapofAppalachia.asp. Accessed February 21, 2019.

Austen, T.A. and B.J. Claborn. 1974. Statistical Models of Short-duration Precipitation Events. Proceedings of the Symposium on Statistical Hydrology, Tucsin, AZ, Aug. 31-Sep.2, 1971. USDA-ARS, Miscellaneous Publication No. 1275, p. 356-365.

Barton, C.D., K. Sena, T. Dolan, P. Angel, and C. Zipper. 2017. Chapter 8: Restoring Forests on Surface Coal Mines in Appalachia: A Regional Reforestation Approach with Global Application. In Spoil to Soil: Mine Site Rehabilitation and Revegetation. Eds. Bolan, N.S., M.B. Kirkham, and Y.S. Ok.

Bell, G., K.L. Sena, C.D. Barton; and M. French. Establishing Pine Monocultures and Mixed Pine-Hardwood Stands on Reclaimed Surface Mined Land in Eastern Kentucky: Implications for Forest Resilience in a Changing Climate.2017. Forestry and Natural Resources Faculty Publications. 8: 1-11.

Bonta, J.V., C.R. Amerman, T.J. Harlukowicz, and W.A. Dick. 1997. Impact of Coal Surface Mining on 3 Ohio Watersheds – Surface Water Hydrology. Journal of the American Water Resources Association 33: 907-907.

Booth, D.B. 1990. Stream-Channel Incision Following Drainage-Basin Urbanization. Journal of the American Water Resources Research Association 26(3): 407-417.

Bosch, D.D., J.M. Sheridan, and F.M. Davis. 1999. Rainfall Characteristics and Spatial Correlation for the Georgia Coastal Plain. Transactions of the ASAE. 42(6): 1637-1644. Doi: 10.13031/2013.13330.

Bradshaw, A. 1997. Restoration of Mined Lands – Using Natural Processes. Ecological Engineering 8: 255-269.Braun, E.L. 1950 Deciduous Forests of Eastern North America. The Blakiston Company, Philadelphia, PA.B

rothers, T.S. 1990. Surface-Mine Grasslands. Geographical Review 80(3): 209-225.Bryant, M.L., S. Bhat, and J.M. Jacobs. 2005. Measurements and Modeling of Throughfall Variability for Five Forest Communities in the Southeastern US. Journal of Hydrology 312: 95-108.

Burger, J. D. Graves, P. Angel, V. Davis, and C. Zipper. 2005. The Forestry Reclamation Approach. U.S. Office of Surface Mining. Forestry Reclamation Advisory No. 2.

Caldwell, P.V., C.R. Jackson, C.F. Miniat, S.E. Younger, J.A. Vining, J. J. McDonnell, D.P. Aubrey. 2018. Woody bioenergy crop selection can have large effects on water yield: A southeastern United States case study. Biomass and Bioenergy. 117: 180–189.

Carlyle-Moses, D.E. 2004. Throughfall, Stemflow, and Canopy Interception Loss Fluxes in a Semi-Arid Sierra Madre Oriental Matorral Community. Joural of Arid Environments 58(2): 181-202.

Carpenter, S.B. and R.L. Rumsey. 1976. Trees and Shrubs of Robinson Forest Breathitt County, Kentucky. Castanea 41(4): 227-282.

Cherry, M.A. 2006. Hydrochemical Characterization of Ten Headwater Catchments in Eastern Kentucky. M.S. Thesis, University of Kentucky, Lexington, Kentucky.

Ciach, G.J. 2003. Local Random Errors in Tipping-Bucket Rain Gauge Measurements. Journal of Atmospheric and Oceanic Technology 20: 752-759.

Colloff, M.J., K.R. Pullen, and S.A. Cunningham. 2010. Restoration of an Ecosystem Function to Revegetation Communities: The Role of Invertebrate Macropores in Enhancing Soil Water Infiltration. Restoration Ecology 18: 65–72.

Cornish, P.M. and R.A. Vertess. 2001. Forest age-induced changes in evapotranspiration and water yield in a eucalypt forest. Journal of Hydrology 242: 43–63.

Crockford, R.H. and D.P. Richardson. 2000. Partitioning of Rainfall into Throughfall, Stemflow and Interception: Effect of Forest Type, Ground Cover and Climate. Hydrological Processes 14: 2903-2920.

Daniels, W.L., C.E. Zipper, Z.W. Orndorff, J.G. Skousen, C.D. Barton, L. McDonald, and M. Beck. 2016. Predicting Total Dissolved Solids Release from Central Appalahian Coal Mine Spoils. Environmental Pollution 216: 371-379.

Dore, M.H.I. 2005. Climate Change and Changes in Global Precipitation Patterns: What Do We Know? Environment International 31: 1167-1181.

Dukes, J.S., J. Pontius, D. Orwig, J.R. Garnas, V.L. Rodgers, N. Brazee, B. Cooke, K.A. Theoharides, E.E. Stange, R. Harrington, J. Ehrenfeld, J. Gurevitch, M. Lerdau, K. Stinson, R. Wick, and M. Ayres. 2009. Response of Insect Pests, Pathogens, and Invasive Plant Species to Climate Change in the Forests of Northeastern North America: What can We Predict? Canadian Journal of Forest Research 39: 231-248.

Ferrari, J.R., T.T. Lookingbill, B. McCormick, P.A. Townsend and K.N. Eshleman.2009. Surface Mining and Reclamation Effects on Flood Response of Watersheds in the Central Appalachian Plateau Region. Water Resources Research. Vol. 45. DOI: 10.1029/2008WR007109.

Guebert, M.D. and T.W. Gardner 2001. Macropore Flow on a Reclaimed Surface Mine: Infiltration and Hillslope Hydrology. Geomorphology 39: 151-169.

Graves, D.H., J.M. Ringe, M.H. Pelkki, R.J. Sweigard, and R.C. Warner. 2000. High Value Tree Reclamation Research. p. 413-421. In Proceedings of the Sixth International Conference on Environmental Issues and Management of Waste in Energy and Mineral Production. SWEMP 2000. Calgary, Alberta, Canada.

Haering, K.C. W.L. Daniels, and J. Galbraith. 2004. Appalachian Mine Spoil Morphology and Properties. Soil Science Society of America Journal 68(4): 1315-1325.

Haydon, S.R., R.G. Benyon, and R. Lewis. 1996. Variation in Sapwood Area and Throughfall with Forest Age in Mountain Ash (Eucalyptus regnans F. Muell.). Journal of Hydrology 187: 351-366.

Hayes, R.A. 1991. Soil Survey of Breathitt County, Kentucky, USDA-NRCS.Helvey, J.D. and J.H. Patric. 1965. Canopy and Litter Interception of Rainfall by Hardwoods of Eastern United States. Water Resources Research 1(2): 193-206.

Herwitz, S.R. 1987. Raindrop Impact and Water Flow on the Vegetative Surfaces of Trees and the Effects on Stemflow and Throughfall. Earth Surface Processes and Landforms 12(4): 425-432.Holl, K.D., C.E. Zipper, and J.A. Burger. 2009. Recovery of Native Plant Communities After Mining. Publication 460-140. Virginia Cooperative Extension, Blacksburg, VA.

Hoomehr, S., J.S. Schwartz, D. Yoder, E.C. Drum, and W. Wright. 2015. Erodibility of Low-Compaction Steep-sloped Reclaimed Surface Mine Lands in the Southern Appalachian Region, USA. Hydrological Processes 29(3): 321-338.

Husic, A., J. Fox, E. Adams, J. Backus, E. Pollock, W. Ford, and C. Agouridis. 2019. Inland Impacts of Atmospheric River and Tropical Cyclone Extremes on Nitrate Transport and Stable Isotope Measurements. Environmental Earth Sciences 78: 36.

Jackson, I.J. 1975. Relationships between Rainfall Parameters and Interception by Tropical Forest. Journal of Hydrology 24 (3-4): 215-238.

Johnson, D.W., P.J. Hanson, and D.E. Todd, Jr. 2002. The Effects of Throughfall Manipulation on Soil Leaching in a Deciduous Forest. Journal of Environmental Quality 31: 204-216.

Jorgensen, D.W. and T.W. Gardner. 1987. Infiltration Capacity of Disturbed Soils: Temporal Change and Lithologic Control. Water Resources Bulletin 23: 116-1172.

Kalisz, P.J., R.W. Zimmerman, and R.N. Muller. 1987. Root Density, Abundance,and Distribution in Mixed Mesophytic Forest of Eastern Kentucky. Soil Science Society of American Journal. 51: 220-225.

Kim, H-Y. 2013. Statistical Notes for Clinical Researchers: Assessing Normal Distribution (2) Using Skewness and Kurtosis. Restorative DentistryEndodontics 38(1): 52-54.

Kuczera, G. 1987. Predictionof Water Yield Reductions Following a Bushfire in Ash-mixed Species Eucalypt Forest. Journal of Hydrology 94: 215-236.

Lafleur, B., D. Paré, A.D. Munson, and Y. Bergeron. 2010. Response of Northeastern North American Forests to Climate Change: Will Soil Conditions Constrain Tree Species Migration? Environmental Reviews 18: 279-289.

Levia, D.F. and E.E. Frost 2006. Variability of Throughfall Volume and Solute Inputs in Wooded Ecosystems. Progress in Physical Geography 30 (5): 605-632.

Levia, D.F., R.F. Keim, D.R. Carlyle-Moses, and E.E. Frost. 2011. Throughfall and Stemflow in Wooded Ecosystems. In Forest Hydrology and Biogeochemistry: Synthesis of Past Research and Future Directions. Eds. D.F. Levia, D. Carlyle-Moses, and T. Tanaka. Springer, New York, NY.

Llorens, P., I. Oliveras, and R. Poyatos. 2003. Temporal Variability of Water Fluxes in a Pinus sylvestris Forest Patch in Mediterranean Mountain Conditions (Vallcebre Research Catchments, Catalan Pyrenees). Hydrology of the Mediterranean and Semiarid Regions. Proceedings of an International Symposium held at Montpellier, April 2003. IAHS Publication No. 278.

Llorens, P., R. Poch, J. Latron, and F. Gallart. 1997. Rainfall Interception by a Pinus sylvestris Forest Patch Overgrown in a Mediterranean Mountainous Abandoned Area. I. Monitoring Design and Results Down to the Event Scale. Journal of Hydrology 199: 331-345.

Lloyd, C.R. and A.D.O. Marques. 1988. Spatial Variability of Throughfall and Stemflow Measurements in Amazonian Rainforest. Agricultural and Forest Meteorology 42: 63-73.

Mao, D. and K.A. Cherkauer 2009. Impacts of Land-Use Change on Hydrologic Responses in the Great Lakes Region. Journal of Hydrology 374: 71-82.

McCarthy, E.J., R.W. Skaggs, and P. Famum. 1991. Experimental Determination of the Hydrologic Components of a Drained Forest Watershed. Transactions of the ASAE 34(5): 2031-2039.

McDowell, R.C., G.J. Grabowski, and S.L. Moore. 1981. Geologic Map of Kentucky. U.S. Geological Survey, scale 1:250,000, 4 sheets.

Miller, J., C. Barton, C. Agouridis, A. Fogle, T. Dowdy, and P. Angel. 2012. Evaluating Soil Genesis and Reforestation Success on a Surface Coal Mine in Appalachia. Soil Science Society of America Journal 76: 950-960.

Miller, A.J. and N.P. Zégre, 2014. Mountaintop Removal Mining and Catchment Hydrology. Water 6: 472-499.

Miralles, D.G., J.H. Gash, T.R.H. Holmes, R.A.M. de Jeu, and A.J. Dolman. 2010.Global Canopy Interception from Satellite Observations. Journal of Geophysical Research 115: D16122.

Negley, T.L. and K.N. Eshleman. 2006. Comparison of Stormflow Responses of Surface-Mined and Forested Watersheds in the Appalachian Mountains, USA. Hydrological Processes 20: 3467-3483.

Orr, S.P., J.S. Rudgers, and K. Clay. 2005. Invasive Plants can Inhibit Native Tree Seedlings: Testing Potential Allelopathic Mechanisms. Plant Ecology 181(2): 153-165.

Osborne, L.L. and D.A. Kovacic 1993. Riparian Vegetated Buffer Strips in Water-Quality Restoration and Stream Management. Freshwater Biology 29: 243-258.

Overstreet, J.C. 1984. Robinson Forest Inventor. 1980-1982. Department of Forestry, College of Agriculture, University of Kentucky, Lexington, Kentucky.

Pericak, A.A., C.J. Thomas, D. A. Kroodsma, M.F. Wasson, M.R.V. Ross, N.E. Clinton, D.J. Campagna, Y. Franklin, E.S. Bernhardt, and J.F. Amos. 2018. Mapping the Yearly Extent of Surface Coal Mining in Central Appalachia Using Landsat and Google Earth Engine. PLOS One.

Pressland, A.J. 1973. Soil Moisture Redistribution as Affected by Throughfall and Stemflow in an Arid Zone Shrub Community. Australian Journal of Botany 24(5): 641-649.

Rhoads, B.L. 1995. Stream Power: A Unifying Theme for Urban Fluvial Geomorphology.In Stormwater Runoff and Receiving Systems: Impact, Monitoring, and Assessment. Eds. E. Herricks and J.R. Jenkins. CRC Lewis Publishers, Boca Raton, FL.

Ricketts, T.H., E. Dinerstein, D.M. Olson, and C. Loucks. 1999. Who's Where in North America?: Patterns of Species Richness and the Utility of Indicator Taxa for Conservation. BioScience 49(5): 369-381.

Roberts, J.A., W.L. Daniels, J.C.Bell, and D.C. Martens. 1998. Tall Fescue Production and Nutrient Status on Southwest Virginia Mine Soils. Journal of Environmental Quality 17: 55-62.

Robson, A.J., C. Neal, G.P. Ryland, and M. Harrow. 1994. Spatial Variations in Throughfall Chemistry at Small Plot Scale. Journal of Hydrology 158: 107-122.

Ruppert, L.F., 2001, Chapter A—Executive summary—Coal resource assessment of selected coal beds and zones in the northern and central Appalachian Basin coal regions, in Northern and Central Appalachian Basin Coal Regions Assessment Team, 2000 resource assessment of selected coal beds and zones in the northern and central Appalachian Basin coal regions: U.S. Geological Survey Professional Paper 1625–C, CD-ROM, version 1.0.

SAS Institute Inc. [SAS] 2016. SAS/CONNECT® 9.4 User's Guide, Fourth Edition. Cary, NC.

Saunders, D.A., R.J. Hobbs, and C.R. Margules. 1991. Biological Consequences of Ecosystem Fragmentation: A Review. Conservation Biology 5(1): 18-32.

Sayler, K.L. 2016. Chapter 10 Central Appalachian Ecoregion. In Status and Trends of Land Change in the Eastern United States – 1973-2000. Eds. K.L. Sayler, W. Acevedo, and J.L. Taylor. U.S. Geological Survey Professional Paper 1794-D.

Sena, K.L. 2014. Influence of Spoil Type on Afforestation Success and Hydrochemical Function on a Surface Coal Mine in Eastern Kentucky. M.S. Thesis, University of Kentucky, Lexington, KY.

Sena, K., C. Barton, S. Hall, P. Angel, C. Agouridis, and R. Warner. 2015. Influence of Spoil Type on Afforestation Success and Natural Vegetative Recolonization on a Surface Coal Mine in Eastern Kentucky, USA. Restoration Ecology 23(2): 131-138.

Sena, K., C. Agouridis, J. Miller, and C. Barton. 2018. Spoil Type Influences Soil Genesis and Forest Development on an Appalachian Surface Coal Mine Ten Years after Placement. Forests 9(12): 780.

Shukla, M.K. R. Lal, J. Underwood, and M. Ebinger. 2004. Physical and Hydrological Characteristics of Reclaimed Minesoils in Southeastern Ohio. Soil Science Society of America Journal 68(4): 1352-1359.

Simmons, J., Currie, W., Eshleman, K., Kuers, K., Monteleone, S., Negley, T., Phlad, B., Thomas, C. 2008. Forest to Reclaimed Mine Land Use Change Leads to Altered Ecosystem Structure and Function. Ecological Applications 18(1): 104-118.

Singh, V., R.K. Rana, and R. Singhal. 2013. Analysis of Repeated Measurement Data in the Clinical Trials. Journal of the Ayrurveda and Integrative Medicine 4(2): 77-81.

Skousen, J., J. Gorman, E. Pena-Yewtukhiw, J. King, J. Stewart, P. Emerson, and C. DeLong. 2009. Hardwood Tree Survival in Heavy Ground Cover on Reclaimed Land in West Virginia: Mowing and Ripping Effects. Journal of Environmental Quality 38: 1400-1409.

Smalley, G.W. 1986. Classification and Evaluation of Forest Sites in the Northern Cumberland Plateau. General Technical Report GTP-SO-50, USDA Forest Service Southern Forest Experiment Station, New Orleans, Louisiana.

Smith, W.D. 1980. Has Anyone Noticed that Trees are not Being Planted Any Longer? Trees for Reclamation in the Eastern U.S. Symposium, Lexington, KY, October 27-29.

Sweigard, R., J. Burger, D. Graves, C. Zipper, C. Barton, J. Skousen, and P. Angel.2007. Loosening Compacted Soils on Mined Sites. Forestry Reclamation Advisory No. 4. U.S. Office of Surface Mining.

Tanaka, N., D. Levia, Y. Igarashi, K. Nanko, N. Yoshifuji, K. Tanaka, C. Tantasirin, M. Suzuki, and T. Kumagai. 2015. Throughfall Under a Teak Plantation in Thailand: A Multifactorial Analysis on the Effects of Canopy Phenology and Meteorological Conditions. International Journal of Biometeorology 59: 1145-1156.

Taylor, C.T. Agouridis, R.C. Warner, C.D. Barton, and P.N. Angel. 2009a. Hydrologic Characteristics of Appalachian Loose-Dumped Spoil in the Cumberland Plateau of Eastern Kentucky. Hydrologic Processes 23: 3372-3381.

Taylor et al 2009b. Runoff Curve Numbers for Loose-Dumped Spoil in the Cumberland Plateau of Eastern Kentucky. International Journal of Mining, Reclamation, and Environment 23(2): 103-120.

Thimonier, A. 1998. Measurement of Atmospheric Deposition Under Forest Canopies: Some Recommendations for Equipment and Sampling Design. Environmental Monitoring and Assessment 52: 353-387.

Townsend, P.A., D.P. Helmers, C.C. Kingdon, B.E. McNeil, K.M. de Beurs, and K.N. Eshleman. 2008. Changes in the Extent of Surface Mining and Reclamation in the Central Appalachians Detected Using a 1976-2006 Lands Landsat Time Series. Remote Sensing of Environment 113: 62-72.

United States Department of Commerce [USDC]. 2002. Climatography of the United States: Monthly Station Normals of Temperature, Precipitation, and Heating and Cooling Degree Days 1971-2000. Weather Bureau No. 81 (15). United States Department of Commerce, Asheville, North Carolina.

United States Environmental Protection Agency [USEPA]. 2011. The Effects of Mountaintop Mines and Valley Fills on Aquatic Ecosystems on the Central Appalachian Coalfields. EPA/600/R09/138F. Office of Research and Development, National Center for Environmental Assessment.

Villines, J.A., C.T. Agouridis, R.C. Warner, and C.D. Barton. 2015. Using GIS to Delineate Headwater Stream Origins in the Appalachian Coalfields of Kentucky. Journal of the American Water Resources Association 51(6): 1667-1687.

Wells, L.G., A.D. Ward, and R.E. Phillips. 1983. Predicting Infiltration and Surface Runoff from Reconstructed Spoils and Soils. Lexington, KY: Water Resources Research Institute, University of Kentucky.

Wickham, J.D., K.H. Ritters, T.G. Wade, M. Coan, and C. Homer. 2007. The Effect of Appalachian Mountaintop Mining on Interior Forest. Landscape Ecology 22: 179-187.

Wiley, J.B. and F.D. Brogan. 2003. Comparison of Peak Discharges Among Sites with and without Valley Fills for July 8-9 2001, Flood in the Headwaters of Clear Fork, Coal River Basin, Mountaintop Coal-Mining Region, Southern West Virginia. U.S. Department of the Interior, U.S. Geological Survey, Charleston, WV.

Witt, E.L. 2012. Evaluating Streamside Management Zone Effectiveness in Forested Watersheds of the Cumberland Plateau. M.S. Thesis. University of Kentucky, Lexington, Kentucky.

Woodwall, C.W., C.M. Oswalt, J.A. Westfall, C.H. Perry, M.D. Nelson, and A.O. Finley. 2009. An Indicator of Tree Migration in Forests of the Eastern United States. Forest Ecology and Management 257: 1434-1444.

Xu, Y., J.A. Burger, W.M. Aust, S.C. Patterson, M. Miwa, and D.P. Peterson. 2002. Changes in Surface Water Table Depth and Soil Physical Properties After Harvest and Establishment of Loblolly Pine (Pinus taeda L.) in Atlantic Coastal Plain Wetlands of South Carolina. Soil and Tillage Research 63: 109-121.

Zipper, C.E. 1990. Variances from “Approximate Original Contour” Requirements in Central Appalachia: History and Prospects. Proceedings of the American Society of Mining and Reclamation, pp. 153-158.

Zipper, C.E., J.A. Burger, J.G. Skousen, P.N. Angel, C.D. Barton, V. Davis, and J.A. Franklin. 2011. Restoring Forests and Associated Ecosystem Services on Appalachian Coal Surface Mines. Environmental Management 47: 751-765.

5.3 Chapter 2

Ab Razak, I. A., Li, A., Christensen, E. R. 1996. Association of PAHs, PCBs, ^{137}Cs, and ^{210}Pb with clay, silt, and organic carbon in sediments. *Water Science and Technology*, *34*(7-8), 29-35.

Adams, M. B. 2017. The forestry reclamation approach: Guide to successful reforestation of mined lands. Gen. Tech. Rep. NRS-169. Newtown Square, PA: U.S. Department of Agriculture, Forest Service, Northern Research Station: Volume 169, 128.

Al Hamarneh, I., Wreikat, A., Toukan, K. 2003. Radioactivity concentrations of ^{40}K, ^{134}Cs, ^{137}Cs, ^{90}Sr, ^{241}Am, ^{238}Pu and ^{239,240}Pu radionuclides in Jordanian soil samples. *J. of Environmental Radioactivity*, *67*(1), 53-67.

Angel, P. N., Burger, J. A., Davis, V. M., Barton, C. D., Bower, M., Eggerud, S. D., Rothman, P. 2009. The forestry reclamation approach and the measure of its success in Appalachia. In *26th Annual National Conference of the American Society of Mining and Reclamation,* Lexington, KY (pp. 18-36).

Angel, P. N., Graves, D. H., Barton, C., Warner, R. C., Conrad, P. W., Sweigard, R. J., Agouridis, C. 2006. Surface mine reforestation research: Evaluation of tree response to low compaction reclamation techniques. In *Proceedings, American Society of Mining and Reclamation* (pp. 45-58).

Arthur, M. A., Coltharp, G. B., Brown, D. L. 2007. Effects of best management practices on forest stream water quality in eastern Kentucky 1. *JAWRA J. of the American Water Resources Association*, *34*(3), 481-495.

Arvidsson, J. 1999. Nutrient uptake and growth of barley as affected by soil compaction. *Plant and Soil*, *208*(1), 9-19.

Baskaran, M. (Ed.). 2011. *Handbook of Environmental Isotope Geochemistry*. Springer Science and Business Media. pp 305-331.

Baskaran, M., Coleman, C. H., Santschi, P. H. 1993. Atmospheric depositional fluxes of ^{7}Be and ^{210}Pb at Galveston and College Station, Texas. *J. of Geophysical Research: Atmospheres*, *98*(D11), 20,555-20,571.

Bauman, J. M., Cochran, C., Chapman, J., Gilland, K. 2015. Plant community development following restoration treatments on a legacy reclaimed mine site. *Ecological Engineering*, *83*, 521-528.

Benmansour, M., Nouira, A., Benkdad, A., MAJAH, M., Bouksirat, H., Oumri, M., Mossadek, R., Duchemin, M. 2011. Estimates of long- and short-term soil erosion rates on farmland in semi-arid West Morocco using caesium-137, excess lead-210 and beryllium-7 measurements. *Impact of Soil Conservation Measures on Erosion Control and Soil Quality,* IAEA-TECDOC-1665, IAEA, Vienna, 159-174.

Bernhardt, E. S., Palmer, M. A. 2011. The environmental costs of mountaintop mining valley fill operations for aquatic ecosystems of the Central Appalachians. *Annals of the New York Academy of Sciences*, *1223*(1), 39-57.

Bernhardt, E. S., Lutz, B. D., King, R. S., Fay, J. P., Carter, C. E., Helton, A., Campagna, D., Amos, J. 2012. How many mountains can we mine? Assessing the regional degradation of central Appalachian rivers by surface coal mining. *Environmental Science and Technology*, *46*(15), 8,115-8,122.

Bernoux, M., Cerri, C. C., Neill, C., de Moraes, J. F. 1998) The use of stable carbon isotopes for estimating soil organic matter turnover rates. *Geoderma*, *82*(1-3), 43-58

Beschta, R. L. 1978. Long-term patterns of sediment production following road construction and logging in the Oregon Coast Range. *Water Resources Research*, *14*(6), 1011-1016.

Black, D., McKinnish, T., Sanders, S. 2005a. The economic impact of the coal boom and bust. *The Economic Journal*, *115*(503), 449-476.

Black, D. A., McKinnish, T. G., Sanders, S. G. 2005b. Tight labor markets and the demand for education: Evidence from the coal boom and bust. *ILR Review*, *59*(1), 3-16.

Boccardy, J. A., Spaulding Jr, W. M. 1968. *Effects of surface mining on fish and wildlife in Appalachia* (No. 65). U.S. Fish and Wildlife Service.

Bohrer, S. L., Limb, R. F., Daigh, A. L. M., Volk, J. M.2017). Below ground attributes on reclaimed surface mine lands over a 40-year chronosequence. *Land Degradation and Development*, 28(7), 2,290-2,297.

Bonta, J. V. 2000. Impact of coal surface mining and reclamation on suspended sediment in three Ohio watersheds. *JAWRA Journal of the American Water Resources Association*, *36*(4), 869-887.

Bovis, M. J., Millard, T. H., Oden, M. E. 1998. Gully processes in coastal British Columbia: the role of woody debris. In Carnation Creek and Queen Charlotte Islands Fish/Forestry Workshop: Applying (Vol. 20, pp. 49-76).

Bradshaw, A. D., Chadwick, M. J. 1980. *The restoration of land: The ecology and reclamation of derelict and degraded land*. University of California Press.

Brais, S., Camiré, C., Paré, D. 1995. Impacts of whole-tree harvesting and winter windrowing on soil pH and base status of clayey sites of northwestern Quebec. *Canadian J. of Forest Research*, *25*(6), 997-1,007.

Brown, G. W., Krygier, J. T. 1971. Clear-cut logging and sediment production in the Oregon Coast Range. *Water Resources Research*, *7*(5), 1189-1198.

Burger, J. A. 2011. Sustainable mined land reclamation in the eastern U.S. coalfields: A case for an ecosystem reclamation approach. In *Proceedings of the National Meeting of the American Society of Mining and Reclamation,* Bismark, ND, USA (Vol. 15, pp. 113-141).

Burger, J. A., Zipper, C. E. 2002. How to restore forests on surface-mined land. Publication 460-123. Virginia Cooperative Extension, Virginia Polytechnic Institute and State University.

Cavender, N., Byrd, S., Bechtoldt, C. L., Bauman, J. M. 2014. Vegetation communities of a coal reclamation site in southeastern Ohio. *Northeastern Naturalist*, *21*(1), 31-46.

Clark, E. V., Zipper, C. E. 2016. Vegetation influences near-surface hydrological characteristics on a surface coal mine in eastern USA. *Catena*, 139, 241-249.

Compton, J. E., Hooker, T. D., Perakis, S. S. 2007. Ecosystem N distribution and $\delta^{15}N$ during a century of forest regrowth after agricultural abandonment. *Ecosystems*, *10*(7), 1,197-1,208.

Crowther, T. W., Maynard, D. S., Leff, J. W., Oldfield, E. E., McCulley, R. L., Fierer, N., Bradford, M. A. 2014. Predicting the responsiveness of soil biodiversity to deforestation: A cross-biome study. *Global Change Biology*, *20*(9), 2,983-2,994.

Curtis, J. B. 2002. Fractured shale-gas systems. *AAPG bulletin*, *86*(11), 1921-1938.

Dawson, T. E., Mambelli, S., Plamboeck, A. H., Templer, P. H., Tu, K. P. 2002. Stable isotopes in plant ecology. *Annual Review of Ecology and Systematics*, *33*(1), 507-559.

Eble, C. F., Hower, J. C. 1997. Coal quality trends and distribution of potentially hazardous trace elements in Eastern Kentucky coals. *Fuel*, *76*(8), 711-715.

Feng, Y., Wang, J., Bai, Z., Reading, L. 2019. Effects of surface coal mining and land reclamation on soil properties: A review. *Earth-Science Reviews*.

Ferrari, J. R., Lookingbill, T. R., McCormick, B., Townsend, P. A., Eshleman, K. N. 2009. Surface mining and reclamation effects on flood response of watersheds in the central Appalachian Plateau region. *Water Resources Research*, *45*(4), W04407, doi:10.1029/ 2008WR007109.

Foil, R. R., Ralston, C. W. 1967. The establishment and growth of Loblolly Pine seedlings on compacted soils 1. *Soil Science Society of America J.*, *31*(4), 565-568.

Fornara, D. A., Tilman, D. 2008. Plant functional composition influences rates of soil carbon and nitrogen accumulation. *J. of Ecology*, *96*(2), 314-322.

Fox, J. F.2009). Identification of sediment sources in forested watersheds with surface coal mining disturbance using Carbon and Nitrogen isotopes 1. *JAWRA J. of the American Water Resources Association*, *45*(5), 1,273-1,289.

Foufoula-Georgiou, E., Ganti, V., & Dietrich, W. E. 2010. A nonlocal theory of sediment transport on hillslopes. *J. of Geophysical Research: Earth Surface*, *115*(F2).

Fritz, K. M., Fulton, S., Johnson, B. R., Barton, C. D., Jack, J. D., Word, D. A., Burke, R. A. 2010. Structural and functional characteristics of natural and constructed channels draining a reclaimed mountaintop removal and valley fill coal mine. *J. of the North American Benthological Society*, *29*(2), 673-689.

Goldberg, E. F., Power, G. 1972. *Legal problems of coal mine reclamation: A study in Maryland, Ohio, Pennsylvania, and West Virginia*. College Park, MD.

Gomez, A., Powers, R. F., Singer, M. J., Horwath, W. R. 2002. Soil compaction effects on growth of young ponderosa pine following litter removal in California's Sierra Nevada. *Soil Science Society of America J.*, *66*(4), 1,334-1,343.

Gough, D. B. 2013. *The value of the commonwealth: An ecocritical history of Robinson Forest*. Ph.D. Dissertation, The University of Iowa.

Greacen, E. L., Sands, R. 1980. Compaction of forest soils. A review. *Soil Research*, *18*(2), 163-189.

Groninger, J., Skousen, J., Angel, P., Barton, C., Burger, J., Zipper, C. 2017. Mine reclamation practices to enhance forest development through natural succession. In: *Adams, Mary Beth, ed. The Forestry Reclamation Approach: Guide to Successful Reforestation of Mined Lands.* Gen. Tech. Rep. NRS-169. Newtown Square, PA: U.S. Department of Agriculture, Forest Service, Northern Research Station: 1-7.

Haering, K. C., Daniels, W. L., Galbraith, J. M. 2004. Appalachian mine soil morphology and properties. *Soil Science Society of America J.*, *68*(4), 1,315-1,325.

Hamlett, J. M., Melvin, S. W., Horton, R. 1990. Traffic and soil amendment effects on infiltration and compaction. *Transactions of the ASAE*, *33*(3), 821-826.

Hamza, M. A., Anderson, W. K. 2005. Soil compaction in cropping systems: A review of the nature, causes and possible solutions. *Soil and Tillage Research*, *82*(2), 121-145.

Harrison, L. H., Klotter, J. C. 2009. *A new history of Kentucky*. University Press of Kentucky.

Hatten, J. A., Segura, C., Bladon, K. D., Hale, V. C., Ice, G. G., Stednick, J. D. 2018. Effects of contemporary forest harvesting on suspended sediment in the Oregon Coast Range: Alsea Watershed Study Revisited. *Forest Ecology and Management*, *408*, 238-248.

He, Q., Walling, D. E. 1996. Interpreting particle size effects in the adsorption of ^{137}Cs and unsupported ^{210}Pb by mineral soils and sediments. *J. of Environmental Radioactivity*, *30*(2), 117-137.

Hillier, S. 2001. Particulate composition and origin of suspended sediment in the R. Don, Aberdeenshire, UK. *Science of the Total Environment*, *265*(1-3), 281-293.

Hobbie, E. A., Werner, R. A. 2004. Intramolecular, compound‐specific, and bulk carbon isotope patterns in C3 and C4 plants: A review and synthesis. *New Phytologist*, *161*(2), 371-385.

Holl, K. D. 2002. Long-term vegetation recovery on reclaimed coal surface mines in the eastern USA. *J. Applied Ecology*, 39(6), 960-970.

Holl, K. D., Cairns Jr, J. 1994. Vegetational community development on reclaimed coal surface mines in Virginia. *Bulletin of the Torrey Botanical Club*, 327-337.

Huang, J., Lacey, S. T., Ryan, P. J. 1996. Impact of forest harvesting on the hydraulic properties of surface soil. *Soil Science*, *161*(2), 79-86.

Huffman, G. P., Mitra, S., Huggins, F. E., Shah, N., Vaidya, S., Lu, F. 1991. Quantitative analysis of all major forms of sulfur in coal by X-ray absorption fine structure spectroscopy. *Energy and Fuels*, *5*(4), 574-581.

Hunter, C. D., Young, D. M. 1953. Relationship of natural gas occurrence and production in eastern Kentucky (Big Sandy gas field) to joints and fractures in Devonian bituminous shale. *AAPG Bulletin*, *37*(2), 282-299.

Jaeger, K. L. 2015. Reach-scale geomorphic differences between headwater streams draining mountaintop mined and unmined catchments. *Geomorphology*, *236*, 25-33.

Jobbágy, E. G., Jackson, R. B. 2000. The vertical distribution of soil organic carbon and its relation to climate and vegetation. *Ecological applications*, *10*(2), 423-436.

Kalisz, P. J., Dotson, D. B. 1989. Land-use history and the occurrence of exotic earthworms in the mountains of eastern Kentucky. *American Midland Naturalist*, *122*(2), 288-297.

Kohn, M. J. 2010. Carbon isotope compositions of terrestrial C3 plants as indicators of (paleo) ecology and (paleo) climate. *Proceedings of the National Academy of Sciences*, *107*(46), 19,691-19,695.

Krishnaswami, S., Benninger, L. K., Aller, R. C., Von Damm, K. L. 1980. Atmospherically-derived radionuclides as tracers of sediment mixing and accumulation in near-shore marine and lake sediments: Evidence from ^{7}Be, ^{210}Pb, and ^{239,240}Pu. *Earth and Planetary Science Letters*, *47*(3), 307-318.

Kochenderfer, J. N. 1970. Erosion control on logging roads in the Appalachians. *Res. Pap. NE-158. Upper Darby, PA: US Department of Agriculture, Forest Service, Northeastern Forest Experiment Station. 28 p.*, *158*.

Koestner, K. A., Carroll, M. D., Neary, D. G., Koestner, P. E., Youberg, A. (2011). Depositional characteristics and sediment availability resulting from the post-Schultz Fire floods of 2010. *24th Annual Symposium of the Arizona Hydrological Society; Watersheds Near and Far: Response to Changes in Climate and Landscape;* September 18-20, 2010; Flagstaff, AZ. 5 p.

Kozlowski, T. T. 1999. Soil compaction and growth of woody plants. *Scandinavian J. of Forest Research*, *14*(6), 596-619.

Larsen, R. J. 1984. *Worldwide deposition of 90 Sr through 1982* (No. EML--430). Department of Energy.

Lima, A. T., Mitchell, K., O'Connell, D. W., Verhoeven, J., Van Cappellen, P. 2016. The legacy of surface mining: Remediation, restoration, reclamation and rehabilitation. *Environmental Science and Policy*, 66, 227-233.

Lubis, A. A. 2013. Constant rate of supply (CRS) model for determining the sediment accumulation rates in the coastal area using ^{210}Pb. *J. of Coastal Development*, *10*(1), 9-18.

Mabit, L., Benmansour, M., Walling, D. E. 2008. Comparative advantages and limitations of the fallout radionuclides ^{137}Cs, $^{210}Pb_{ex}$ and ^{7}Be for assessing soil erosion and sedimentation. *J. of Environmental Radioactivity*, *99*(12), 1,799-1,807.

Maharaj, S., Barton, C. D., Karathanasis, T. A., Rowe, H. D., Rimmer, S. M. 2007. Distinguishing" new" from" old" organic carbon in reclaimed coal mine sites using thermogravimetry: II. Field validation. *Soil Science*, *172*(4), 302-312.

Mangena, S. J., Brent, A. C. 2006. Application of a life cycle impact assessment framework to evaluate and compare environmental performances with economic values of supplied coal products. *Journal of Cleaner Production*, *14*(12-13), 1,071-1,084.

Martin, C. W. 1988. Soil disturbance by logging in New England, review and management recommendations. *Northern J. of Applied Forestry*, *5*(1), 30-34.

Martin, C. W., Hornbeck, J. W. 1994. Logging in New England need not cause sedimentation of streams. *Northern J. of Applied Forestry*, *11*(1), 17-23.

Martin, L. L. 2006. Effects of Forest and Grass Vegetation on Fluviokarst Hillslope Hydrology. *Bowman's Bend, Kentucky (Ph.D. dissertation) University of Kentucky, Lexington (Available at: http://uknowledge.uky. edu/gradschool_diss/362/)*.

Matisoff, G., Bonniwell, E. C., Whiting, P. J. 2002. Soil erosion and sediment sources in an Ohio watershed using beryllium-7, cesium-137, and lead-210. *J. of Environmental Quality*, *31*(1), 54-61.

Megahan, W. F., & Kidd, W. J. 1972. Effects of logging and logging roads on erosion and sediment deposition from steep terrain. *Journal of Forestry*, *70*(3), 136-141.

McCashion, J. D., & Rice, R. M. 1983. Erosion on logging roads in northwestern California: How much is avoidable?. *Journal of Forestry*, *81*(1), 23-26.

Meier, A. J., Bratton, S. P., Duffy, D. C. 1995. Possible ecological mechanisms for loss of vernal-herb diversity in logged eastern deciduous forests. *Ecological Applications*, *5*(4), 935-946.

Mensah, A. K. 2015. Role of revegetation in restoring fertility of degraded mined soils in Ghana: A review. *International J. of Biodiversity and Conservation*, *7*(2), 57-80.

Milici, R. C. 2000. Depletion of Appalachian coal reserves—how soon? *International Journal of Coal Geology*, *44*(3-4), 251-266.

Miura, T., Hayano, K., Nakayama, K. 1999. Determination of ^{210}Pb and ^{210}Po in environmental samples by alpha ray spectrometry using an extraction chromatographic resin. *Analytical Sciences*, *15*(1), 23-28.

Moehring, D. M., Rawls, I. W. 1970. Detrimental effects of wet weather logging. *J. of Forestry*, *68*(3), 166-167.

Narita, H., Harada, K., Burnett, W. C., Tsunogai, S., McCabe, W. J. 1989. Determination of ^{210}Pb, ^{210}Bi and ^{210}Po in natural waters and other materials by electrochemical separation. *Talanta*, *36*(9), 925-929.

O'Leary, M. H. 1988. Carbon isotopes in photosynthesis. *Bioscience*, *38*(5), 328-336.

O'loughlin, C. L., Pearce, A. J. 1976. Influence of Cenozoic geology on mass movement and sediment yield response to forest removal, North Westland, New Zealand. *Bulletin of the International Association of Engineering Geology 13*(1), 41-46.

O'Loughlin, C. L., Rowe, L. K., Pearce, A. J. 1980. Sediment yield and water quality responses to clear felling of evergreen mixed forests in western New Zealand. *IAHS-AISH Publication (IAHS). no. 130.*

O'Loughlin, C. L., Rowe, L. K., Pearce, A. J. 1982. *Exceptional storm influences on slope erosion and sediment yield in small forest catchments, North Westland, New Zealand*. Institution of Engineers, Australia.

Palmer, M. A., Bernhardt, E. S., Schlesinger, W. H., Eshleman, K. N., Foufoula-Georgiou, E., Hendryx, M., Lemly, A., Likens, G., Loucks, O., Power, M., White, P., Wilcock, P. 2010. Mountaintop mining consequences. *Science*, *327*(5962), 148-149.

Persson, B. R., Holm, E. 2011. Polonium-210 and lead-210 in the terrestrial environment: A historical review. *J. of Environmental Radioactivity*, *102*(5), 420-429.

Peterson, B. J., Fry, B. 1987. Stable isotopes in ecosystem studies. *Annual Review of Ecology and Systematics*, *18*(1), 293-320.

Phillips, J. D. 2004. Impacts of surface mine valley fills on headwater floods in eastern Kentucky. *Environmental Geology*, *45*(3), 367-380.

Phillips, D. L., Gregg, J. W. 2001. Uncertainty in source partitioning using stable isotopes. *Oecologia*, *127*(2), 171-179.

Plouffe, A., Hall, G. E., Pelchat, P. 2001. Leaching of loosely bound elements during wet grain size separation with sodium hexametaphosphate: Implications for selective extraction analysis. *Geochemistry: Exploration, Environment, Analysis*, *1*(2), 157-162.

Poet, S. E., Moore, H. E., Martell, E. A. 1972. Lead 210, bismuth 210, and polonium 210 in the atmosphere: Accurate ratio measurement and application to aerosol residence time determination. *J. of Geophysical Research*, *77*(33), 6,515-6,527.

Pond, G. J. 2010. Patterns of Ephemeroptera taxa loss in Appalachian headwater streams (Kentucky, USA). *Hydrobiologia*, *641*(1), 185-201.

Pond, G. J., Passmore, M. E., Pointon, N. D., Felbinger, J. K., Walker, C. A., Krock, K. J., Fulton, J. B., Nash, W. L. 2014. Long-term impacts on macroinvertebrates downstream of reclaimed mountaintop mining valley fills in central Appalachia. *Environmental Management*, *54*(4), 919-933.

Price, P., Wright, I. A. 2016. Water quality impact from the discharge of coal mine wastes to receiving streams: Comparison of impacts from an active mine with a closed mine. *Water, Air, and Soil Pollution*, *227*(5), 155

Price, S. J., Muncy, B. L., Bonner, S. J., Drayer, A. N., Barton, C. D. 2016. Effects of mountaintop removal mining and valley filling on the occupancy and abundance of stream salamanders. *J. of Applied Ecology*, *53*(2), 459-468.

Ramani, R. V. 2012. Surface mining technology: progress and prospects. *Procedia Engineering*, *46*, 9-21.

Rani, L. M., Jeevanram, R. K., Kannan, V., Govindaraju, M. 2014. Estimation of Polonium-210 activity in marine and terrestrial samples and computation of ingestion dose to the public in and around Kanyakumari coast, India. *J. of Radiation Research and Applied Sciences*, *7*(2), 207-213.

Reisinger, T. W., Simmons, G. L., Pope, P. E. 1988. The impact of timber harvesting on soil properties and seedling growth in the south. *Southern J. of Applied Forestry*, *12*(1), 58-67.

Rice, D. L. 1986. Early diagenesis in bioadvective sediments: Relationships between the diagenesis of beryllium-7, sediment reworking rates, and the abundance of conveyor-belt deposit-feeders. *J. of Marine Research*, *44*(1), 149-184.

Rice, R. M., Tilley, F. B., Datzman, P. A. 1979. A watershed's response to logging and roads: South Fork of Caspar Creek, California, 1967-1976. *Res. Paper PSW-RP-146. Berkeley, CA: US Department of Agriculture, Forest Service, Pacific Southwest Forest and Range Experiment Station. 12 p*, *146*.

Ritchie, J. C., McHenry, J. R. 1990. Application of radioactive fallout cesium-137 for measuring soil erosion and sediment accumulation rates and patterns: A review. *J. of Environmental Quality*, *19*(2), 215-233.

Robinson, R. A., Slingerland, R. L. 1998. Origin of fluvial grain-size trends in a foreland basin: The Pocono Formation on the central Appalachian basin. *J. of Sedimentary Research*, *68*(3), 473-486.

Ryan, M., Meiman, J. 1996. An examination of short-term variations in water quality at a karst spring in Kentucky. *Groundwater*, *34*(1), 23-30.

Santschi, P. H., Guo, L., Walsh, I. D., Quigley, M. S., Baskaran, M. 1999. Boundary exchange and scavenging of radionuclides in continental margin waters of the Middle Atlantic Bight: Implications for organic carbon fluxes. *Continental Shelf Research*, *19*(5), 609-636.

Santschi, P. H., Allison, M. A., Asbill, S., Perlet, A. B., Cappellino, S., Dobbs, C., McShea, L. 1999. Sediment transport and Hg recovery in Lavaca Bay, as evaluated from radionuclide and Hg distributions. *Environmental Science and Technology*, *33*(3), 378-391.

Schuler, R., Lowery, B., Wolkowski, R., Bundy, L. 1986. Soil Compaction: Causes, Concerns, and Cures. *University of Wisconsin-Extension Report A3367*.

Schuler, T. M., Gillespie, A. R. 2000. Temporal patterns of woody species diversity in a central Appalachian forest from 1856 to 1997. *J. of the Torrey Botanical Society*, *127*(2), 149-161.

Sharma, P., Gardner, L. R., Moore, W. S., Bollinger, M. S. 1987. Sedimentation and bioturbation in a salt marsh as revealed by ^{210}Pb, ^{137}Cs, and ^{7}Be studies. *Limnology and Oceanography*, *32*(2), 313-326.

Shaw III, C. G., Sidle, R. C., Harris, A. S. 1987. Evaluation of planting sites common to a southeast Alaska clear-cut. III. Effects of microsite type and ectomycorrhizal inoculation on growth and survival of Sitka spruce seedlings. *Canadian J. of Forest Research*, *17*(4), 334-339.

Sheoran, V., Sheoran, A. S., Poonia, P. 2010. Soil reclamation of abandoned mine land by revegetation: A review. *International J. of Soil, Sediment and Water*, *3*(2), art. 13.

Simmons, J. A., Currie, W. S., Eshleman, K. N., Kuers, K., Monteleone, S., Negley, T. L., Pohlad, B.R, Thomas, C. L. 2008. Forest to reclaimed mine land use change leads to altered ecosystem structure and function. *Ecological Applications*, *18*(1), 104-118.

Stevenson, B. A., Kelly, E. F., McDonald, E. V., Busacca, A. J. 2005. The stable carbon isotope composition of soil organic carbon and pedogenic carbonates along a bioclimatic gradient in the Palouse region, Washington State, USA. *Geoderma*, *124*(1-2), 37-47.

Swab, R. M., Lorenz, N., Byrd, S., Dick, R. 2017. Native vegetation in reclamation: Improving habitat and ecosystem function through using prairie species in mine land reclamation. *Ecological Engineering*, *108*, 525-536.

Swer, S., Singh, O. P. 2004. Status of water quality in coal mining areas of Meghalaya, India. In *Proceedings of the national seminar on environmental engineering with special emphasis on mining environment* (pp. 19-20). NSEEME-2004.

Tiwary, R. K. 2001. Environmental impact of coal mining on water regime and its management. *Water, Air, and Soil Pollution*, *132*(1-2), 185-199.

Turekian, K. K., Nozaki, Y., Benninger, L. K. 1977. Geochemistry of atmospheric radon and radon products. *Annual Review of Earth and Planetary Sciences*, *5*(1), 227-255.

Updegraff, K., Pastor, J., Bridgham, S. D., Johnston, C. A. 1995. Environmental and substrate controls over carbon and nitrogen mineralization in northern wetlands. *Ecological Applications*, *5*(1), 151-163.

Ussiri, D. A., Lal, R. 2005. Carbon sequestration in reclaimed minesoils. *Critical Reviews in Plant Sciences*, *24*(3), 151-165.

Ussiri, D. A., Lal, R., Jacinthe, P. A. 2006. Post-reclamation land use effects onproperties and carbon sequestration in minesoils of southeastern Ohio. *Soil Science*, *171*(3), 261-271.

Vaaramaa, K., Aro, L., Solatie, D., Lehto, J. 2010. Distribution of ^{210}Pb and ^{210}Po in boreal forest soil. *Science of the Total Environment*, *408*(24), 6,165-6,171.

Vesterbacka, P., Ikäheimonen, T. K. 2005. Optimization of ^{210}Pb determination via spontaneous deposition of ^{210}Po on a silver disk. *Analytica Chimica Acta*, *545*(2), 252-261.

Walling, D. E. 1998. *Use of 137 Cs and other fallout radionuclide in soil erosion investigations: progress, problems and prospects* (No. IAEA-TECDOC--1028).

Walling, D. E., Zhang, Y., He, Q. 2011. Models for deriving estimates of erosion and deposition rates from fallout radionuclide (caesium-137, excess lead-210, and beryllium-7) measurements and the development of user-friendly software for model implementation. *Impact of soil conservation measures on erosion control and soil quality.* IAEA-TECDOC-1665, 11-33.

Wan, G. J., Chen, J. A., Wu, F. C., Xu, S. Q., Bai, Z. G., Wan, E. Y. Wang, C. S., Huang, R. G., Yeager, K. M. Santschi, P. H. 2005. Coupling between $^{210}Pb_{ex}$ and organic matter in sediments of a nutrient-enriched lake: An example from Lake Chenghai, China. *Chemical Geology*, *224*(4), 223-236.

Wang, J., LeDoux, C. B., Edwards, P., Jones, M. 2005. Soil bulk density changes caused by mechanized harvesting: A case study in central Appalachia. *Forest Products J., 55* (11): 37-40.

Wentworth, C. K. 1922. A scale of grade and class terms for clastic sediments. *The J. of Geology*, *30*(5), 377-392.

Wickham, J. D., Riitters, K. H., Wade, T. G., Coan, M., Homer, C. 200). The effect of Appalachian mountaintop mining on interior forest. *Landscape Ecology*, *22*(2), 179-187.

Wickham, J., Wood, P. B., Nicholson, M. C., Jenkins, W., Druckenbrod, D., Suter, G., Strager, M., Mazzarella, C., Galloway, W., Amos, J. 2013) The overlooked terrestrial impacts of mountaintop mining. *BioScience*, *63*(5), 335-348.

Wood, P. J., & Armitage, P. D. 1997. Biological effects of fine sediment in the lotic environment. *Environmental management*, *21*(2), 203-217.

Wyatt, J. L., Silman, M. R. 2010. Centuries-old logging legacy on spatial and temporal patterns in understory herb communities. *Forest Ecology and Management*, *260*(1), 116-124.

Wynn, J. G., Harden, J. W., Fries, T. L. 2006. Stable carbon isotope depth profiles and soil organic carbon dynamics in the lower Mississippi Basin. *Geoderma*, *131*(1-2), 89-109.

Yang, M. Y., Walling, D. E., Tian, J. L., Liu, P. L. 2006. Partitioning the contributions of sheet and rill erosion using beryllium-7 and cesium-137. *Soil Science Society of America Journal*, *70*(5), 1579-1590.

Yeager, K. M., Santschi, P. H., Phillips, J. D., Herbert, B. E. (2005). Suspended sediment sources and tributary effects in the lower reaches of a coastal plain stream as indicated by radionuclides, Loco Bayou, Texas. *Environmental Geology*, *47*(3), 382-395.

Yeager, K. M., Santschi, P. H., Rifai, H. S., Suarez, M. P., Brinkmeyer, R., Hung, C., Schindler, K., Andres, M., Weaver, E. 2007. Dioxin chronology and fluxes in sediments of the Houston Ship Channel, Texas: Influences of non-steady-state sediment transport and total organic carbon. *Environmental Science and Technology*, *41*(15), 5,291-5,298.

Zipper, C. E., Burger, J. A., Skousen, J. G., Angel, P. N., Barton, C. D., Davis, V., Franklin, J. A. 2011. Restoring forests and associated ecosystem services on Appalachian coal surface mines. *Environmental Management*, *47*(5), 751-765.

5.4 Chapter 3

Agouridis, C.T., P.N. Angel, T.J. Taylor, C.D. Barton, R.C. Warner, X. Yu, and C. Wood. 2012. Water quality characteristics of discharge from reforested loose-dump mine spoil in eastern Kentucky. *J Environ Qual* 41: 454-468.

Bernhardt, E.S., M. Palmer, J.D. Allan, G. Alexander, K. Barnas, S. Brooks, and E. Sudduth. 2005. Synthesizing U.S. river restoration efforts. *Science* 308: 636-637.

Blackburn-Lynch, W. 2015. Development of techniques for assessing and restoring streams on surface mined lands. Ph.D. Dissertation, University of Kentucky.

Brannon, M.P. and B.A. Purvis. 2008. Effects of sedimentation on the diversity of salamanders in a southern Appalachian headwater stream. *Journal of the North Carolina Academy of Science* 124 18-22.

Burger, J., D. Graves, P. Angel, V. Davis, and C. Zipper. 2005. The forestry reclamation approach. Appalachian Regional Reforestation Initiative, Office of Surface Mining. Forestry Reclamation Advisory Number 2.

Clark, A. R. MacNally, N. Bond, and P.S. Lake. 2008. Macroinvertebrate diversity in headwater streams: a review. *Freshwater Biol* 53: 1707-1721.

Gomi, T., R.C. Sidle, and J.S. Richardson. 2002. Understanding processes and downstream linkages of headwater systems. *BioScience* 52: 906-916.

Graves, D.H., J.M. Ringe, M.H. Pelkki, R.J. Sweigard, and R.C. Warner. 2000. High value tree reclamation research. In *Environmental issues and management of waste in energy and mineral production*, ed. R.K. Singhal and A.K. Mehrotra, 413-421. Balkema: Rotterdam.

Green, J., M. Passmore, and H. Childers. 2000. A survey of the condition of streams in the primary region of mountaintop mining/valley fill coal mining. Appendix In *Mountaintop mining/valley fill programmatic environmental impact statement*. Wheeling: U.S. Environmental Protection Agency, Region III.

Greenberg, A.E., L.S. Clesceri, and A.D. Eaton. 1992. *Standard Methods for the Examination of Water and Wastewater*. Washington, D.C.: American Public Health Association.

Hey, R.D. 2006. Fluvial geomorphological methodology for natural stable channel design. *Journal of the American Water Resources Association* 42: 357-374.

Lowe, W. and G.E. Likens. 2005. Moving headwater streams to the head of the class. *BioScience* 55: 196-197.

Maupin, T.P. 2012. Assessment of conductivity sensor performance for monitoring mined land discharged waters and an evaluation of the hydrologic performance of the Guy Cove Stream Restoration Project. M.S. Thesis, University of Kentucky.

May, C.L. and R.E. Gresswell. 2003. Processes and rates of sediment and wood accumulation in the headwater streams of the Oregon Coast Range, U.S.A. *Earth Surf Proc Land* 28: 409-424.

McDonough, O.T., J.D. Hosen, and M.A. Palmer. 2011. Temporary streams: the hydrology, geography, and ecology of non-perennially flowing waters. In *River Ecosystems: Dynamics, Management and Conservation* ed. H.S. Elliot and L.E. Martin. New York: Nova Science Publishers, Inc.

Meyer, J.L., D. L. Strayer, J. B. Wallace, S.L. Eggert, G.S. Helfman, and N.E. Leonard. 2007. The contribution of headwater streams to biodiversity in river networks. *Journal of the American Water Resources Association* 43: 86-103.

Palmer, M.A. and K.L. Hondula. 2004. Restoration as mitigation: analysis of stream mitigation for coal mining impacts in southern Appalachia. *Environ Sci Technol* 48: 10552-10560.

Petranka, J.W. and S.S. Murray. 2001. Effectiveness of removal sampling for determining salamander density and biomass: a case study in an Appalachian streamside community. *J Herpetol* 35: 36-34.

Pond, G.J. 2004. Effects of surface mining and residential land use on headwater stream biotic integrity in the Eastern Kentucky Coalfield region. Kentucky Department for Environmental Protection, Division of Water, Water Quality Branch.

Pond, G.J., M.E. Passmore, F.A. Borsuk, L. Reynolds, and C.J. Rose. 2008. Downstream effects of mountaintop coal mining: comparing biological conditions using family- and genus-level macroinvertebrate bioassessment tools. *Journal of the North American Benthological Society* 27: 717-737.

Rosgen, D.L. 1998. The reference reach – a blueprint for natural channel design. *In* Proceedings of the Wetland Engineering and River Restoration Conference, ASCE, CDROM.

Sena, K., C. Barton, P. Angel, C. Agouridis, and R. Warner. 2014. Influence of spoil type on chemistry and hydrology of interflow on a surface coal mine in the Eastern US Coalfield. *Water Air Soil Pollut* 225: 2171.

Sena, K., C. Barton, S. Hall, P. Angel, C. Agouridis, and R. Warner. 2015. Influence of spoil type on afforestation success and natural vegetative recolonization on a surface coal mine in Appalachia. *Restoration Ecol* 23: 131-138.

Shreve, R.L. 1969. Stream lengths and basin areas in topographically random channel networks. *J Geol* 77: 397-414.

Taylor, T.J., C.T. Agouridis, R.C. Warner, C.D. Barton, and P.N. Angel. 2009a. Hydrologic characteristics of Appalachian loose-dumped spoil in the Cumberland Plateau of eastern Kentucky. *Hydrol Process* 23: 3372-3381.

Taylor, T.J., C.T. Agouridis, R.C. Warner, and C.D. Barton. 2009b. Runoff curve numbers for loose-dumped spoil in the Cumberland Plateau of eastern Kentucky. *Int J Min Reclam Env* 23: 103-120.

Torbert, J.L. and J.A. Burger. 1994. Influence of grading intensity on ground cover establishment, erosion, and tree establishment on steep slopes. Proceedings of the International Land Reclamation and Mine Drainage Conference and the Third International Conference on the Abatement of Acid Drainage, Pittsburg.

U.S. DC (Department of Commerce). 2002. Climatography of the United States, No. 81 monthly station normal of temperature, precipitation, and heating and cooling degree 1971-2000.

U.S. EPA (Environmental Protection Agency). 2011. The effects of mountaintop mines and valley fills on aquatic ecosystems of the central Appalachian Coalfields. Office of Research and Development, National Center for Environmental Assessment, Washington, D.C. EPA/600/R-09/138F.

Zipper, C., J. Burger, J. Skousen, P. Angel, C. Barton, V. Davis, and J. Franklin. 2011. Restoring forests and associated ecosystem services on Appalachian coal surface mines. *Environ Manag* 47: 751-765.

5.5 Chapter 4

Amoozegar, A. 1992. Compact constant head permeameter: a convenient device for measuring hydraulic conductivity. Advances in Measurement of Soil Physical Properties: Bringing Theory into Practice. Soil Science Society of America, Madison, WI. p. 31-42.

Baker, T.J., Williamson, T.N., Lee, B.D. 2015. Translating soil properties to simulated soil-water availability under forecasted climate. Soil Science Society of America Annual Meeting, Minneapolis, MN.

Beijing Climate Center. 2018. BCC BCC-CSM2MR model output prepared for CMIP6 CMIP historical. Earth System Grid Federation, Beijing Climate Center. http://cera-www.dkrz.de/WDCC/meta/CMIP6/CMIP6.CMIP.BCC.BCC-CSM2-MR.historical.

Beijing Climate Center. 2018. BCC BCC-CSM2MR model output prepared for CMIP6 ScenarioMIP ssp585. Earth System Grid Federation, Beijing Climate Center. http://cera-www.dkrz.de/WDCC/meta/CMIP6/CMIP6.ScenarioMIP.BCC.BCC-CSM2-MR.ssp585.

Beven, K.J. and M.J. Kirkby. 1979. A physically based, variable contributing area model of basin hydrology / Un modèle à base physique de zone d'appel variable de l'hydrologie du bassin versant. Hydrological Sciences Bulletin 24: 43-69. doi:10.1080/02626667909491834.

Bock, A.R., L.E. Hay, G.J. McCabe, S.L. Markstrom and R.D. Atkinson. 2018. Do Downscaled General Circulation Models Reliably Simulate Historical Climatic Conditions? Earth Interactions 22: 1-22. doi:10.1175/ei-d-17-0018.1.

Boucher, O., S. Denvil, A. Caubel and M.A. Foujols. 2018. IPSL IPSL-CM6A-LR model output prepared for CMIP6 CMIP historical. Earth System Grid Federation, Institut Pierre Simon Laplace. https://doi.org/10.22033/ESGF/CMIP6.5195.

Boucher, O., S. Denvil, A. Caubel and M.A. Foujols. 2019. IPSL IPSL-CM6A-LR model output prepared for CMIP6 ScenarioMIP ssp585. Earth System Grid Federation, Institut Pierre Simon Laplace. https://doi.org/10.22033/ESGF/CMIP6.5271.

Canadian Centre for Climate Modelling and Analysis. 2018. CCCma CanESM5 model output prepared for CMIP6 CMIP historical. Earth System Grid Federation, Canadian Centre for Climate Modelling and Analysis. http://cera-www.dkrz.de/WDCC/meta/CMIP6/CMIP6.CMIP.CCCma.CanESM5.historical.

Canadian Centre for Climate Modelling and Analysis. 2018. CCCma CanESM5 model output prepared for CMIP6 ScenarioMIP ssp585. Earth System Grid Federation, Canadian Centre for Climate Modelling and Analysis,. http://cera-www.dkrz.de/WDCC/meta/CMIP6/CMIP6.ScenarioMIP.CCCma.CanESM5.ssp585.

Centre National de Recherches Meteorologiques and Centre Europeen de Recherche et de Formation Avancee en Calcul Scientifique. 2018. CNRM-CERFACS CNRM-ESM2-1 model output prepared for CMIP6 ScenarioMIP ssp585. Earth System Grid Federation, Centre National de Recherches Meteorologiques, Centre Europeen de Recherche et de Formation Avancee en Calcul Scientifique. http://cera-www.dkrz.de/WDCC/meta/CMIP6/CMIP6.ScenarioMIP.CNRM-CERFACS.CNRM-ESM2-1.ssp585.

Eyring, V., S. Bony, G.A. Meehl, C.A. Senior, B. Stevens, R.J. Stouffer, et al. 2016. Overview of the Coupled Model Intercomparison Project Phase 6 (CMIP6) experimental design and organization. Geosci. Model Dev. 9: 1937-1958. doi:10.5194/gmd-9-1937-2016.

Guo, H., J.G. John, C. Blanton, C. McHugh, S. Nikonov, A. Radhakrishnan, et al. 2018. NOAA-GFDL GFDL-CM4 model output prepared for CMIP6 ScenarioMIP ssp585. Earth System Grid Federation, National Oceanic and Atmospheric Administration, Geophysical Fluid Dynamics Laboratory. https://doi.org/10.22033/ESGF/CMIP6.9268.

Guo, H., J.G. John, C. Blanton, C. McHugh, S. Nikonov, A. Radhakrishnan, et al. 2018. NOAA-GFDL GFDL-CM4 model output prepared for CMIP6 CMIP historical. Earth System Grid Federation, National Oceanic and Atmospheric Administration, Geophysical Fluid Dynamics Laboratory. https://doi.org/10.22033/ESGF/CMIP6.8594.

Hamon, W.R. 1963. Computation of direct runoff amounts from storm rainfall. International Association of Scientific Hydrology Symposium Publication No. 63: 52-62.

Met Office Hadley Centre. 2018. MOHC UKESM1.0-LL model output prepared for CMIP6 CMIP historical. Earth System Grid Federation, Met Office Hadley Centre. http://cera-www.dkrz.de/WDCC/meta/CMIP6/CMIP6.CMIP.MOHC.UKESM1-0-LL.historical.

Met Office Hadley Centre. 2018. MOHC UKESM1.0-LL model output prepared for CMIP6 ScenarioMIP ssp585. Earth System Grid Federation, Met Office Hadley Centre. http://cera-www.dkrz.de/WDCC/meta/CMIP6/CMIP6.ScenarioMIP.MOHC.UKESM1-0-LL.ssp585.

Nash, J.E. and J.V. Sutcliffe. 1970. River flow forecasting through conceptual models part I — A discussion of principles. J. Hydrol. 10: 282-290. doi:10.1016/0022-1694(70)90255-6.

O'Neill, B.C., C. Tebaldi, D.P. van Vuuren, V. Eyring, P. Friedlingstein, G. Hurtt, et al. 2016. The Scenario Model Intercomparison Project (ScenarioMIP) for CMIP6. Geosci. Model Dev. 9: 3461-3482. doi:10.5194/gmd-9-3461-2016.

Schoeneberger, P.J., D.A. Wysocki and E.C. Benham. 2012. Field book for describing and sampling soils. Version 3.0 ed. Natural Resources Conservation Service, National Soil Survey Center, Lincoln, NE.

Seferian, R. 2018. CNRM-CERFACS CNRM-ESM2-1 model output prepared for CMIP6 CMIP historical. Earth System Grid Federation, Centre National de Recherches Meteorologiques, Centre Europeen de Recherche et de Formation Avancee en Calcul Scientifique. https://doi.org/10.22033/ESGF/CMIP6.4068.

Shiogama, H., M. Abe and H. Tatebe. 2019. MIROC MIROC6 model output prepared for CMIP6 ScenarioMIP ssp585. Earth System Grid Federation, Japan Agency for Marine-Earth Science and Technology, Atmosphere and Ocean Research Institute, National Institute for Environmental Studies, RIKEN Center for Computational Science. https://doi.org/10.22033/ESGF/CMIP6.5771.

Tatebe, H. and M. Watanabe. 2018. MIROC MIROC6 model output prepared for CMIP6 CMIP historical. Earth System Grid Federation, Japan Agency for Marine-Earth Science and Technology, Atmosphere and Ocean Research Institute, National Institute for Environmental Studies, RIKEN Center for Computational Science. https://doi.org/10.22033/ESGF/CMIP6.5603.

U.S. Department of Agriculture - Natural Resource Conservation Service [USDA-NRCS]. 2010. Soil Survey Geographic (SSURGO) Database for KY. Soil Survey Staff, Natural Resources Conservation Service, United States Department of Agriculture. http://soildatamart.nrcs.usda.gov.

Voldoire, A. 2018. CMIP6 simulations of the CNRM-CERFACS based on CNRM-CM6-1 model for CMIP experiment historical. Earth System Grid Federation, Centre National de Recherches Meteorologiques, Centre Europeen de Recherche et de Formation Avancee en Calcul Scientifique. https://doi.org/10.22033/ESGF/CMIP6.4066.

Voldoire, A. 2019. CNRM-CERFACS CNRM-CM6-1 model output prepared for CMIP6 ScenarioMIP ssp585. Earth System Grid Federation, Centre National de Recherches Meteorologiques, Centre Europeen de Recherche et de Formation Avancee en Calcul Scientifique. https://doi.org/10.22033/ESGF/CMIP6.4224.

Williamson, T.N., C.T. Agouridis, C.D. Barton, J.A. Villines and J.G. Lant. 2015. Classification of ephemeral, intermittent, and perennial stream reaches using a TOPMODEL-based approach. Journal of the American Water Resources Association 51: 1739-1759. doi:10.1111/1752-1688.12352.

Williamson, T.N. and P. Claggett. 2019. Sensitivity of streamflow simulation in the Delaware River Basin to forecasted land-cover change for 2030 and 2060. Hydrological Processes 33: 115-129. doi:10.1002/hyp.13315.

Williamson, T.N., B.D. Lee, P.J. Schoeneberger, W.M. McCauley, S.J. Indorante and P.R. Owens. 2014. Simulating Soil-Water Movement through Loess-Veneered Landscapes Using Nonconsilient Saturated Hydraulic Conductivity Measurements. Soil Sci. Soc. Am. J. 78: 1320-1331. doi:10.2136/sssaj2014.01.0045.

Publications

Sena, Kenton, Carmen Agouridis, Jarrod Miller and Chris Barton. 2018. Spoil type influences soil genesis and forest development on Appalachian surface coal mine ten years after placement. Forests, 9, 730: doi:10.3390/f9120780.

Gerlitz, Morgan F., "Evaluating the Influence of the Forestry Reclamation Approach on the Hydrology of Appalachian Coal Mined Lands" (2019). *Theses and Dissertations--Biosystems and Agricultural Engineering*. 65.
https://uknowledge.uky.edu/bae_etds/65

Sena, Kenton, Kevin Yeager, Tyler Dreaden and Christopher Barton. 2018. *Phytophthora cinnamomi* Colonized Reclaimed Surface Mined Sites in Eastern Kentucky: Implications for the Restoration of Susceptible Species. Forests. 9, 203; doi:10.3390/f9040203.

Presentations

2018 Sustainability Forum in Lexington, KY

- William Bond - *The Forestry Reclamation Approach: Measuring Sediment Mass Accumulation Rates in Reclaimed Mines and Regenerated Logging Sites in Eastern Kentucky.*

- Morgan Gerlitz - *Evaluating the Influence of the Forestry Reclamation Approach on the Hydrology of Appalachian Coal Mined Lands*

2018 ARRI Conference in Indiana, Pennsylvania

- Kenton Sena, Kevin Yeager, Tyler Dreaden, and Chris Barton - *Phytophthora cinnamomi colonized reclaimed surface mined sites in Eastern Kentucky: Implications for restoration of susceptible species*

- Kenton Sena, Joseph Frederick, Jarrod Miller, and Chris Barton - *Mine spoil type impacts tree growth and soil development 10 years after site establishment*

2019 ARRI Conference in Cambridge, OH

- Morgan Gerlitz - *Evaluating the Influence of the Forestry Reclamation Approach on the Hydrology of Appalachian Coal Mined Lands*

- Kenton Sena, Kevin Yeager, John Lhotka and Chris Barton – *Development of Mine Soils in a Chronosequence of FRA Reclaimed Sites in Eastern KY*